THE JOURNAL OF CHEMICAL PHYSICS

VOLUME 11 NUMBER 10

OCTOBER, 1943

Published by the

AMERICAN INSTITUTE OF PHYSICS

Lancaster, Pa., and New York, N. Y.

The Journal of Chemical Physics

ADVISORY EDITORIAL BOARD

R. T. Birge
A. H. Compton
James Franck
Irving Langmuir
John T. Tate
Harold C. Urey

BOARD OF EDITORS

Joseph E. Mayer, *Editor*

Associate Editors

Term ending December 31, 1944

Charles O. Beckman
Bryce L. Crawford, Jr.
P. Debye
David Harker
Frank H. Westheimer

Term ending December 31, 1945

L. O. Brockway
Ronald W. Gurney
Kenneth S. Pitzer
Alfred L. Sklar
E. W. R. Steacie
Hugh S. Taylor

The Journal of Chemical Physics is published monthly by the American Institute of Physics. Its purpose is to provide a medium for publication of physical and physicochemical research of interest to chemists and physicists. Its boundary between chemistry and physics has been a actual fact for many years and a large and active group is engaged in research which is as much the one as the other. It is to this group that the Journal is rendering its principal service and makes its greatest appeal, both as a prompt and efficient medium for publication of research and as a convenient and carefully edited assemblage of pertinent information.

Communication should be submitted to the Editor, Mayer Hall, Columbia University, New York, N. Y.

Manuscripts should be submitted in duplicate. Papers should be sent to the Publication Office, 175 Fifth Avenue, New York, N. Y.

Subscriptions should be sent to the Publication Office, Prince and Lemon Streets, Lancaster, Pennsylvania, or to the American Institute of Physics, 175 Fifth Avenue, New York, N. Y.

Subscription Price

The United States and Possessions, Canada and Mexico $10.00
Elsewhere 11.00

Back Numbers

Complete set: Vol. 1, 1933—Vol. 10, 1942 ..... $100.00
Yearly rate: $11.00.
Single copies: $1.00 each.

The Journal of Chemical Physics is published monthly by Prince and Lemon Streets, Lancaster, Pennsylvania.

Entered as second class matter at the post office at Lancaster, Pa., under the act of August 24, 1912. Acceptance for mailing at special rate of postage provided for in paragraph (d) Section 538, P. L. & R. authorized [illegible]

THE JOURNAL
OF
CHEMICAL PHYSICS

VOLUME 11, NUMBER 10 OCTOBER, 1943

Atomic and Electronic Distributions in Liquid Nitrogen, Nitric Oxide, and Nitrous Oxide

PAUL C. SHARRAH*
University of Missouri, Columbia, Missouri

(Received May 17, 1943)

The monochromatic x-ray diffraction patterns for liquid nitrogen, nitric oxide and nitrous oxide have been obtained and analyzed by the Fourier integral method to obtain the atomic or electronic distributions. The diffraction patterns show one main peak and only faint peaks or plateaus at larger angles. The distribution curves show diatomic aggregates in liquid nitrogen and nitric oxide comparable to those found in the gaseous states. A linear molecule for nitrous oxide is consistent with the present data while a triangular molecule is not.

INTRODUCTION

THE diffraction patterns produced by x-rays when scattered by liquids are of interest both in a qualitative way and as regards the information they can give concerning the "structure" of the liquid. The x-ray diffraction patterns produced by monatomic liquids may be analyzed in a systematic way to give the radial distribution of atoms about a given atom, using the theory of Zernicke and Prins,[1] and Debye and Menke.[2] The diffraction pattern produced by a polyatomic liquid is not so directly interpreted in terms of the distribution of atoms, but does give, by a direct analysis, the distribution of electrons in the liquid. A successful analysis by either of these theories depends first on a careful determination of the diffraction pattern out to large angles for that liquid, the relative intensity of the scattered x-rays, as well as the position of the diffraction peaks, being of importance.

The present work was undertaken both to seek to improve on earlier work on the diffraction pattern produced by liquid nitrogen and for the first time actually to carry out analyses of this pattern and those of liquid nitric oxide and nitrous oxide so as to obtain direct information concerning the atomic and electronic distributions in these liquids.

The diffraction pattern produced by liquid nitrogen was one of the first to be obtained, pictures having been taken by Keesom and de Smedt[3] about 1923. Using molybdenum radiation filtered through zirconium and an evacuated camera of 2.75-cm radius, they found two peaks in the pattern for liquid nitrogen, the main peak at $\sin\theta/\lambda=0.139$ and a second peak at about 0.208.

THEORY AND METHOD OF EVALUATING THE FOURIER INTEGRAL

The equation used for liquid nitrogen has been developed previously[4] in the literature and may

* Now at University of Arkansas, Fayetteville, Arkansas.

[1] F. Zernicke and J. Prins, Zeits. f. Physik **41**, 184 (1927); Zeits. f. Physik **56**, 617 (1929).

[2] P. Debye and H. Menke, Physik. Zeits. **31**, 797 (1930); Ergeb. d. Tech. Rontgenk. (1931), Vol. 2.

[3] W. H. Keesom and J. de Smedt, Proc. Amst. Akad. Sci. **26**, 112 (1923).

[4] B. E. Warren, J. App. Phys. **8**, 645 (1937).

be written

$$4\pi R^2\rho(R)=4\pi R^2\rho_0+2R/\pi\int_0^\infty si(s)\sin rsds,$$

where

$$s=4\pi\sin\theta/\lambda, \qquad i(s)=(I-Nf^2)/Nf^2,$$

I is the experimentally determined scattered intensity which has been corrected for absorption in the sample, the partial polarization of the scattered x-rays and the incoherent scattering background, Nf^2 is the scattering which would be expected if the scattering by the different atoms did not interfere, and ρ_0 is the average density of atoms (atoms per cubic angstrom). The function $4\pi R^2\rho(R)$ gives the distribution of atoms about any given atom in the liquid.

The equation used for the polyatomic liquids nitric oxide and nitrous oxide has been given in connection with the analysis of certain compounds and glasses.[5] The development of this equation is based on the assumption that the dependence of the atomic scattering factors upon $\sin\theta/\lambda$ for the different atoms in the liquids is such that they may be taken proportional to an average structure factor f_e per electron with Z (or K, an effective number of electrons per atom) as the proportionality factor. It should be pointed out that this assumption is particularly good for compounds of nitrogen and oxygen, which elements are adjacent in the periodic table. The equation is

$$\sum_M K_m 4\pi R^2\rho_m(R)=4\pi R^2\rho_0\sum_M Z_m+2R/\pi\int_0^\infty si(s)\sin Rsds,$$

where $i(s)=(I-N\sum_M f_m^2 m)/Nf_e^2$, I is the fully corrected experimentally determined scattering intensity, $N\sum_M f_m^2$ is the scattering which would be expected if the scattering from the different atoms did not interfere, $f_e=\sum_M f_m/\sum_M Z_m$, and ρ_0 is the average density of the electrons (electrons per cubic angstrom). $\sum_M$ signifies summation over the unit of composition in the liquid. The graph of $\sum_M K_m 4\pi R^2\rho_m(R)$ *vs.* R thus obtained is the result of a superposition of the electronic distribution curves about each atom of the composition, each curve multiplied by the effective number of electrons in the origin atom for that curve. Thus this curve is more difficult to interpret unambiguously than one obtained for liquids composed of one kind of atom.

The experimentally determined and fully corrected intensity curve was placed on an absolute basis by choosing a value of N so that $I=Nf^2$ (or, for the generalized method, $I=N\sum_M f_m^2$) out at some large angle where it is assumed that all interference effects have ceased. The Fourier integral appearing in these two equations was evaluated in two ways, one using graphical integration and the other using the method of trigonometric interpolation which is described elsewhere.[6]

The appearance of discrete peaks in the distribution curves is of significance. The area under the first peak of the $4\pi R^2\rho(R)$ curve gives directly the number of nearest neighbor atoms at this position for liquids of one kind of atom. Two methods suggest themselves for interpreting discrete peaks in the $4\pi R^2\sum_M K_m\rho_m(R)$ curve in terms of atomic distributions. The first is to calculate from the measured area of a peak the number of atoms of type j surrounding one atom of type i using the formula $n=\text{area}/2n_iK_iK_j$ where n_i is the number of atoms of type i in the smallest possible unit of composition. The other is the calculation from an assumed plausible structure of the area of the expected peak using the relation that the area is equal to $\sum_M K_m\sum_a K_j$ where $\sum_a K_a$ serves to add up all the electrons due to atoms at a distance R' (inside a shell with R' as average radius) from atom m and $\sum_M K_m$ serves to move the origin of the shell over all atoms of the composition. This last method was of special value in interpreting the results for nitrous oxide.

EXPERIMENTAL

The apparatus consisted primarily of the x-ray source, the system for recording the scattered x-ray intensity, and the cooling system for maintaining the liquid at a known temperature and pressure. Auxiliary apparatus also had to be provided for obtaining and purifying the substances to be studied. The source of radiation was a molybdenum target tube with the $K\alpha$ radiation

[5] B. E. Warren, H. Krutter, and O. Morningstar, J. Am. Ceramic Soc. **19**, 202 (1936).

[6] G. C. Danielson and C. Lanczos, J. Frank. Inst. **233**, 365, 435 (1942).

TABLE I.

	System	Pressure	Temp.	Cooling agent
N_2	Closed, photographic, counter	3.3 atmos.	89°K	Liquid air
N_2	Closed, photographic	3.3 "	64°K	Liquid air and pump
NO	Closed, photographic	2 "	125°K	Liquid methane (natural gas)
N_2O	Closed, photographic	3 "	196°K	Dry ice and ether
N_2O	Closed, photographic	3 "	173°K	Dry ice and ether and pump

being reflected from rocksalt. For the photographic work a General Electric CA-2 tube was used and with the Geiger-Mueller counter system,[7] used to obtain valuable supplementary data on liquid nitrogen, a demountable grid-controlled molybdenum target tube[8] was used.

Most of the work was done photographically with a specially designed[9] camera. A glass Dewar and sample holder 8 mm in diameter were sealed to the camera and the camera was evacuated. The x-rays monochromatized by the rocksalt crystal were collimated by two slits and the width of the incident beam at the sample was about 1.5 mm. The photographic film to record the intensity of the diffracted x-rays was placed around the outside of the cylindrical evacuated camera, the x-rays passing through a thin (0.004") aluminum window to reach the film. The radius of the camera was 9.53 cm. The "camera" used with Geiger counter detection for liquid nitrogen consisted of a metal Dewar with a sample chamber having flat beryllium windows.[10]

The cooling system used for the liquids reported on here used a closed sample system, as contrasted with the open system used on liquid oxygen.[11] The closed system has the great advantage that it doesn't require as large quantities of the substance to be studied as is true for the open system. Furthermore, the pressure on the gas being studied could be increased to produce liquefaction in some cases where the cooling agent used would not liquefy the gas at atmosphere pressure. The cooling agents used were liquid air, liquefied natural gas (high percentage methane) and dry ice. The liquid air and dry ice were used as the cooling agents for nitrogen and nitrous oxide, respectively. Nitric oxide was the most inconvenient of the gases to liquefy since it is a solid at liquid-air temperature and since its critical temperature is below the temperature of dry ice. Liquid methane has a boiling point which made it of value as a cooling agent and the natural gas available was a rather high percent methane so that it was used. A brass liquid-air container was supported in the reservoir of the glass Dewar to serve as a condenser for the natural gas which would fall to the bottom of the Dewar to boil and maintain a fairly constant temperature at the sample. (There was a gradual rise of this temperature due to fractional distillation as the liquefied natural gas boiled away.)

Table I summarizes the temperatures and cooling agents used for the various liquids studied. The temperatures listed for nitrogen and nitrous oxide are probably correct to within two degrees. The temperature for nitric oxide is only an average, the rise during an exposure being from 8° to 10°. A pump was used to reduce the pressure and hence lower the temperature in certain cases, as shown in Table I.

The nitrogen used was of two qualities, one the usual commercial product, and the other somewhat more pure (99.8%).* Commercial nitrogen was passed through sulfuric acid and phosphorous pentoxide in being admitted to the sample holder for the photographic method. The purer nitrogen was passed through a dry ice trap in admitting it to the sample holder for use with the Geiger counter system.

Nitric oxide was obtained from the reaction of sulfuric acid dropped into a dilute solution of sodium (or potassium) nitrite and potassium iodide.[12,13] The gas resulting from this reaction was condensed and frozen out in a liquid-air trap. But even with great care a large percent of impurities appeared with N_2O_5 and N_2O_4 being easily detected. The first purification step sought to eliminate most of the N_2O_5 and N_2O_4 by permitting a large portion of the liquid in the trap

[7] A. Eisenstein and N. S. Gingrich, Rev. Sci. Inst. **12**, 582 (1941).
[8] A. Eisenstein, Rev. Sci. Inst. **13**, 208 (1942).
[9] A. Eisenstein and N. S. Gingrich, Phys. Rev. **58**, 307 (1940).
[10] A. Eisenstein and N. S. Gingrich, Phys. Rev. **62**, 261 (1942).
[11] P. C. Sharrah and N. S. Gingrich, J. Chem. Phys. **10**, 504 (1942).

* Ohio Chemical Company, 1177 Marquette Street, N. E., Cleveland, Ohio.
[12] W. A. Noyes, J. Am. Chem. Soc. **47**, 2170 (1925).
[13] H. L. Johnston and W. F. Giauque, J. Am. Chem. Soc. **51**, 3194 (1929).

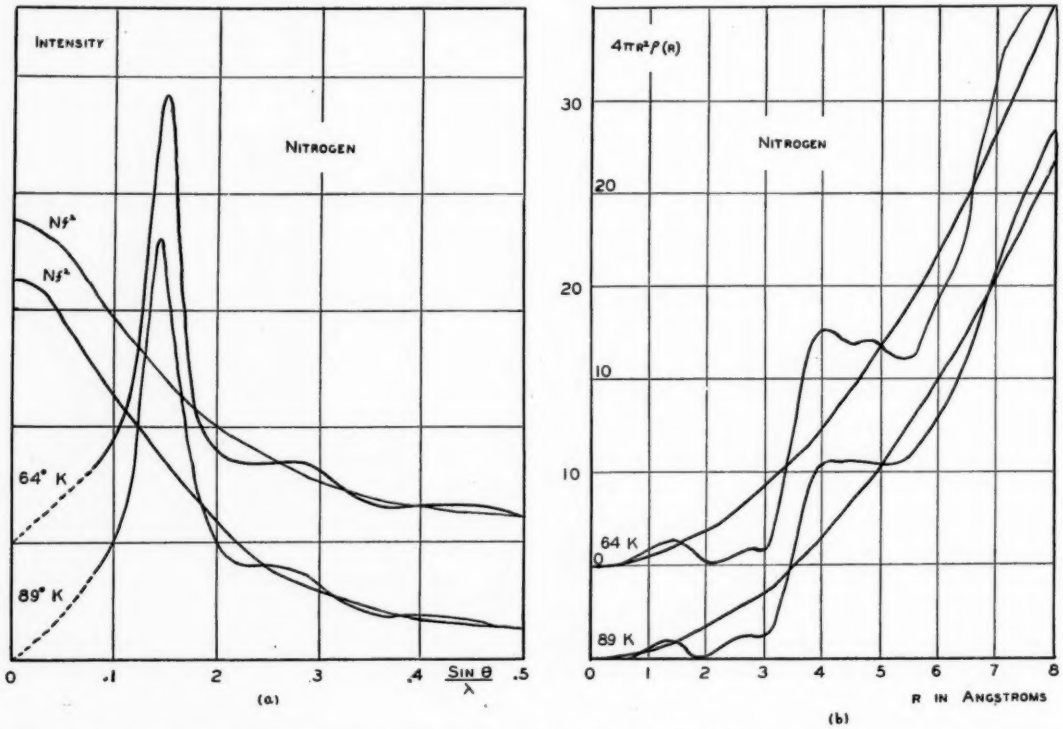

FIG. 1. (a) The x-ray diffraction patterns of liquid nitrogen at 89°K and at 64°K. (b) The atomic distribution curves for liquid nitrogen at 89°K and at 64°K.

to boil off and be condensed in a second liquid-air trap, the remaining liquid in the first trap being rich in these impurities which then were discharged from the system through a second tube with stopcock. The remaining amount of these two impurities was then further greatly reduced by boiling the liquid in one trap and freezing it out in the other liquid-air trap, thus driving it repeatedly back and forth through a potassium hydroxide wash and a dry ice trap placed between them. The purified nitric oxide was finally frozen out and held in reserve in one of the liquid-air traps from which it could be introduced directly into the closed sample holder where it would be maintained in the liquid state by the liquefied natural gas used as a cooling agent there.

Nitrous oxide (N_2O) of 99%* purity was passed through an ice and salt trap in which the temperature was around -10°C. This would tend to eliminate any traces of moisture, N_2O_3 and N_2O_4 which might be present.

Five pictures were taken of liquid nitrogen at 89°K and four at 64°K. Three pictures were taken of liquid nitric oxide in the neighborhood of 125°K. Pictures were taken of liquid nitrous oxide at both 196°K and 175°K, but the difference between the resulting patterns was so slight that the three pictures taken at the lower temperature were the only ones used in the analysis. A large number of patterns were determined for each substance because of the broad peaks or plateaus beyond the main peak, which were typical of all the liquids studied. These relatively small peaks are of importance in the analysis and thus had to be determined with considerable accuracy.

DISCUSSION OF RESULTS

Figures 1(a), 2(a), and 3(a) show the experimentally determined diffraction patterns fully corrected for absorption and polarization.[14] For the patterns obtained photographically, the absorption correction used was that for a cylindrical sample completely bathed in a parallel

* See asterisk footnote, p. 437.

[14] S. Katzoff, J. Chem. Phys. 2, 841 (1934).

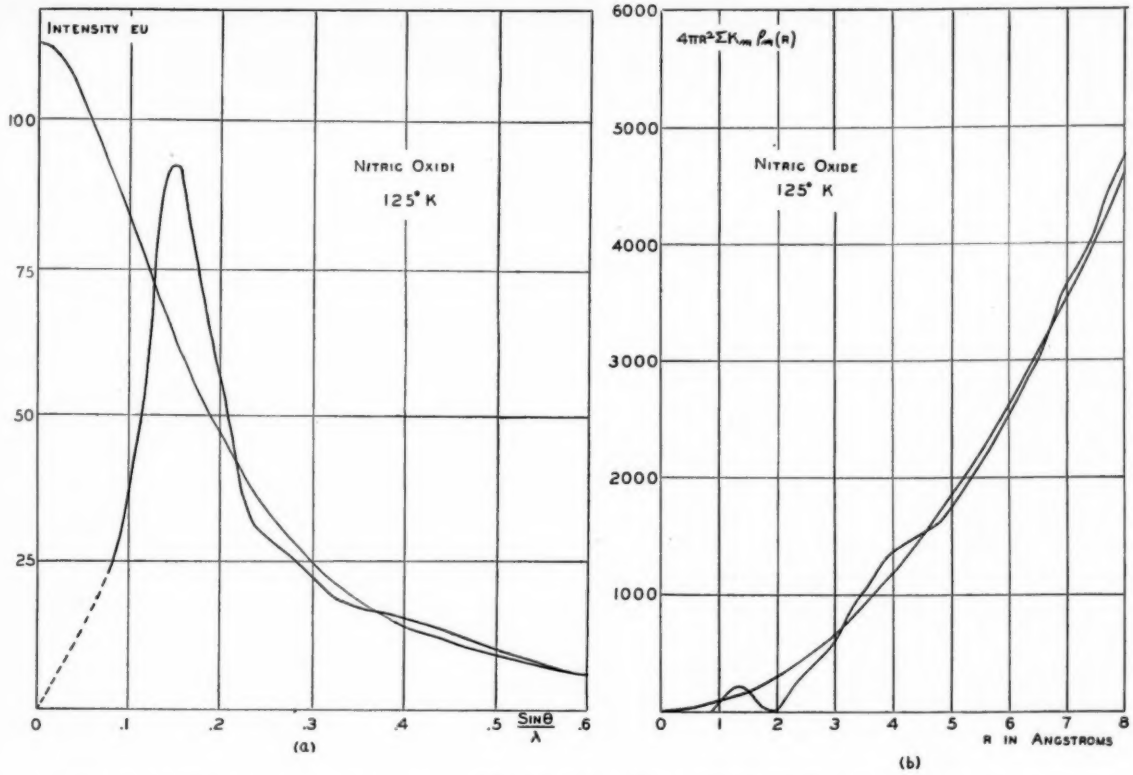

FIG. 2. (a) The x-ray diffraction pattern of liquid nitric oxide at 125°K. (b) The electronic distribution curve for liquid nitric oxide at 125°K.

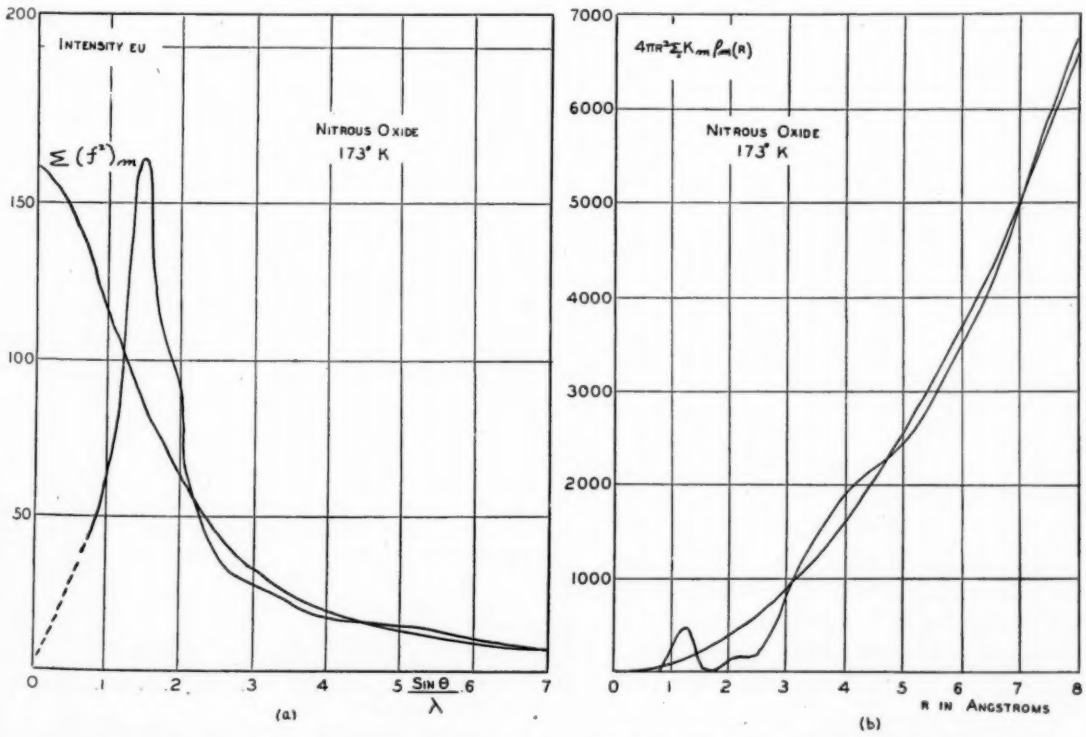

FIG. 3. (a) The x-ray diffraction pattern of liquid nitrous oxide at 173°K. (b) The electronic distribution curve for liquid nitrous oxide at 173°K.

TABLE II. Diffraction pattern peak positions in $\sin\theta/\lambda$.

Substance	First	Second	Third
Nitrogen*	0.139	0.208	
Nitrogen 89°K	.144	.26	0.42
Nitrogen 64°K	.148	.26	.42
Nitric oxide 125°K	.15	.26	.44
Nitrous oxide 173°K	.155	.30	.50

* See footnote 3, p. 435.

beam of x-rays, as discussed by Blake.[15] However, it has been shown[16] that for sodium, with cylindrical samples having diameters of from one to five times the width of the beam, there is little difference in the ratio of the intensity of scattering at the main peak to that at angles as large as were used here. The absorption correction applied to the patterns obtained for nitrogen using the Geiger-Mueller counter was for a flat sample. These curves are averages from several experimental patterns. Table II gives the position, in terms of $\sin\theta/\lambda$, of the intensity peaks (or plateaus). Values for nitrogen from the previous values of Keesom and de Smedt[3] are given for comparison. The weak plateau appearing at about $\sin\theta/\lambda=0.42$ in Fig. 1(a) was not reported by them. The position of the main peak and the existence of their second peak are open to question. It is believed that with the larger camera here used the present peak positions are likely to be more nearly correct.

Figures 1(b), 2(b), and 3(b) show the atomic and electronic distribution curves obtained from analyses of the intensity patterns. These curves are averages, more than one complete Fourier analysis having been carried through for each substance. In all the analyses carried out for a given substance, the final distribution curves were fairly reproducible up to nearly 6A, but beyond that distance the various analyses differed noticeably. The shape of the discrete peak obtained for all the liquids analyzed depended somewhat on the fitting, and hence its area was altered to some extent. A feature of all the distribution curves which persisted to a greater or lesser extent, depending on the fitting, but which never completely disappeared, is the rise immediately following the fall to zero of the distribution curve after the first peak. This rise leveled off in the case of nitrogen and nitrous oxide but did not resolve itself into a discrete peak.

The peak positions for the distribution curves are given in Table III.

Resolving the more distant aggregations into two peaks (third and fourth) for nitric oxide and nitrous oxide is somewhat artificial, but convenient for comparison with the graphs for nitrogen (and oxygen[11]). An interatomic distance of 1.095A has been reported elsewhere for the nitrogen molecule and 1.15A for the nitric oxide molecule.[17] Distances within the triatomic nitrous oxide molecule N—N—O have been reported as 1.15A, 1.23A, and 2.38A, respectively.[18] Recent values for these same distances in nitrous oxide, based on electron diffraction experiments, are 1.12A, 1.19A, and 2.31A, respectively.[19]

The area of the first peak of the distribution curve for liquid nitrogen at both 89° and 64°K is 1.03 atoms. The area of the first peak in the distribution curve for nitric oxide is 108.9 electrons[2] and for nitrous oxide 225.5 electrons.[2]

The area under the first peak for nitrogen is only slightly different from one, so that, within the experimental error, each atom in the liquid has one permanent nearest neighbor at the distance of the first peak, which is comparable to the interatomic distance found by other methods for the diatomic nitrogen molecule.

In order to interpret the meaning of the discrete peak for nitric oxide and nitrous oxide, the formula $n=\text{area}/2n_iK_iK_j$ may be used to calculate the number of nearest neighbors from the known area of the peak in electrons.[2] Applying this equation to nitric oxide and seeking to calculate the number of nitrogen atoms surrounding each oxygen atom, one has $n_i=n_O=1$. Further-

TABLE III. Atomic concentration positions in angstroms.

Substance	First	Second	Third	Fourth
Nitrogen 89°K	1.3	2.6	4.0	4.8
Nitrogen 64°K	1.3	2.6	4.0	4.8
Nitric oxide 125°K	1.3	(2.6)	3.4	4.0
Nitrous oxide 173°K	1.2	2.1	3.4	4.2

[15] F. C. Blake, Rev. Mod. Phys. **5**, 180 (1933).
[16] G. A. Mitchell, unpublished work.
[17] G. Herzberg, *Molecular Spectra and Molecular Structure* (Prentice-Hall, 1939) p. 491.
[18] W. G. Penney and G. B. B. M. Sutherland, Proc. Roy. Soc. London, **A156**, 672 (1936).
[19] Verner Shomaker and Robert Spurr, J. Am. Chem. Soc. **64**, 1184 (1942).

more, one assumes plausible values for the effective number of electrons per atom which may be taken as $K_i=K_O=8.3$ and $K_j=K_N=6.7$. Substitution gives $n=(108.9)/2(1)(8.3)(6.7)=0.978$, which is close to one which is the number of nitrogen atoms per oxygen atom, showing that, within the experimental error, nitric oxide shows a diatomic aggregation in the liquid state with the interatomic distance shown by the position of the first peak in the distribution curve.

Now applying the same equation to nitrous oxide to seek to determine the number of nitrogen atoms around one oxygen atom at the distance of the first peak, one has $n_i=n_O=1$, and using the approximate values for $K_i=K_O=8$ and $K_j=7$, one gets $n=225.5/2(1)(8)(7)=2.05\doteq 2$. This result is two, within the experimental error, and it suggests a triatomic unit in the liquid state, but the fact that the scattering from nitrogen and oxygen is comparable demands some further calculations. With no information about the structure assumed in other work for N_2O, one might reasonaly assume two structures; one an approximately equilateral triangular array of three atoms with the side of the triangle equal to the peak position on the distribution curve, and the other a linear array of three atoms in the molecule, with the short interatomic distances approximately the same and equal to the first peak position in the distribution. Assuming these two, the expected area of the first peak will be calculated according to the equation area$=\sum_M K_m \sum_a K_a$ and compared with the observed.

For the triangular array, using $Ko=8$ electrons and $K_N=7$ electrons, the area of the peak at $R'=1.2$A is $Ko(K_{N(1)}+K_{N(2)})+K_{N(1)}(Ko+K_{N(2)})+K_{N(2)}(Ko+K_{N(1)})=8(14)+7(15)+7(15)=322$ elect.$^2\neq 225.5$ elect.^{2}, and since the observed area was 225.5 elect.^{2}, the equilateral triangular array is rather definitely eliminated.

The area for the linear array $N_{(1)}-N_{(2)}-O$, using the same equation is $Ko(K_{N(2)})+K_{N(2)}(Ko+K_{N(1)})+K_{N(1)}(K_{N(2)})=8(7)+7(8+7)+(7)(7)=209$ elect.$^2\doteq 225.5$ elect.^{2}. Recalling that the peak areas are probably not known to better than 10 percent this makes the observed 225.5 elect.^{2} approach 209 elect.^{2} almost within the experimental error. The observed distribution curve is thus found to be consistent with the existence of the linear molecule N−N−O in the liquid state comparable to the linear molecule found in the gaseous state.[18] The present data alone, however, could not decide between N−N−O and N−O−N, the latter requiring an area of the first peak of 224 elect.^{2}, this being itself in favor of the latter. Now assuming the linear molecule to be correct, it is interesting to calculate the area of the peak which one would expect due to the large N−O distance (2.4A). Its area would be $K_NKo+KoK_N=2(7)(8)=112$ elect.^{2}. This peak is evidently masked by the interpenetration within this distance of the atoms of adjacent molecules in thermal motion.

ACKNOWLEDGMENTS

The author wishes to thank Professor N. S. Gingrich, under whose direction this problem was conceived and carried out, for the encouragement and assistance given and for making available certain apparatus and materials obtained through grants-in-aid-of-research made by the American Academy of Arts and Science, the American Association for the Advancement of Science, and the Elizabeth Thompson Science Fund.

THE JOURNAL OF CHEMICAL PHYSICS VOLUME 11, NUMBER 10 OCTOBER, 1943

The Magnetic Susceptibility of Oxygen and Nitric Oxide at Low Field Strengths

A. BURRIS* AND C. D. HAUSE
Michigan State College, East Lansing, Michigan

(Received April 5, 1943)

The Rankine magnetic balance has been used to determine the magnetic susceptibility of oxygen and nitric oxide at atmospheric pressure in a field of about 15 oersteds. The mass susceptibility of water at 20°C is assumed to be -0.7200×10^{-6}. The mean of ten separate measurements on oxygen gives $(106.3\pm0.2)\times10^{-6}$ for the mass susceptibility, with an average deviation from the mean of 0.9×10^{-6}. The value of $\chi_M T$ is 0.997 ± 0.002; the average deviation from the mean being 0.008. The mean of six separate measurements on nitric oxide gives 47.2×10^{-6} for the mass susceptibility, and 0.0590×10^{-6} for the volume susceptibility, with an average deviation from the mean of 0.6×10^{-6} and 0.0007×10^{-6}, respectively.

INTRODUCTION

IN 1934 Rankine[1] described a magnetic balance suitable for the comparison of feebly magnetic materials in extremely weak fields. He later constructed such a balance but it did not function with the high sensitivity anticipated, largely because of ferromagnetic impurities in some of the structural materials.[2] An improved form of the balance which functioned with the requisite sensitivity was first developed by Iskenderian,[3] who used it to determine the susceptibility of oxygen in a field of about 40 oersteds.[4] His measurements gave the value 0.979 for $\chi_M T$, which he interpreted as being in good agreement with the theoretical value[5] of 1.000,[6] considering that the gas used was tank oxygen which probably contained some diamagnetic impurities.

The present work was undertaken to obtain more precise measurements on oxygen and to obtain measurements on nitric oxide at low fields. Oxygen is of particular interest since the theoretical value of $\chi_M T$ can hardly be questioned, and is the value obtained by experiment, within 1 percent or so, at high field strengths. If, therefore, measurements relative to water were made at low fields and a close check with theory obtained, it would remove any doubts as to a discrepancy between the susceptibility of water in high and low fields and would furnish additional evidence of the fitness of the Rankine balance for magnetic measurements on gases.

Nitric oxide was chosen because the theoretical value of the susceptibility is known and no results on this gas at low fields have been reported. However, the mass susceptibility has been measured at high fields by several investigators with results as follows: 46.68×10^{-6} (Weiss and Piccard[7]); 48.7×10^{-6} (Bauer, Weiss, and Piccard[8]); 48.80×10^{-6} (Sone[9]). Van Vleck[10] has made a careful calculation of the volume susceptibility using data from the molecular spectrum of the molecule. The value[6] obtained at 20°C and 760-mm pressure is 0.0597×10^{-6}. The corresponding volume susceptibilities from the data of Bauer, Weiss, and Piccard and of Sone are 0.0609×10^{-6} and 0.0610×10^{-6}, respectively, or a little more than 2 percent above the theoretical value.

THE RANKINE BALANCE

The Rankine balance depends for its action upon the fact that when a test specimen is placed near a suspended magnet the magnet experiences a force arising from a distortion of its field by the specimen. This force is proportional to the susceptibility of the specimen, and is balanced by the application of a small non-uniform field over

* Now at Eastern New Mexico College, Portales, New Mexico.

[1] A. O. Rankine, Proc. Phys. Soc. **46**, 1 (1934).
[2] A. O. Rankine, Proc. Phys. Soc. **46**, 391 (1934).
[3] Haig P. Iskenderian, Phys. Rev. **51**, 1092 (1937).
[4] Haig P. Iskenderian, Phys. Rev. **52**, 1244 (1937).
[5] J. H. Van Vleck, *The Theory of Electric and Magnetic Susceptibilities* (Oxford University Press, London, 1932), p. 266.
[6] Calculated from Van Vleck's formula, using recent values of the physical constants. (See Raymond T. Birge, Rev. Mod. Phys. **13**, 233 (1941).)
[7] P. Weiss and A. Piccard, Comptes rendus **157**, 916 (1913).
[8] E. Bauer, P. Weiss, and A. Piccard, Comptes rendus **167**, 484 (1918).
[9] T. Sone, Sci. Rep. **11**, 139 (1922).
[10] J. H. Van Vleck, Phys. Rev. **31**, 587 (1928).

the magnet, produced by current in a nearby wire. From the magnitudes of the currents necessary to balance the forces arising from various test samples their relative susceptibilities can be deduced. The procedure in determining the magnetic susceptibility of a liquid or gas with this type of balance has been given elsewhere.[3]

Figure 1 is a schematic diagram of the balance used in the present work. The magnet *C* is of an alloy called Nipermag and was obtained from Cinaudagraph Corporation. The weight is 0.5 g and the pole strength about 10 e.m.u. The beam *F* is a very thin Duralumin strip about 6 cm long, to which is attached a counterweight *G* and a small plane electrometer mirror *E* for measuring the deflection. The torsion head *H* is of OFHC copper and is supported by a tripod made of Pyrex tubing. The base plate *A* is also of OFHC copper and is secured to a heavy hard wood board by means of four short OFHC copper legs. The lengths of the upper and lower quartz fibers are about 24 cm and 17 cm, respectively, and their torsion constants of the order of 10^{-4} and 10^{-6} dyne-cm per radian. The test cell *B* is of Pyrex and is approximately a cylinder about 4 cm in diameter and 1.5 cm long. The suspended system was enclosed in the heavy Pyrex cylinder *N*, provided with a plane glass window and a plate glass top which could be sealed on with soft wax.

Preliminary work indicated that radiation falling on the instrument apparently affected the suspension. To guard against this, a polished copper cylinder *M* was fitted inside the Pyrex cylinder and the upper fiber enclosed in the heavy-walled copper tube *K*. To avoid troublesome electrostatic effects, a thin copper box was placed over the test cell to shield it from the magnet. The cell-connecting tubes and filling arrangement, as well as the balance proper, were protected from temperature fluctuations by Celotex housings. Continuous circulation of air within the housings was necessary to avoid small temperature gradients which affected greatly the operation of the balance. The temperature of the room was kept constant to about 0.1°C. The motion of the suspended system was controlled from an adjoining room by varying the current in a straight wire beneath the base of the instrument. This control current was measured by means of a standard resistance and a L & N type *K* potentiometer.

As was expected, it was almost impossible to obtain any consistent readings during the day when the laboratory was in general use. Consequently, measurements were made late at night when conditions were best. During a run, which required about two hours, it was necessary to keep under strict control the motions of all laboratory apparatus containing iron. It was observed that the parking of cars in certain locations outside the building produced a noticeable deflection of the beam. Even alternating currents, under certain conditions, were observed to affect

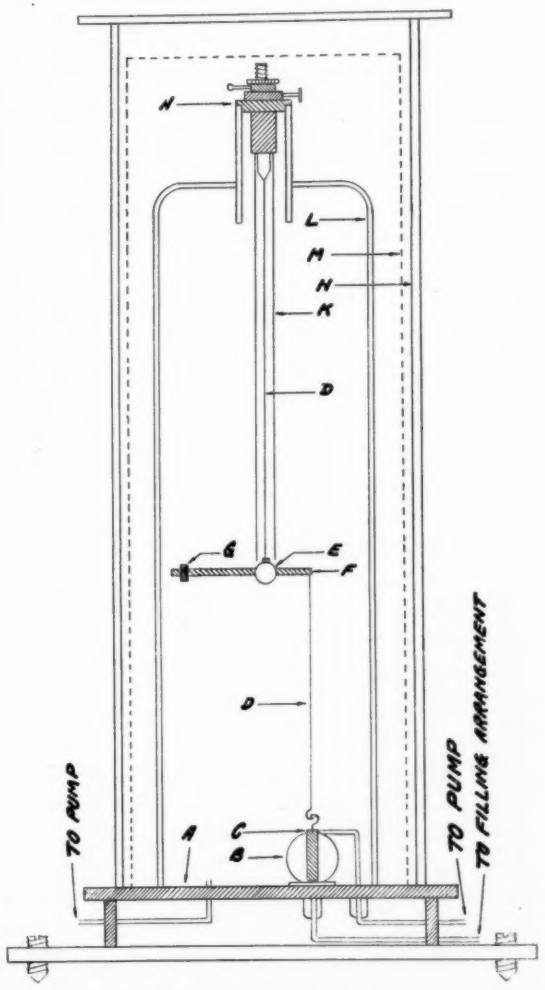

FIG. 1. Magnetic balance. *A*—OFHC copper base plate; *B*—test cell; *C*—magnet; *D*—quartz fibers; *E*—electrometer mirror; *F*—Duralumin beam; *G*—counterweight; *K*—copper tube; *H*—torsion head; *L*—Pyrex tripod; *M*—copper shield; *N*—Pyrex cylinder.

TABLE I. The magnetic susceptibility of oxygen at 20°C and 760-mm pressure.

Trial	$(\Delta i)_{O_2}\times10^7$	$(\Delta i)_W\times10^7$	$\kappa\times10^6$	$\chi\times10^6$	$\chi_M T$
1	1893	9959	0.1407	105.7	0.992
2	1907	9830	0.1429	107.3	1.007
3	1909	9830	0.1437	107.9	1.012
4	1857	9821	0.1395	104.8	0.983
5	1878	9866	0.1407	105.9	0.994
6	1890	9867	0.1420	106.6	1.000
7	1887	9867	0.1418	106.5	0.999
8	1876	9897	0.1409	105.8	0.993
9*	1857	9892	0.1389	104.3	0.979
10*	1860	9943	0.1382	103.8	0.974
11*	1840	9826	0.1384	104.0	0.976
12	1893	9779	0.1430	107.4	1.008
13	1863	9829	0.1397	104.9	0.984
Mean values			0.1415	106.3	0.997
Av. deviation from mean			0.0012	0.9	0.008
Probable error in mean			0.0003	0.2	0.002

* Deleted from the final calculations.

the balance. However, only a very few trials were vitiated by such disturbances when measurements were made late at night.

OXYGEN

Oxygen was prepared by electrolysis of water acidulated with sulfuric acid. After leaving the generating apparatus the gas was bubbled through distilled water, then passed through a tube containing copper oxide heated to 400°–500°C. After passing through tubes containing calcium chloride and phosphorus pentoxide, the gas was collected in a 500-ml bulb, from which it could be led directly into the test cell by turning a stopcock.

Table I shows the results of thirteen consecutive measurements on oxygen. In this table $(\Delta i)_{O_2}$ is the difference between the control currents, in amperes, with oxygen in the test cell and with the cell evacuated. $(\Delta i)_W$ is the corresponding quantity for water. The last three columns in the table give, respectively, the volume susceptibility, the mass susceptibility, and the product of the molar susceptibility by the absolute temperature. Those trials marked with an asterisk have been deleted in calculating the mean values and probable error. There was reason to believe that the gas had become contaminated when these measurements were made. Before making the next run (No. 12) the entire system was pumped out and refilled.

NITRIC OXIDE

Nitric oxide was prepared by the reduction of nitrous acid by mercury.[11] The mixture used was a 20 percent sulfuric acid solution containing 2 percent by weight of sodium nitrite, with enough mercury to provide the necessary surface for a reasonable rate of evolution of the gas. After leaving the generating flask, the gas was bubbled through mercury to remove nitrogen dioxide and some of the higher oxides probably present, and to prevent too violent a reaction by maintaining some pressure on the reacting solution. The gas was dried by passing over phosphorus pentoxide.

Analysis of the gas was carried out by absorbing the nitric oxide and measuring the volume of the residual gas. Two different absorbing solutions were used; the first a saturated solution of sodium sulphite,[12] made slightly alkaline with potassium hydroxide, and the second a saturated solution of potassium dichromate,[13] mixed with one-fifth its volume of concentrated sulfuric acid. The average purity of the gas as indicated by this method of analysis was 99 percent nitric oxide by volume, with very little variation.

The correction to the observed value of χ was made assuming the additivity law and also that the residual gas was entirely nitrogen. This latter assumption is supported by the work of Moser,[14] Weiss and Piccard,[7] and Sone.[9] The value of χ at 20°C was calculated assuming Curie's law.

Table II shows the results of seven consecutive measurements on nitric oxide. The symbols, here applied to nitric oxide, have the same significance

TABLE II. The magnetic susceptibility of nitric oxide at 20°C and 760-mm pressure.

Trial	$(\Delta i)_{NO}\times10^7$	$(\Delta i)_W\times10^7$	$\chi\times10^6$	$\kappa\times10^6$
1	756	9796	46.5	0.0581
2*	699	9740	43.2	0.0540
3	789	9740	48.5	0.0606
4	757	9534	47.4	0.0592
5	742	9538	46.4	0.0580
6	763	9580	47.6	0.0594
7	748	9551	47.0	0.0587
Mean values			47.2	0.0590
Average deviation from mean			0.6	0.0007

* Deleted from the final calculations.

[11] F. Emich, Monatsh. f. Chemie **13**, 73 (1892).
[12] E. Divers, J. Chem. Soc. **75**, 82 (1899).
[13] G. von Knorre, Die Chem. Ind. p. 531 (1902).
[14] L. Moser, Zeits. f. anal. Chemie **50**, 401 (1911).

as those of Table I. Trial No. 2 is definitely out of line with the other values and has been deleted in calculating the mean and average deviation from the mean.

DISCUSSION OF RESULTS

The performance of the Rankine balance in this experiment has been found thoroughly satisfactory, with the precision in a single determination limited largely by accidental disturbances which could not be controlled. The data show that the effect of these disturbances is an entirely random one, with the maximum deviation of any one measurement from the mean of less than 2 percent and an average deviation of less than 1 percent in the case of oxygen. The corresponding figures for nitric oxide are only slightly higher. It is felt that considerable significance may, therefore, be attached to the mean values. These values are, in the authors' opinion, about as precise as can be obtained with the balance in its present form under ordinary laboratory conditions.

Measurements on electrolytic oxygen give a mean value of 0.997 for $\chi_M T$, which is in excellent agreement with the theoretical value of 1.000. The agreement with the results obtained by other methods using high field strengths is also good. The average of the results of seven other investigations,[15] using different methods, is 0.990, with a maximum deviation from the mean of about 3 percent.

In view of the results on oxygen, it is difficult to reconcile, on the basis of experimental error, the 3 percent difference between the value obtained here and that obtained by Sone for nitric oxide. The highest single value obtained in the present work is a little more than 0.5 percent below that given by him.

An important factor which enters into measurements on nitric oxide is the question of the purity of the gas. Most measurements have been made on the more or less impure gas and the observed value of the susceptibility corrected for the impurities. In the present analysis the two different absorbing solutions gave results in agreement to 0.2 percent. Since it is usually agreed that absorption methods are reliable, especially when used on a gas of high purity, it is probable that the 99 percent purity stated is very close to the correct value. It therefore seems improbable that a more accurate analysis would change the susceptibility by more than a fraction of 1 percent. The gas used by Sone was 95 percent nitric oxide by volume. He states: ". . . thus the correction for the susceptibility due to nitrogen was about 3 percent." According to the authors' calculations, the correction would be nearer 5 than 3 percent. However, this would result in an even greater discrepancy between the two values.

It will also be noted that the volume susceptibility obtained here is about 1.2 percent below the theoretical value. Van Vleck[10] points out in his paper that x in his equation $x=h\Delta\nu/3kT$, might be about 5 percent larger, due to the fact that the value of B is different in the two-component normal states of the molecule. He states that by a crude estimate this would affect the susceptibility by about 1 percent. It is apparent from his final equation that an increase in x lowers the susceptibility. Hence, it is possible that his value 0.0597×10^{-6} may be as much as 1 percent too high. This would bring the value 0.0590×10^{-6} into excellent agreement with the theoretical value, while it would appear that 0.0610×10^{-6}, obtained by Sone, is too high.

[15] E. C. Stoner, *Magnetism and Matter* (Methuen and Company, London, 1934), p. 342.

THE JOURNAL OF CHEMICAL PHYSICS VOLUME 11, NUMBER 10 OCTOBER, 1943

Depolarization Studies of Raman Lines. A Simplified Method*

GEORGE GLOCKLER AND HAROLD T. BAKER†
The State University of Iowa, Iowa City, Iowa

(Received July 20, 1943)

A simplified method for the determination of the depolarization factor of Raman lines is reported which requires only *one* exposure and is, therefore, independent of fluctuation of arc current and any other factors influencing the intensity of Raman lines. Two Polaroid films are placed at the front of the slit of the spectrograph, one above the other. The electric vectors of the radiation are at right angles to one another. Between the Polaroid films and the slit are introduced two half-wave mica plates (one above the other) which orient the electric vectors of the light so that they are both vibrating in the same direction upon striking the prism faces. Thus differential reflection at these faces is eliminated. The method was checked with carbon tetrachloride.

INTRODUCTION

SINCE the discovery of the Raman effect, workers in this field have been interested in the determination of the factor of depolarization for the Raman lines of the liquids they have studied. This information is necessary to a better understanding of the type of vibration or rotation involved. Cabannes and his co-workers[1] were among the first to devise an accurate method for this type of measurement. The diffuse radiation was broken up into its two components by means of a double-image prism and then depolarized by means of a suitably orientated crystal. The two components were then focused one above the other on the slit of the spectrograph. Trumpy[2] and Rao[3] also made use of the double-image prism. Reitz[4] carried out a very intensive study of the method. Both Cabannes and Reitz made use of the calcite combination of Hanle.[5] Gupta[6] developed a unique arrangement. A double-image prism was used in such a way that the entering light was vibrating at an angle of 45° from the principal plane. It would leave the crystal vibrating in the same way, but the separation of the two components is in the vertical plane or in the direction of the length of the slit. Thus the differential reflection of the prism was greatly reduced. Langseth *et al.*[7] used a Wollaston prism behind the slit of the spectrograph in the collimator tube. This arrangement resulted in a displacement of one of the components so that they were recorded in different positions on the plate. Bhagavantam[8] interposed a Nicol between the Raman tube and the slit of the spectrograph. Two spectrograms were taken on the same plate with the vibration direction of the Nicol parallel to the track of the light in the liquid and the other perpendicular, the conditions of illumination being identical in both cases. Corrections were introduced for the differential reflections at the prism faces. Cleveland and Murray[9] used a fixed film of Polaroid between the slit and the Raman tube. The position of the arcs was changed by 90° in two exposures. The tube containing the filter solution acted as a lens causing the light from the arc to converge onto the Raman tube. Edsall and Wilson[10] also employed the tube of filter solution as a lens. They used plane-polarized light, obtained with a Polaroid film, as the primary source of light in the first exposure and unpolarized light in the second exposure. The

* We gratefully acknowledge a fellowship in chemistry from the Allied Chemical and Dye Corporation of which Mr. Harold T. Baker was the recipient for the year 1942–1943.

† Submitted by Harold T. Baker to the Graduate College of the State University of Iowa, in partial fulfillment of the requirements for the degree of Doctor of Philosophy, July, 1943.

[1] J. Cabannes and co-workers, Ann. de Phys. [X] **19**, 229 (1933).
[2] B. Trumpy, Zeits. f. Physik **88**, 226 (1934).
[3] A. V. Rao, Proc. Ind. Acad. Sci. **2A**, 49 (1935).
[4] A. W. Reitz, Zeits. f. physik. Chemie **B33**, 368 (1936).
[5] W. Hanle, Ann. d. Physik **11**, 885 (1931).
[6] J. Gupta, Ind. J. Phys. **10**, 313 (1936).
[7] A. Langseth, J. U. Sorensen, and J. R. Nielsen, J. Chem. Phys. **2**, 407 (1934).
[8] S. Bhagavantam, Ind. J. Phys. **5**, 60 (1930); **7**, 79 (1932).
[9] F. F. Cleveland and M. J. Murray, J. Chem. Phys. **7**, 396 (1939).
[10] J. T. Edsall and E. B. Wilson, Jr., J. Chem. Phys. **6**, 124 (1938).

intensity of the unpolarized light was reduced so as to obtain equal densities for lines having a depolarization factor of 6/7. Stitt and Yost[11] introduced a half-wave mica plate before the Nicol prism. In the first exposure the diffuse rays passed through the mica plate vibrating in the same direction as upon entering and in the second exposure, the mica plate was so orientated that the rays were rotated through 90° upon leaving the crystal. Some of the methods recorded above involve one exposure only, which, however, is of great length and they are not simple in execution, while others having features of simplicity require two exposures. It was desirable to devise a method which would feature both of these *desiderata*. The use of a Polaroid film[10] and a mica half-wave plate[11] are most convenient and both are used in the method described below. However, the particular arrangement developed here allows one to obtain results with one exposure only.

Two separate experiments are obviously undesirable because all the experimental conditions for the two runs must be kept constant. The light fluctuations, change in the liquid (decomposition), temperature, humidity conditions, etc., cannot be easily controlled. With a single exposure, however, these conditions may vary without affecting the results.

METHOD

An attempt has been made to develop a method that would not demand any elaborate equipment and would, at the same time, satisfy most of the requirements necessary to give a fairly accurate quantitative measurement of the depolarization factor. For the determination of this factor, the following simple method was employed. Two pieces of Polaroid were cut in such a way that one of them permitted light vibrating vertically and the other one allowed radiation vibrating horizontally to pass. The first piece was placed above the other one in front of the slit. Between each Polaroid film and the slit was placed a half-wave-length mica plate. One of these mica plates allows the light to pass through unchanged in its direction of vibration. The other one causes the light vector to be rotated through 90°. In the latter case, the mica half-wave plate was so orientated that it separated the polarized light passing through into its two components, one of which was retarded a half-wave-length with respect to the other. When these two waves leave the mica, they recombine in a wave that is plane polarized, but whose direction of vibration is at an angle of 90° from its original direction. The arrangement is shown diagrammatically in Fig. 1.

The two components are measured *simultaneously* and are found on the plate, the one above the other. The Polaroid films and mica plates are mounted in a special metal slide that can be pushed into place in the front of the slit of the spectrograph. This equipment is used only for depolarization measurements and is removed for regular Raman runs.

With many compounds, the time of exposure for ordinary Raman work may take as long as twenty or more hours. When the ideal arrangement of Cabannes[1] and Reitz[4] is used for determination of the depolarization factor, the intensity of the light becomes many times less and so almost prohibitive lengths of exposure are necessary. To get around this difficulty, Placzek and Van Wijk,[12] Ornstein and Stoutenbeck,[13]

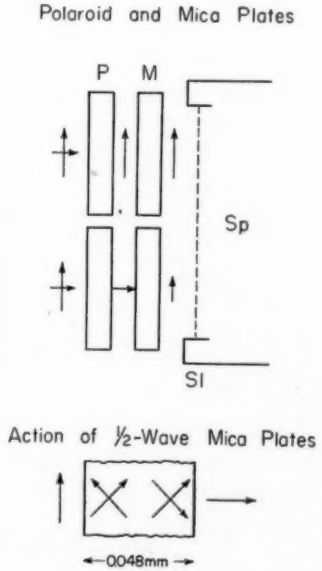

FIG. 1. P = Polaroid films, M = mica half-wave plates, Sl = slit, Sp = spectrograph. Arrows indicate electric vector. Dotted line indicates height of slit. Thickness of mica plate is 0.048 mm.

[11] F. Stitt and D. M. Yost, J. Chem. Phys. **5**, 90 (1937).

[12] G. Placzek and W. Van Wijk, Zeits. f. Physik **67**, 582 (1931).

[13] L. Ornstein and P. Stoutenbeck, Zeits. f. Physik **85**, 754 (1933).

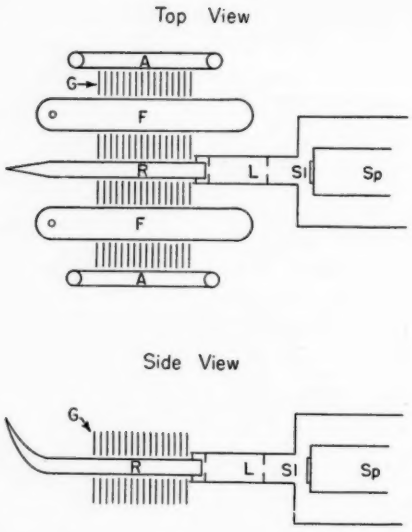

FIG. 2. Raman apparatus. A = arcs, F = filters, R = Raman tube, Sl = slit (carrying Polaroid films and mica plates), L = lens, G = grid, Sp = spectrograph. Side view = longitudinal cut through the axis of the Raman tube.

and Nijveld and Gerding,[14] have employed Wood's arrangement in order to obtain greater light intensity. Use was made of liquids whose depolarization factor (ρ) was known by the ideal method. The values obtained by this method were plotted against those obtained with Wood's arrangement. Since highly polarized lines have a depolarization factor of about 0.4 when this method is used, and lines that are somewhat less polarized give almost identical results, it is nearly impossible to differentiate very accurately between lines with $\rho=0.05$ and $\rho=0.30$. Lines that are near 6/7 in value can be determined accurately because they are almost completely depolarized, and so the orthogonality of the system is not such a crucial factor.

If an arrangement were used somewhere between the ideal and the conventional Raman set-up, then it should be possible to obtain values lower than 0.4 and thus be able to differentiate better between highly polarized and moderately polarized lines. The experimental arrangement here described is an attempt in this direction.

RAMAN EQUIPMENT

The general features of the apparatus used are shown in Fig. 2. The placement of the Raman tube, filter solutions, and arcs is similar to that described by Cleveland and Murray.[9] The two arcs, the two filter tubes, and the Raman tube lie in a horizontal plane—all being parallel to one another. It was found convenient to build a completely adjustable metal frame to hold the Raman tube, filter solutions, arcs, and grid. The exciting radiation from the arcs passes through a grid of blackened tin strips which keeps the light nearly perpendicular to the Raman tube. Two elliptical, polished metal pieces were placed behind the arcs in order to increase the intensity of the light. The metal framework and equipment were mounted on a platform, which moved on a track, making it easy to push the equipment up to the spectrograph. The outside diameter of the arcs and Raman tube was 15 mm and that of the filter tubes was 21 mm. The distance from the center of the Raman tube to the center of a filter tube was 33 mm and the distance from the center of the filter tube to the center of an arc was 35 mm. The front plate of the Raman tube and the slit of the spectrograph were about 17 to 18 cm apart, and in this region was placed a lens of focal length 4 to 4.5 cm, which converged the scattered light onto the slit. The ratio of image size to object size was approximately 1 : 1.

The support of the arcs, filters, Raman tube, and grids consisted of a rectangular metal frame. Two pieces of steel ($1''\times\frac{1}{8}''\times41''$) were each bent twice at right angles to form open end rectangles of sides 14, 13, and 14″, respectively. These two open rectangles were placed one above the other with a $\frac{3}{16}''$ opening between them. A piece ($2\frac{3}{16}''\times\frac{1}{8}''\times13''$) was welded onto the open ends of these rectangles. The other two corners were made rigid by welding on two small rectangular strips ($2\frac{3}{16}''\times\frac{1}{8}''\times\frac{1}{2}''$). This unit gave a framework with slots on three sides permitting the sliding of the equipment. A sliding center piece was made by taking two pieces ($1''\times\frac{1}{8}''\times17''$) and bending each of them at right angles (both bends inward) at a distance of $2\frac{1}{8}''$ from each end. These pieces were placed one above the other and spaced $\frac{3}{16}''$ apart, and welded together with two strips ($\frac{3}{16}''\times\frac{1}{8}''\times\frac{1}{2}''$). This section can slide in the slots of the frame perpendicularly to the 14″ sides and parallel to the 13″ sides.

Into another piece ($\frac{1}{4}''\times1''\times4\frac{3}{16}''$) two $\frac{3}{16}''$ holes and $\frac{1}{2}''$ hole were drilled. The half-inch hole is located $\frac{1}{2}''$ from one end and the other smaller holes are needed to attach the piece to the middle of the solid 13″ side of the frame. A metal rod (10″ long and $\frac{1}{2}''$ in diameter) is fitted into the hole just described and soldered or welded in place. This unit is the support for the back half of the framework. The front end is arranged similarly, except that a suitably sized metal tube is attached to a metal plate. When the frame is

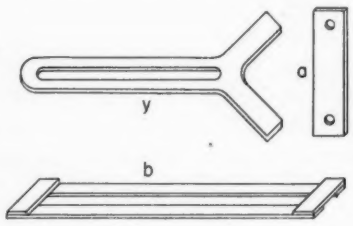

FIG. 3. Raman assembly. y = tube and filter support; a, b = blackened grid pieces.

[14] W. J. Nijveld and H. Gerding, Rec. trav. chim. 59, 1198 (1940).

fixed onto the platform it can be rotated about the axis of the Raman tube. The 14″ sides are parallel to the Raman tube axis.

To support the Raman tube, arcs, and filter tubes, adjustable metal supports move in the slots of the 13″ front piece and the 13″ movable piece. These supports are elongated Y's as shown in Fig. 3. A bolt with a wing nut holds the support to the frame. It can be raised and lowered or moved sideways. Thus any desired spacing of the Raman tube, arcs, and filter tubes can be secured. The grid of metal strips which gives the exciting light a direction perpendicular to the Raman tube was also made adjustable, so that changes in dimensions could be obtained when reassembling the grid. Two types of pieces as shown in Fig. 3 are the main parts. Blackened washers serve as spacers. The "a" metal pieces ($3\frac{1}{2}''\times\frac{1}{2}''$ or $3\frac{1}{2}''\times\frac{3}{8}''$) form the light grid and are made of thin tin sheet. The "b" pieces ($\frac{7}{8}''\times 8''$) are of heavier metal and thus give it more rigidity. They are made by taking two metal strips and soldering a small metal piece across each end. In order to assemble the grid, four long bolts ($\frac{1}{8}''$ diameter) are passed through each of two "b" pieces. The "a" pieces are then placed perpendicularly onto the "b" pieces, while the washers serve as spacers. Two "b" are necessary for every four "a" pieces. This arrangement is repeated until the desired width is obtained. Different sizes can be made to suit other purposes.

SPECIAL ITEMS

Two useful techniques in connection with Raman work which have been found very useful are ultrafiltration and the employment of a Tyndall beam in order to test for optical clearness. Solutions of salts cannot be purified by distillation and so filtration must be resorted to. Since ordinary filter paper will not remove much colloidal matter, ultra-filtration was employed to great advantage as described by Holmes.[15] The Tyndall beam is secured by focusing the light from a carbon arc into a narrow beam. The Raman tube is then held in this beam and observed at right angles. If colloidal matter is present in only small amount, the beam can scarcely be seen as it passes through the liquid. Distilled water is a good reference standard.

TABLE I. Depolarization factors (ρ) of carbon tetrachloride.

Raman line (cm^{-1})	Run I	Run II	Run III	Average	Accepted values Ref. (17)
218	0.80	0.83	0.82	0.82	0.857
314	.81	.85	.84	.83	.857
459	.07	.06	.09	.08	.05
762, 790	.82	.79	.80	.80	.79

[15] H. N. Holmes, *Manual of Colloid Chemistry* (John Wiley and Sons, New York, 1934) third edition, pp. 28–30.

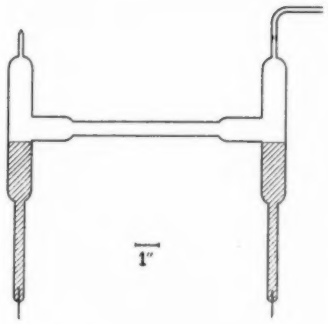

FIG. 4. Pyrex mercury arc.

After a number of trials, a very satisfactory design for a mercury arc was evolved and used for the polarization measurements. The glow discharge tubes containing neon and mercury,[16] while found very satisfactory for the measurement of Raman lines, did not furnish enough radiation when their illumination was cut down by the grid. The exposure times became quite prohibitive in length. For this reason, a change was made to a very satisfactory design of a Pyrex mercury arc. When such an arc operates at moderately cool temperature, very little continuous background is found on the photographic plates. Low temperature operation is, therefore, an important fact to consider in their construction. Arcs having large heat capacity are able to dissipate energy more readily than those of smaller size. A large mercury reservoir for each of the two electrodes will accomplish this purpose. The arcs are built in the shape of the letter "H" as shown in Fig. 4. The cross bar (15 mm Pyrex tubing) serves as the source of illumination. When these arcs are cooled by a breeze from fans and from compressed air jets, very efficient light sources are obtained.

RESULTS

When the depolarization factor was measured with the described arrangement, set to give the best possible orthogonality and the least possible convergence error, the results obtained for carbon tetrachloride were in good agreement with the accepted values[17] as shown in Table I.

It appears that the method is sufficiently accurate for all ordinary purposes of Raman spectroscopy. The relative ease of operation and the speed of execution commend it to the investigator of Raman spectra.

[16] G. Glockler and C. E. Morrell, J. Chem. Phys. **4**, 15 (1936).

[17] F. F. Cleveland and J. M. Murray, Res. Pub. Illinois Inst. Tech. **2**, 1 (1941).

Raman Spectra of Acetylenes. VII. Symmetrical-Top Acetylenes*

FORREST F. CLEVELAND, *Department of Physics*
AND
M. J. MURRAY, *Department of Chemistry*
Illinois Institute of Technology, Chicago, Illinois

(Received July 22, 1943)

Raman frequencies, relative intensities, and depolarization factors are listed for 1-iodo-1-propyne, 1-bromo-1-propyne, 1-chloro-1-propyne, and 3,3-dimethyl-1-butyne. The relative intensities and depolarization factors were obtained by use of a Gaertner microdensitometer. Assignments of the frequencies to the different vibration types and calculated values of the heat capacities for the ideal gaseous state at 1 atmos. pressure are given for 1-iodo-1-propyne and 1-bromo-1-propyne. Examination of the results in the 2200-cm^{-1} region leads to the suggestion that the resonance splitting of the triple bond fundamental for disubstituted acetylenes may frequently be due to the combination frequencies (2900−700) and (1375+700); and that the doubling of the 2100-cm^{-1} fundamental for the monosubstituted acetylenes, 3-methyl-1-butyn-3-ol and 3,3-dimethyl-1-butyne, may be due to the second overtones of the highly polarized, "breathing" frequencies near 700 cm^{-1} of the groups 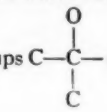 and 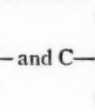 , respectively.

INTRODUCTION

DISUBSTITUTED acetylenes almost invariably have two or more lines near 2200-cm^{-1}, rather than the expected single line corresponding to the triple bond carbon vibration frequency. Badger[1] has suggested that the multiplicity is caused by a Fermi resonance interaction of the acetylenic fundamental with an overtone. However, not a great deal of success has accompanied attempts to point out which vibrations are involved in the interaction. Crawford[2] in his study of dimethylacetylene ascribed the doubling to the first overtone of the infra-red active fundamental at 1126 cm^{-1}. Murray and Cleveland[3] by use of both Raman and infra-red data for methylphenylacetylene found it necessary to assume a rather large anharmonicity to account for the phenomenon.

The splitting of the 2200-cm^{-1} fundamental is so general for disubstituted acetylenes that the fundamental or fundamentals involved must occur consistently in a wide variety of these compounds at approximately the same frequency. The carbon-hydrogen frequencies[4] near 1375 and 2920 cm^{-1} and probably also the carbon stretching frequency near 700 cm^{-1} satisfy this condition reasonably well. The (1375+700) combination frequency falls near the 2200-cm^{-1} fundamental but the difference tone (2920−700) comes even nearer to coincidence. A number of acetylenes for which spectra have been reported show a line near 700 cm^{-1}, but it is missing in others. In the authors' own work, for example, this line is not found in those cases for which the spectra as a whole are easily obtainable with short exposures. The weakness of the line corresponding to the 700-cm^{-1} fundamental does not, however, necessarily preclude its interaction with the 2920-cm^{-1} fundamental to give the resonance effect with the 2200-cm^{-1} acetylenic frequency.

Since rather simple symmetrical-top molecules are possible in the disubstituted acetylenes and since all of the fundamentals for molecules of this symmetry are permitted in the Raman spectra by the selection rules, it was hoped that compounds of this type would aid in solving the problem. The molecules selected were methyl-

* Presented at the American Physical Society meeting, Columbia University, January 1943; Phys. Rev. **63**, 220 (1943).

[1] R. M. Badger, J. Chem. Phys. **5**, 178 (1937).

[2] B. L. Crawford, Jr., J. Chem. Phys. **7**, 555 (1939).

[3] M. J. Murray and Forrest F. Cleveland, J. Chem. Phys. **8**, 133 (1940).

[4] It was suggested to the authors, see J. Am. Chem. Soc. **62**, 3185 (1940), that hydrogen atoms on adjacent carbons might in some way be responsible for the doubling.

iodoacetylene (1-iodo-1-propyne) and methylbromoacetylene (1-bromo-1-propyne). The spectrum of *t*-butylacetylene (3,3-dimethyl-1-butyne) was also obtained since it had been observed[5] that a *monosubstituted* acetylene, dimethylethynyl carbinol (3-methyl-1-butyn-3-ol), with the group 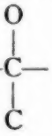 adjacent to the triple bond gave a double line, 2089 and 2112 cm^{-1}. It was expected that *t*-butylacetylene would show a similar doubling, which indeed it did, although the intensity order of the lines differs in the two compounds.

EXPERIMENTAL

The spectrograms used in obtaining the frequencies and the polarization spectrograms were made with the technique and apparatus described in previous papers from this laboratory.[6] The spectrograms were obtained with the samples in the liquid state and excitation was by Hg 4358A. The intensities were determined by use of a Gaertner microdensitometer. This instrument was calibrated for the Agfa Superplenachrome Press film by replacing the Raman tube by a white cardboard diffuser and varying the distance of an auto-lamp from the cardboard in order to get known relative intensities of illumination. One-hour exposures were made for each position of the lamp. A calibration curve was then made by plotting the densities, at a wavelength corresponding to $\Delta\nu \sim 1400$ cm^{-1}, against the relative intensities.

The inverse square law method, described above, was subsequently checked by a method involving the use of crossed Nicol prisms. Finally, the calibration curve was checked, with satisfactory results, by obtaining Raman spectrograms of various known mixtures of ethyl bromide and carbon tetrachloride.

The relative intensities are only semi-quantitative since no correction was made for variation of the sensitivity of the Agfa film with wave-length. This correction was, of course, not necessary for the depolarization factors.

The methylacetylene used for the preparation of the halogen derivatives was made by the method of Heisig and Davis[7] using propylene bromide with potassium hydroxide in *n*-butyl alcohol. The methylacetylene was liquefied in a dry-ice trap. Excellent yields were obtained. An outline of the method of preparation of the other compounds follows:

1-Iodo-1-propyne,

$CH_3C{\equiv}CI$, C_3H_3I: Two-fifths mole of magnesium was converted into Grignard reagent, using ethyl bromide in ethyl ether. The flask containing the Grignard reagent was provided with stirrer, a dry-ice cooled reflux condenser, and a tube through which a slight excess of methylacetylene was introduced. After evolution of ethane ceased, a saturated solution of iodine in dry ether[8] was added, with stirring, until a slight color remained. Water was added, the ether layer separated, and the methyliodoacetylene purified by distillation through a Podbielniak-type column. B. p. 109–110°C. The compound is colorless when freshly distilled, but turns slightly yellow upon standing. It is much more stable to air than is the corresponding bromo derivative.

1-Bromo-1-propyne,

$CH_3C{\equiv}CBr$, C_3H_3Br: This compound was synthesized by a modification of the method which Straus, Kollek, and Heyn[9] used for the preparation of several other bromoacetylenes. Potassium hypobromite was prepared by addition of 35 cm^3 of bromine to 150 g of potassium hydroxide in one liter of water at 0°C. Through this solution (in two flasks, in series) was bubbled the methylacetylene obtained from 150 g of propylene dibromide. Considerable methylbromoacetylene formed in the flask was swept over by unreacted methylacetylene. Part of the product was caught in a tube cooled by ice water; the remainder and somewhat more than half of the methylacetylene were received in a dry-ice trap. The recovered methylacetylene was again passed through the hypobromite solution and the process repeated until almost all had reacted. The lower layer from the hypobromite and the condensate in the traps were combined and distilled in an atmosphere of nitrogen. B. p. 64.5°C at 750 mm. This agrees with the boiling point of a sample prepared by Loevenich, Losen, and Dierichs[10] by dehydrobromination of 1,1,2-tribromopropane.

The freshly distilled product is not spontaneously combustible, but the residue, or the pure compound, ignites quickly when it comes in contact with air and gives dense clouds of black smoke having an irritating odor. All transfers of the material from flasks to Raman tube, etc., were made in an atmosphere of nitrogen.

1-Chloro-1-propyne,

$CH_3C{\equiv}CCl$, C_3H_3Cl: The authors were unable to discover any reported synthesis of methylchloroacetylene. An attempt to prepare the compound by the action of methylacetylenesodium (freshly prepared sodamide and methylacetylene followed by removal of ammonia) on *p*-toluenesulfonyl chloride in dibutyl ether was unsuccessful. Another synthesis, using methylacetylene-magnesium bromide in dibutyl ether, resulted in a very small yield. The Raman

[5] Forrest F. Cleveland and M. J. Murray, J. Am. Chem. Soc. **62**, 3185 (1940).
[6] Forrest F. Cleveland, M. J. Murray, J. R. Coley, and V. I. Komarewsky, J. Chem. Phys. **10**, 18 (1942).
[7] G. B. Heisig and H. M. Davis, J. Am. Chem. Soc. **57**, 339 (1935).
[8] V. Grignard and H. Perrichon, Ann. chim. **5**, 5 (1926).
[9] F. Straus, L. Kollek, and W. Heyn, Ber. **63B**, 1868 (1930).
[10] J. Loevenich, J. Losen, and A. Dierichs, Ber. **60B**, 950 (1927).

TABLE I. Raman spectra of 1-iodo-1-propyne and 1-bromo-1-propyne.*

$CH_3C\equiv CI$				$CH_3C\equiv CBr$			
$\Delta\nu$	I	ρ	Assignment	$\Delta\nu$	I	ρ	Assignment
163	2	(0.8)	E	171	1		E
±343	60	0.8	E	±343	50	6/7	E
±405	10	0.3	A_1	464	6	0.3	A_1
497	1		163+343=506, A_1+A_2+E				
691	1	P	A_1	692	1	P	A_1
1021	1	D	E	1026	1	D	E
1150	vw	(D)	1438−343=1095, A_1+A_2+E	1154	vw		1443−343=1100, A_1+A_2+E
1375	10	0.7	A_1	1375	9	0.6	A_1
1438	1	0.9	E	1443	2	D	E
2011	vw		1375+691=2066, A_1	2060	vw		1375+692=2067, A_1
2182	vw		2(1030)=2060, A_1+E	2213	(16)	(0.3)	2(1035)=2070, A_1+E
2197	100	0.4	2892−691=2201, A_1	2230	80	0.35	2900−692=2208, A_1
			A_1				
2730	vw		2(1375)=2750, A_1				
2851	2	0.3	2(1438)=2876, A_1+E	2853	5	0.2	2(1443)=2886, A_1+E
			A_1	2921	100	0.15	A_1
2913	100	0.2	E	2968	8	6/7	E
2958	3	0.9					

* $\Delta\nu$ is the Raman frequency in cm^{-1}, I is the relative intensity based upon 100 for the strongest Raman line on the spectrogram, ρ is the depolarization factor, vw (very weak) designates lines that were too weak to measure with the microdensitometer, P indicates lines for which the weaker component of the polarization doublet was too weak to measure with the microdensitometer, D means depolarized, ± indicates lines that were obtained both as Stokes and as anti-Stokes lines, and the parentheses inclose data in regard to which there is some uncertainty.

spectrum of the small amount of product which was obtained (b. p. 37–41°C) showed that ethyl bromide was the main impurity. In working up the product, considerable quantities of methylacetylene and of unreacted *p*-toluenesulfonyl chloride were recovered. The yield of the product, however, was not increased by heating on a water bath for several hours the vigorously stirred reaction mixture containing the acetylenic Grignard and the sulfonyl chloride.

3,3-Dimethyl-1-butyne,

$(CH_3)_3CC\equiv CH$, C_6H_{10}: Fifty grams of pinacolone (Eastman Kodak Company product) were converted to the dichloride by action of 110 g of PCl_5.[11] After the addition of water the dichloride was isolated by steam distillation. To obtain *t*-butylacetylene, the method of Heisig and Davis[7] was again employed, with entirely satisfactory results. The solid pinacolone dichloride was introduced, a small amount at a time, into 200 cm^3 of *n*-butyl alcohol and 90 g of potassium hydroxide. The *t*-butylacetylene was caught in a dry-ice trap. Distillation through a Podbielniak-type column yielded a product whose boiling point was 37.5–38.0°C. A small amount of olefinic impurity was present in the final sample, as indicated by a weak Raman line at 1630 cm^{-1}.

RESULTS

The experimental results for 1-iodo-1-propyne and 1-bromo-1-propyne, which were obtained in the pure state, are listed in Table I. It was not possible to obtain pure 1-chloro-1-propyne, but the data for the impure sample, which contained ethyl bromide and a trace of some olefinic impurity, are listed in Table II. The lines that are certainly due to 1-chloro-1-propyne are indicated by asterisks. Also included in Table II are the data obtained for the 3,3-dimethyl-1-butyne.

DISCUSSION

The symmetry of each of the methyl halogen acetylenes concerned in the present paper is C_{3v}; the *t*-butylacetylene also has this symmetry if one of the hydrogen atoms of each methyl group lies in one of the vertical symmetry planes. Using group theory methods, one can work out not only the selection rules for the fundamentals, combinations, and overtones but also the number of fundamentals of each vibration type.[12] The results are summarized in Table III, from which it is seen that five totally symmetrical A_1 and five doubly degenerate E vibrations are permitted by the selection rules for the methyl halogen acetylenes. The A_1 vibrations should be polarized, the E vibrations depolarized, in the Raman spectra.

[11] A. Faworsky, J. Prakt. Chem. **37**, 393 (1888).

[12] For an elementary account of these methods see Arnold G. Meister, Forrest F. Cleveland, and M. J. Murray, Am. J. Phys. **11**, 239 (1943).

With the aid of the polarization data it is not difficult to pick out the A_1 and E fundamentals for the 1-iodo-1-propyne and 1-bromo-1-propyne; the assignments are indicated in Table I. One selection which may be somewhat questionable is the choice of the 1375-cm^{-1} line as an A_1 fundamental, since it is not very highly polarized. However, there are five E type fundamentals and only four A_1 fundamentals, if this line is excluded, and it thus seems fairly certain that it must be of the A_1 type. Crawford[13] was confronted with the same difficulty in his analysis of methylacetylene (another symmetrical-top acetylene); there the corresponding line was listed as "1380(2)D?", but was nevertheless chosen as an A_1 fundamental.

In the 2200-cm^{-1} region, three lines were observed for each of the compounds. These could arise from the resonance interactions of the triple-bond fundamental with the combinations and overtones indicated in Table I. In addition to the approximate coincidence of the combination or overtone frequency with the fundamental frequency, it is necessary that a symmetry condition be met in order for resonance doubling to appear. This symmetry condition is that the overtone or combination must have the same symmetry as the fundamental, or at least have one component which is the same as that of the fundamental.[12] Thus the combinations and overtones listed in Table I for the 2200-cm^{-1} region can produce resonance interaction with the A_1 triple-bond fundamental because they are either of type A_1 or contain A_1 as a component. The combinations (1438+691)=2129 and (2958−691)=2267 for 1-iodo-1-propyne and (1443+692)=2135 and (2968−692)=2276 for 1-bromo-1-propyne are of type E, and hence by the symmetry restriction cannot cause resonance doubling of the triple-bond fundamental. Several other cases of resonance doubling appear in Table I and it will be noted that in each case the symmetry condition is fulfilled.

TABLE II. Raman spectra of 1-chloro-1-propyne and 3,3-dimethyl-1-butyne.

$CH_3C\equiv CCl$+ C_2H_5Br		$(CH_3)_3CC\equiv CH$			$CH_3C\equiv CCl$+ C_2H_5Br		$(CH_3)_3CC\equiv CH$		
$\Delta\nu$	I	$\Delta\nu$	I	ρ	$\Delta\nu$	I	$\Delta\nu$	I	ρ
*184	3	183	100	0.90	1449	7	1390	vw	
±293	4	359	3		**1637	2	1453	9	D
*±353	35	389	2		*2102	1	2105	32	0.35
*439	2	544	2		*2134	2	2138	7	P
564	40	633	5		*2235	11	2714	1	
842	vw	690	16	0.10	*2263	20	2865	9	P
955	vw	722	3		2733	2	2887	10	P
*1029	vw	885	4	P	2864	18	2905	20	P
(1068)	vw	931	6	D	2926	100	2923	35	0.15
1152	2	1029	1		2971	35	2968	50	0.75
1246	3	1205	8	D			3307	1	
*1380	7	1247	1						

* These lines belong to the 1-chloro-1-propyne molecule.
** This line is due to a trace of some olefinic impurity.

TABLE III. Selection rules for any molecule of symmetry C_{3v} and the number of vibrations of each type for $CH_3C\equiv CX$ and $(CH_3)_3CC\equiv CH$.

	Type	Activity* Raman	Activity* Infra-red	No. of fundamentals $CH_3C\equiv CX$	No. of fundamentals $(CH_3)_3CC\equiv CH$
Fundamentals	A_1	a	a	5	10
	A_2	ia	ia	0	4
	E	a	a	5	14
Combinations					
†$A_1\times A_1$	A_1	a	a		
$A_1\times A_2$	A_2	ia	ia		
$A_1\times E$	E	a	a		
$A_2\times A_2$	A_1	a	a		
$A_2\times E$	E	a	a		
$E\times E$	A_1+A_2+E	a	a		
Overtones					
††A_1^n	A_1	a	a		
A_2^n (n even)	A_1	a	a		
A_2^n (n odd)	A_2	ia	ia		
E^2	A_1+E	a	a		
E^3	A_1+A_2+E	a	a		

* a = active, ia = inactive.
† $A_1\times A_1$ represents a combination frequency ($\nu_i\pm\nu_j$) of an A_1 frequency ν_i with another A_1 frequency ν_j.
†† A_1^n represents the $(n-1)$th overtone of an A_1 frequency.

Since the CH deformation vibration near 1375 cm^{-1}, the CH stretching frequency near 2920 cm^{-1}, and the carbon stretching frequency near 700 cm^{-1} are present in a great number of disubstituted acetylenes, the combinations (1375+700) and (2920−700) represent two other possibilities for the resonance doubling in addition to the overtone of the carbon stretching frequency near 1100 cm^{-1} as proposed by Badger[1] and by Crawford.[2] In addition, as suggested by Badger,[1] the second overtone of the 700 cm^{-1} frequency, which would be of type A_1, may sometimes be involved. Thus there exist four overtone or combination frequencies which are satisfactory for explaining the multiplicity of lines usually observed in the 2200 cm^{-1} region for the disubstituted acetylenes. Whether two or more lines are observed depends upon the frequency of the triple bond fundamental in the compound under consideration.

These possibilities would not apply to monosubstituted acetylenes since for them the 700-

[13] B. L. Crawford, Jr., J. Chem. Phys. **8**, 526 (1940).

TABLE IV. Fundamental frequencies.*

$CH_3C{\equiv}CI$		$CH_3C{\equiv}CBr$		$CH_3C{\equiv}CI$		$CH_3C{\equiv}CBr$	
$\Delta\nu$	D	$\Delta\nu$	D	$\Delta\nu$	D	$\Delta\nu$	D
163	2	171	2	1375	1	1375	1
343	2	343	2	1438	2	1443	2
410	1	464	1	2192	1	2225	1
691	1	692	1	2892	1	2900	1
1030	2	1035	2	2958	2	2968	2

* $\Delta\nu$ = Raman frequency in cm^{-1}. D = degeneracy.

and 1100-cm^{-1} lines are replaced by lines near 925 and 3300 cm^{-1}, respectively. Hence the few cases in which doubling has been observed for a monosubstituted acetylene must involve some other vibration. Dimethylethynyl carbinol which

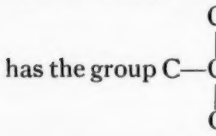

has the group C—C(=O)— adjacent to the triple bond was previously found[5] to have a double line at 2089 and 2112 cm^{-1} and the *t*-butylacetylene concerned in the present study also had a double line at 2105 and 2138 cm^{-1}; the latter has the

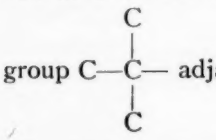

group C—C(C)— adjacent to the triple bond. The symmetrical, "breathing" frequency of these groups falls at 709 for dimethylethynyl carbinol and at 690 cm^{-1} for *t*-butylacetylene. In both cases this frequency is highly polarized and thus, at least for *t*-butylacetylene, corresponds to an A_1 type fundamental whose second overtone could produce resonance doubling of the triple-bond frequency, which for most monosubstituted acetylenes appears at 2118 cm^{-1}.

For *t*-butylacetylene, the selection rules (see Table III) permit 24 frequencies to appear in the Raman spectrum. Twenty-three were observed, but not all of these can correspond to fundamentals. The polarized lines at 690, 885, 2105, and 2923 as well as the lines at 1390 and 3307 cm^{-1} can rather safely be taken as A_1 fundamentals, and the depolarized lines at 183, 931, 1205, 1453, and 2968 as *E* fundamentals. The lines at 2138, 2865, 2887, and 2905 cm^{-1} probably owe their appearance to resonance interactions. A complete interpretation of this spectrum is not possible upon the basis of the present data.

HEAT CAPACITY CALCULATIONS

Since all of the fundamental frequencies were obtained for 1-iodo-1-propyne and 1-bromo-1-propyne, it is possible to calculate the heat capacities of these compounds for the ideal gaseous state at one atmosphere pressure. The tables given by Wilson[14] were used in the calculations. The results are only approximate since the frequencies were obtained for the liquid rather than the gaseous state. Because of the several cases of resonance interaction, it was necessary to make slight adjustments of the frequencies in these cases; the adjustments were made by consideration of the relative intensities of the components of the resonance doublet or multiplet. The fundamentals used for the calculations are listed in Table IV; the numbers appearing under the letter D are the degeneracies. The values of the heat capacities calculated from these frequencies are given in Table V.

TABLE V. Heat capacities at constant pressure.

Temperature	$CH_3C{\equiv}CI$	$CH_3C{\equiv}CBr$
250.0°K	16.95*	16.77
298.16	18.23	18.08
400.	20.67	20.56
600.	24.56	24.47
800.	27.49	27.42
1000.	29.71	29.65

* Calories/(mole-degree).

ACKNOWLEDGMENTS

The optical parts of the spectrograph used in obtaining the frequencies were obtained with a grant to the authors from the Society of the Sigma Xi and the microdensitometer used in obtaining the intensities was obtained with a grant to one of us (F. F. C.) from the Penrose Fund of the American Philosophical Society. The authors are grateful for this assistance.

[14] E. B. Wilson, Jr., Chem. Rev. **27**, 17 (1940).

THE JOURNAL OF CHEMICAL PHYSICS VOLUME 11, NUMBER 10 OCTOBER, 1943

Theory of the Elastic Properties of Rubber

HUBERT M. JAMES,* *Purdue University, Lafayette, Indiana*

AND

EUGENE GUTH, *University of Notre Dame, Notre Dame, Indiana*

(Received July 8, 1943)

Previous discussions of the kinetic theory of rubber elasticity have dealt with individual long chain molecules, but the theory of the structure of bulk rubber has been almost entirely undeveloped. The present paper goes beyond earlier ones both in the more detailed treatment of the individual chains and in the development of a clear-cut model of the bulk material. From the consideration of familiar properties of rubber, it is concluded that in the lightly vulcanized state it consists of a coherent network of flexible molecular chains (this involving a considerable fraction of the total material) together with other molecules not actively involved in the network, but acting like a fluid mass through which the network extends and in which it moves with Brownian motion. The idea of an effective internal pressure is advanced and discussed. A simplified model for bulk rubber is proposed, consisting of a network of idealized flexible chains extending through the material and a fluid filling it, the bounding surfaces being in equilibrium under all the forces acting on them—internal pressure, pull of the molecular network, and any external forces. For the quantitative treatment of this model the principal problem is that of computing the forces exerted by the molecular network, because of its thermal agitation, on the bounding surfaces. Two models of the flexible molecular chains have been used—one with a linear stress-extension relation (Gaussian chain), the second with independent links of fixed length, having, like real molecular chains, a definite maximum extension. Methods for the statistical treatment of chains of independent links at all extensions are developed and applied to the computation of stress-strain relations for the second of the above models. It is shown that an irregular network of Gaussian chains is equivalent to a simple set of independent chains; the corresponding reduction in the case of non-Gaussian chains is only approximate. Making this reduction in all cases, the model is applied to the quantitative computation of stress-strain curves for unilateral stretch of rubber and for stretch in two directions. A prediction is made of the change in elastic properties of rubber in the swollen state. The thermoelastic properties of rubber are worked out, and the change in slope of the nearly linear stress-temperature curves from negative to positive values with increasing strain is explained. The location of the thermoelastic inversion point, at which this slope is zero, is shown to depend only upon the cubic expansion coefficient of unstretched rubber. The linear thermal expansion coefficient of stretched rubber in the direction of the stress is shown to be positive (and of the order of the same coefficient for unstretched rubber) below the thermoelastic inversion point. Above the thermoelastic inversion point this coefficient becomes negative and is—for appreciable extensions—of the order of the cubic expansion coefficient for a gas, independent of the composition of rubber. The linear coefficient of thermal expansion perpendicular to the direction of stress is always positive. Stress-strain curves for bulk rubber at constant temperature have been compared with the theory for extensions up to 400 percent. The agreement is particularly good as concerns that part of the total stress due to changing entropy. In some rubber compounds minor deviations, variable from sample to sample, are found for small extensions. These are attributed to van der Waals forces not taken into account by the theory. The characteristic knee in rubber stress-strain curves is shown to be due to change in internal pressure in the material. This varies inversely with the extended length, and in unstretched rubber is of the order of 5 kg/cm². The upward curvature of the stress-strain curve for larger extensions, which appears even before the onset of crystallization, is explained as due to the approach of the molecular network to its maximum extension, which is of the order of 10 times its extension in the unstretched bulk rubber. Crystallization may in general enhance the S-shape of the stress-strain curve for natural cured rubber, Neoprene and butyl rubber. Synthetic rubber of the Buna type, while having an S-shaped stress-strain curve, does not exhibit any crystallization at all. It is estimated that, in the materials considered, roughly a fourth of the rubber chains are actively involved in the network. Internal pressure, maximum extensions, and the fraction of active material all change with the state of vulcanization. The general theory developed in this paper provides a basis for the treatment of many other physical properties of stretched rubber.

1. INTRODUCTION

RUBBER is the best known representative of a class of materials set apart from other solids by their characteristic elastic and thermoelastic behavior. The most striking property of rubber is its long-range reversible elasticity. This property is so characteristic that any material possessing it may be called a "rubber" regardless of its chemical constitution. With soft rubber,

* On leave of absence at the Radiation Laboratory, Massachusetts Institute of Technology, Cambridge, Massachusetts.

elongations of some 1000 percent (greater than those possible with ordinary solids by a factor of 10^5) are obtainable with relatively small deviations from complete reversibility; the elastic constants are, correspondingly, of a quite different order of magnitude. The stress-strain curves have, also, an unusual S-form, the differential Young's modulus at first decreasing with increasing strain until it is of the order of one-third its value for small strain, and thereafter increasing more and more rapidly (cf. Fig. 1).

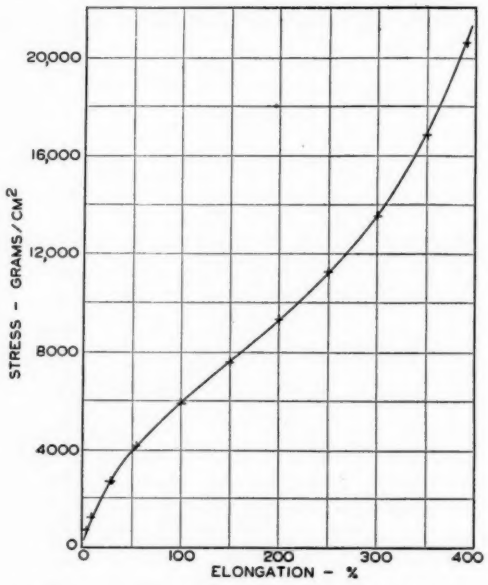

FIG. 1. Typical stress-strain curve for rubber.

The thermoelastic properties of rubber-like substances are equally striking, and perhaps more suggestive as to the mechanism involved. Rubber extended under constant load contracts when heated; the stress of rubber kept at constant length increases with rising temperature, under not too extreme conditions very nearly proportionally to the absolute temperature. The striking generation of heat when rubber is adiabatically stretched is thermodynamically related to these other elements in the behavior of the material and needs no special explanation.

In a general way the existence of long range reversible elasticity in rubber and the temperature dependence of stress for constant strain have been understood for some years;[1,2] an attempt[3] has even been made to get an estimate of the order of magnitude of the elastic constants. These previous discussions have, however, been of a very general character, or have involved the use of models which were vaguely defined, physically unsatisfactory, or incompletely worked out.[4] It is our purpose in the present paper to present a definite and reasonable model for rubber-like materials in bulk, and to employ it in the quantitative explanation of various properties of rubber, especially the hitherto little understood form of the stress-strain curves at constant temperature.

Many qualitative conclusions about the mechanism of rubber-like elasticity can be drawn from the most elementary features in the behavior of these materials.

The behavior of rubber as a *solid*, the possibility of elastic deformations, shows that bulk rubber possesses a definite structure which determines its form in the absence of external forces. The elements of structure must, however, be of a quite different sort from those in normal solids, in which bonds of electrostatic, chemical, or van der Waals type connect atoms or molecules into a definite and rigid three-dimensional structure. The long-range extensibility suggests that the structure of rubber must be of a much more flexible, more open, type with the relationships between atoms less completely defined. The small forces needed to produce considerable distortions suggest that the elastic restoring forces cannot be of any of the types listed above. One must suppose that ordinary distortions of bulk rubber do not appreciably change the distances between atoms linked by chemical or other strong bonds. That is, in distorting rubber one does not act against the strong bonds which suppress the plasticity and maintain the coherence of the material. Only for the very large extensions, at which rubber begins to crystallize or approaches the breaking point, do these bonds come into play. For instance, ordinary chemical bonds appear to contribute to the tensile strength of

[1] E. Guth and H. Mark, Monats. f. Chemie **65**, 93 (1934).
[2] E. Guth, Kautschuk **13**, 201 (1937).
[3] W. Kuhn, Kolloid Zeits. **76**, 258 (1936).
[4] For a more detailed discussion, with reference to the literature, see E. Guth and H. M. James, Ind. Eng. Chem. **33**, 1624 (1941); and H. M. James and E. Guth, *ibid.* **34**, 1365 (1942). In these two papers a preliminary discussion is given of the new theory developed in detail in the present paper.

rubber, which (taken with regard to the cross section at the breaking point) is about that of copper.

Rubber resembles a *liquid* in possessing high volume rigidity together with small rigidity of shape. The compressibility of rubber is that of an ordinary liquid. In consideration of the stretching of rubber this is quite negligible, and one may treat rubber as incompressible for extensions up to 300 or 400 percent; Poisson's modulus is thus $\frac{1}{2}$ for small deformations. Furthermore, the coefficient of thermal expansion for rubber is of the same order of magnitude as for liquids. These points suggest that the interactions between adjacent molecules in bulk rubber are, for the most part, similar to those which maintain the fixed volume of ordinary liquids. In addition to these forces, which do not maintain a fixed coupling of molecule to molecule or atom to atom, there must be strong bonds between the molecules, constituting the elements of structure previously mentioned. These bonds may, however, affect only relatively small portions of the very large rubber molecules, and thus have relatively small effect on the above properties of the material.

Rubber resembles a *gas* very strikingly in its thermoelastic behavior. The proportionality of stress to absolute temperature under constant strain suggests that the tension in stretched rubber, like the pressure in a gas, is associated with a change in entropy of the material when it is deformed, rather than with a change in internal energy. Quantitatively, the behavior of stretched rubber, or of a gas under pressure, is determined by its free energy, which in the case of rubber under simple tension may be written

$$F(L, T) = U(L, T) - TS(L, T). \qquad (1.1)$$

Here L represents the length of the stretched material and the other symbols have their customary significance. The tension is

$$\begin{aligned} Z(L, T) &= (\partial F/\partial L)_T = (\partial U/\partial L)_T - T(\partial S/\partial L)_T \\ &= (\partial U/\partial L)_T + T(\partial Z/\partial L)_T. \end{aligned} \qquad (1.2)$$

In the case of a gas one has only to replace L by the volume V, and Z by the negative pressure $(-p)$. The simple and uniform thermoelastic behavior of ideal gases, independent of their chemical composition, is due to two characteristics of these gases: (1) the internal energy is in all cases nearly independent of the volume; (2) the entropy consists of two parts, one associated with the thermal capacity of the gas, dependent on the chemical composition, but making no contribution to $(\partial S/\partial V)_T$, and the second associated with the number of positional configurations available to the system, independent of the composition, and making a contribution to $(\partial S/\partial V)_T$ which is independent of T. The uniform and simple thermoelastic behavior of "ideal" rubber-like materials, independent of their composition, may be understood in a similar way, consistently with our previous discussion of their properties. The internal energy of the liquid-like mass of molecules will be practically independent of its form, such strong chemical bonds as may exist being but little stretched by the relatively small forces which produce moderate deformations of the material; $(\partial U/\partial L)_T$ will be small. As we shall indicate later in more detail, the entropy will consist of two parts, one associated with the heat capacity and not contributing to $(\partial S/\partial L)_T$, the other associated with the number of configurations available to the molecules within the material. The number of these configurations will depend on the external form of the material but not on the temperature, on the general structure of the masses of molecules but not on their precise chemical composition. $(\partial S/\partial L)_T$ will, accordingly, be independent of temperature, and we will have, approximately,

$$Z(L, T) = Z_0(L)T. \qquad (1.3)$$

The setting up of models for bulk rubber consistent with all these ideas, and the calculation of their entropies and the associated forces, is the main problem considered in this paper.

2. MODELS OF THE STRUCTURE OF RUBBER

In earlier discussions of rubber elasticity as an entropy effect, attention has been concentrated not on bulk rubber, but on a single rubber molecule.

The rubber molecule is a very long unbranched hydrocarbon chain composed of isoprene groups

linked end to end:

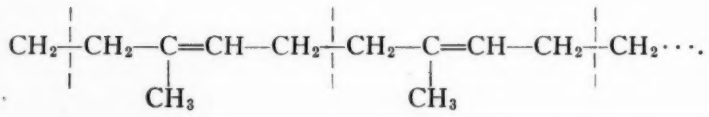

The first essential characteristic of this molecule is its great length. The second is its flexibility. Of the carbon-carbon bonds in the chain, three-fourths are single, one-fourth double. Now the molecule can have its two parts rotated with respect to each other at any one of the single bonds without change in the energy, to the approximation in which interactions are neglected between atoms in the chain farther apart than third neighbors. Indeed it possesses the possibility of free rotation, in the usual quantum-mechanical sense,[5] to the better approximation which does take account of interaction of the atoms directly bound to adjacent carbon atoms in the chain. It is sufficient for the following general discussion that there exist configurations of the molecule differing by rotations of one part with respect to the other about any given single bond and having the same minimum energy; the configurations may be separated by energy barriers, provided only that they are not so high as to prevent transitions from one configuration to another in a time small compared to that in which a distortion is applied to the bulk rubber. By twisting about all the single bonds, the molecule can take on[6] an enormous number of configurations, all of the same energy, to the approximation just mentioned. Given the direction of one carbon-carbon bond in the chain, that of the next bond is restricted to the neighborhood of two or three definite directions. That of the second bond along the chain will be less definitely fixed, there being more different orientations of maximum probability, while bonds only a little farther down the chain will take on their orientations practically independently of the prescribed orientation of the first. So long as it is not necessary to consider in detail the configurations of short segments of the molecule, one may treat it like a perfectly flexible chain, which can take on any configuration without change of energy.[7]

One may treat such a long chain molecule, consisting of very many units, by the methods of statistical mechanics. To a chain in thermal equilibrium with a temperature bath and subject only to the constraint that the ends have a separation L, one may assign the entropy

$$S=k \log C(L)+h(T), \tag{2.1}$$

where k is Boltzmann's constant and $C(L)$ is the relative number of configurations of the chain consistent with the separation L of its ends. The term $h(T)$ arises from the thermal capacity of the chain, and, because of the flexibility of the chain, is independent of L. For a flexible chain the internal energy is completely independent of the configuration of the chain, and thus of L; hence, we have

$$u=u(T). \tag{2.2}$$

The free energy becomes

$$F=u(T)-kT \log C(L)-Th(T) \tag{2.3}$$

[5] Cf. for instance, R. H. Fowler and E. A. Guggenheim, *Statistical Thermodynamics* (Cambridge, 1939), pp. 107–109.

[6] Measurements of the heat capacity of ethane indicate that the energy barrier hindering the free rotation of the two CH_3 groups relative to each other is of the order of 3 kcal./mole. However, for isoprene the presence of the double C=C bonds may very well lower the barrier by a factor of 3 or more. In fact for dimethylacetylene ($CH_3-C\equiv C-CH_3$), the presence of the triple $C\equiv C$ bond lowers the barrier so much that the two CH_3 groups rotate practically freely relative to each other. These points seem to have been overlooked by S. Bresler and J. Frenkel, Acta Physicochem. U.S.S.R. **11**, 485 (1939) in their attempt to calculate the influence of the potential barrier on the contracting force in single long chain hydrocarbon chains.

[7] For the mathematical development of the theory one may introduce the flexibility of the chain in a variety of idealized ways, as by treating the chain as involving only single bonds about which perfectly free rotation is possible, or as consisting of rigid links each of which can take on its orientations independently of its neighbors. These are the models of the rubber molecules employed in the present work. The general character of the results will be independent of the way in which the flexibility is introduced, but there will be differences in details, and to some degree in estimated magnitudes, from model to model. Concerning such details, the theory will be reliable only in proportion as the model is well chosen for the particular long chain molecules to be treated. In the present paper we have chosen the second and simpler model indicated above, as it has all the essential characteristics of the real chains. The other, and quantitatively more reliable, model will be treated in a second, more mathematical, paper.

and the tension in the chain

$$Z(L, T) = -k \cdot [1/C(L)] \cdot [dC(L)/dL] \cdot T. \quad (2.4)$$

The functions $u(T)$ and $h(T)$ drop out of the computation of Z, which is proportional to the absolute temperature. This will clearly be the case with any system of flexible chains which one might use as a model for bulk rubber.

This problem could also be discussed from the point of view of kinetic theory. A chain molecule immersed in a temperature bath will undergo constant changes in configuration through its thermal agitation—an internal Brownian motion. For a perfectly flexible and unconstrained molecule, all configurations will have the same energy and the same probability of occurrence. However, since knotted and coiled configurations are far more numerous than relatively straight and extended ones, the probability is overwhelming that at any given time the molecule will be found in a highly twisted state, with its ends separated by a distance small compared to the total length of the chain. If the ends of the molecule are constrained to lie at fixed points, the thermal agitation will result in a constant jerking of the molecule against the constraints. Unless the ends of the molecule are coincident, jerks in the different directions will not be equally probable; they will result in a net force tending to bring the ends of the molecule closer together—an effective tension. If the temperature is raised, the thermal agitation will be more violent and the effective tension will increase. If the distance between the ends of the chain is slowly increased at constant temperature, work must be done against the forces in the jerking chain. The energy of thermal agitation of the chain will, however, be unchanged, and the energy given to the chain will appear as heat. In all these respects the single molecular chain would show the behavior observed with bulk rubber, and the same would be true of any system of chain molecules so connected together that the intramolecular Brownian motion is not suppressed. This approach to the understanding of rubber elasticity as due to the tendency of long chain molecules to curl up under the influence of thermal agitation is qualitatively useful. For quantitative purposes, however, methods involving the enumeration of the configurations of the chain under the imposed constraints are usually the only practicable ones.

In order to investigate the dependence of Z upon L, one must determine the form of the function $C(L)$, which will vary as to details from model to model. Guth and Mark[1] treat the case of chains of N independent links, each of length l, in both one and three dimensions. With L denoting the component of the extension in a fixed direction, they find in either case that for small L a Gaussian distribution applies:

$$C(L) = A \exp(-L^2/2\langle L^2\rangle_{Av}). \quad (2.5)$$

For the one-dimensional case $\langle L^2\rangle_{Av} = Nl^2$; for the three-dimensional case $\langle L^2\rangle_{Av} = (1/3)Nl^2$. Kuhn[3] considers a three-dimensional chain in which each independent link can contribute $\pm l/\sqrt{3}$ to the extension in any or all of the coordinate directions, and obtains the same result. Both make the extension to the case of a chain of links each making a fixed valence angle δ with its neighbors, but otherwise independent of them, by assuming the same form for $C(L)$ and noting that in this case $\langle L^2\rangle_{Av} = (1/3)Nl^2 \tan^2 \delta/2$. The limited accuracy of such results will be discussed in Part 6 of this paper.

With this form for $C(L)$, one obtains

$$Z = [kT/\langle L^2\rangle_{Av}]L. \quad (2.6)$$

In order to extend this discussion to bulk rubber, it is necessary to make some assumption as to how the material is built up from single chains. The implicit assumption of Guth and Mark is that a unit cube of rubber can be treated as a bundle of M similar, parallel, and independent chains. These chains would exert equal restoring forces; one has at once as the restoring force in stretched rubber, per unit cross section of the unstretched material,

$$Z = M[kT/\langle L^2\rangle_{Av}] \cdot L. \quad (2.7)$$

This model is much oversimplified. It is anisotropic, being stretchable only in the direction of the bundle, and has length and volume zero when acted upon by no external forces. The proportionality of tension to length given by this model is, correspondingly, far simpler than the observed relation for rubber-like materials.

Kuhn gives a rather vague description of his model and his formalism is actually inconsistent

with his textual picture of the situation. He does picture a transition from a hypothetical melted rubber, in which the molecules take on all the different configurations possible for isolated molecules, to the actual solid, in which each molecule is immobilized in the configuration it possessed at the instant of solidification. The picture of a complete immobilization of the molecular chain is certainly incorrect; such a suppression of the internal Brownian motion would destroy the rubber-like properties of the material. However, Kuhn's mathematical treatment actually corresponds to the assumption that, after the freezing, each molecule is fixed at the end points and at points $\frac{1}{4}$, $\frac{1}{2}$, and $\frac{3}{4}$ of the way along its length, with the Brownian motion otherwise unhampered. He assumes that, when the bulk material is distorted, the configurations of the molecules (in his mathematical treatment the fixed points) have the motion which would be assigned to them by a continuum theory of elasticity. He provides no adequate picture of the mechanism by which this might be brought about; the basis of his discussion is essentially the *assumed* variation of the distribution function with distortion of the material. This consideration of what happens to the material perpendicular to the direction of stretch makes the model, in contrast to that of Guth and Mark, a three-dimensional one; a complete treatment of his formalism would, in fact, lead to our preliminary form of the stress-strain curve as discussed in Section 3. Kuhn, however, determines only the slope of the stress-strain curve for very small stresses and not its complete form.

Wall[8] gives a formal discussion of bulk rubber similar to Kuhn's, based on an *assumed* distribution function without an associated physical picture, and obtains in his second paper the stress-strain curve previously described by the authors.[4] Kuhn and Wall treat, in an identical way, the problem of the "molecular weight" of rubber molecules in bulk rubber. A different view of the situation is presented in Section 7 of the present paper. Kuhn's model and its relation to our model is further discussed in that section and in the Appendix.

[8] F. T. Wall, J. Chem. Phys. **10**, 132, 485 (1942). In the first paper, the incompressibility of stretched rubber was not taken into account.

The picture of the structure of rubber on which we base our model is as follows.[9] Raw rubber consists of a tangled mass of long chain molecules, of which some may be linked together by chemical bonds, while others can move more or less freely past each other, impeded only by the tendency of the Brownian motion to keep the chains tangled. The possibility of an unlimited relative displacement of the molecules is responsible for the plasticity of raw rubber, while the tangling of the chains keeps the internal viscosity high—higher the longer the molecular chains. Raw rubber deformed rapidly and immediately released will return to its original shape with little plastic deformation because there has been time for only a little motion of the molecules with respect to each other.[10]

Vulcanization appears to consist of the reinforcing of cross-links already present in raw rubber *and* the introduction of new cross-links.[11] These bonds will be formed at random, sometimes connecting different parts of a single molecule, but more often linking parts of two different molecules which happen to be adjacent at the time. As more and more bonds are formed, the whole mass of molecules will come to be linked together in a coherent network, very irregular in detail and quite open in structure, there being only a few bonds formed for each of the long molecules. These bonds introduce fixed relations between the molecules which will be undisturbed by later distortions of the body, and result in the suppression of the plasticity of the material. On the other hand, they affect only a small portion of each molecule; the intramolecular Brownian motion is largely undisturbed, and over the

[9] A convenient summary of the great variety of ideas concerning the structure of rubber is provided in the monograph, Chemistry and Technology of Rubber, edited by C. C. Davis and J. T. Blake (New York, 1937).

[10] The recent work by L. R. G. Treloar, Trans. Faraday Soc. **36**, 538 (1940), shows that the plasticity of raw rubber is largely of a semi-permanent character. On release after stretching, the material returns almost completely to its original unstretched length, though this recovery may take a long time, require additional heat treatment and the application of solvents.

[11] The exact chemical nature of vulcanization is irrelevant for the purposes of this paper. The cross-links may be van der Waals bonds or chemical bonds. Where the latter are concerned, it is very likely that the double C=C bonds are involved in the formation of cross-links. At any rate, saturated long chain hydrocarbons (which may show the properties of raw rubber to a marked extent) cannot be vulcanized.

greater part of their lengths the molecules will be free to move past each other, as in a liquid or in raw rubber. Rubber vulcanized to this degree will show all the properties of raw rubber except the plasticity. If the vulcanization is carried further, the intermolecular bonds will eventually become so numerous as to suppress the intramolecular Brownian motion to a great extent and to change markedly the relationship of adjacent molecules. The extensibility of the material then approaches that of ordinary solids. We must exclude from consideration such highly vulcanized rubbers, and even soft rubber under high strains, in which there is known to be induced a crystallization which radically modifies the properties of the material. Our discussion will be restricted entirely to the case of ideal soft rubber-like materials, characterized by negligible plasticity and at least approximate proportionality of stresses to the absolute temperature.

The first essential element in the structure of rubber of which our model must take account is, then, the existence of a complicated network of flexible molecular chains extending throughout the material. Such a network will, as already shown, exert restoring forces proportional to the absolute temperature. An idealized network of this type would alone, however, be quite inadequate as a model for rubber. For instance, such a model would extend through a very small volume in the absence of external forces. It is not possible to neglect completely, as one does in the treatment of idealized flexible chains, the volume-filling property of the rubber molecules.

The volume of the bulk rubber will be regulated by lateral forces between the chains quite unrelated to those effective tensions along the chains which tend to maintain the shape of the material. The chains, for the most part moving freely past each other, will jostle each other, and any bounding surfaces, as they would in a liquid. The bounding surfaces may be those of other solids, or free surfaces of the material at which the outward forces of the jostling molecules are balanced by the inward pull of the coherent network. The effect of the sidewise thrusts and pulls will be the same as in an ordinary liquid—the production of an effective hydrostatic pressure in the material, which will depend on its volume. This will clearly be uniform throughout the material so long as this undergoes no irregular distortions. It is likely that the mobility of the rubber molecules within the bulk rubber is sufficient to assure the usefulness of the idea of a hydrostatic pressure under somewhat more general conditions, but such an extension of our model is beyond the scope of the present paper.

In our model of bulk rubber, we separate and idealize the two aspects of the molecular network. We replace the real molecular network by a similar network of idealized flexible chains, very irregular in detail, but homogeneous and isotropic on the average. The space-filling aspect of the network we represent by filling the model with a fluid. This fluid can, as a first approximation, be taken as incompressible; further refinements may be introduced by attributing to it an appropriate compressibility and thermal expansion. To prevent the collapse of the idealized network into a small volume, we must then constrain it to stretch throughout the whole of the model by constraining appropriate points of it to lie on the bounding surfaces. This completes the representation of volume-filling properties of the network. Under equilibrium conditions, to which we restrict ourselves, every surface of the model must of course be in equilibrium under all the forces which act on it—the push of the hydrostatic forces, the pull of the network, and any external forces.

It should be pointed out that not all of the molecular chains will be involved actively in the network. A chain connected into the network at a single point will not contribute to its tendency to pull against constraints. The same may be said of closed loops in chains in the network, and chains threaded through the network but not linked to it. Finally, some of the chains may be completely dissociated from the main network, either removable by solvents, or, if connected into large and complicated snarls, not so easily separable from it. All these "inert" molecular chains will play just the role of the fluid filling our model and can be omitted from the idealized network. In the final section of this paper we shall arrive at an estimate of the fraction of the molecular chains actively involved in the network.

It may be objected that, in idealizing the molecular chains and neglecting their interactions with other chains, we neglect a factor which affects the configurations possible to the network, and therefore the forces which it will exert. For the most part, however, the effect of these other chains will be that of a foreign fluid, even though they are not of the "inert" sort just described. They will not modify the probability distribution of the configurations eventually available to the chain, since they do not occupy fixed positions, and they will thus not modify the forces which it exerts. An obvious exception occurs in the case of portions of chains near a junction, where relative positions are more or less fixed. However, if the material is lightly vulcanized a relatively small fraction of the total chain length will be thus affected, and the approximation should not be serious.

We begin the treatment of this model by a discussion of the stress-strain relation which it exhibits when the distribution function $C(L)$ for each segment of molecular chain between two junctions is taken to have the Gaussian form (Section 3). The principal calculation required for this discussion, the reduction of the forces exerted by an irregular network of flexible chains to those of an equivalent regular network, is to be found in the Appendix. Other properties of the model with Gaussian chains are discussed in Section 4. Agreement with experiment is satisfactory for moderate strains, testifying to the value of the idea of internal hydrostatic pressure. However, the deviation of the theory from experiment at large strains is of such a character as to suggest that we have here to deal with flexible chains approaching their maximum extension, for which the Gaussian distribution does not hold. We shall then develop methods for discussing the stress-strain relations in flexible chains when the extensions are comparable to the maximum length, in Section 5. Section 6 deals specifically with chains consisting of completely independent links, and describes an improved model involving such chains. The problem of imperfectly flexible chains in general, and of chains with free rotation and fixed valence angle in particular, is deferred to a later paper. Finally, in Section 7, a comparison of theory with experiment is carried out, and further conclusions are drawn as to the conditions existing in soft rubber compounds.

3. THE NEW MODEL FOR RUBBER: GAUSSIAN CHAINS

We shall now discuss the stress-strain relation for our model of rubber, treating the material as essentially incompressible. This assumption is well substantiated by the experiments of Holt and McPherson[12] who have found that the volume is essentially unchanged when soft gum compounds are given extensions of up to 300 percent.

We shall consider a unit cube of rubber stretched by forces of magnitude Z and having the z direction, and applied uniformly to cube faces perpendicular to the z axis. The cube will be deformed into a parallelopiped of dimensions L_x, L_y, L_z, with $L_x=L_y$. According to the assumption of incompressibility we have then

$$L_xL_yL_z=L_x^2L_z=1. \tag{3.1}$$

In the treatment of the model thus stretched the first task is to compute the pull of the irregular molecular network. This may be thought of as a system of junction points connected by segments of flexible chains which are independent of each other. The theoretical treatment of this network may be split into two parts:
(a) Determination of the configuration function for a single chain segment, $C(\mathbf{r}_\alpha, \mathbf{r}_\beta)$. This function of the positions of the endpoints of the chain will depend only on the separation $r_{\alpha\beta}$ of the ends.
(b) Determination of the configuration function for the whole net when a number of the junction points, specified by the vectors $\mathbf{r}_1$, $\mathbf{r}_2 \cdots$ are kept fixed, as at the surface of the model. This configuration function will be a function $P(\mathbf{r}_1, \mathbf{r}_2 \cdots)$ of the positions of the fixed junction points, obtainable by integration of a product of the functions $C(\mathbf{r}_\alpha, \mathbf{r}_\beta)$ over the positions of all junctions which are not fixed.

Problem (a) is solved in this paper for several types of flexible chain, and for all extensions. Problem (b) has been solved rigorously only when each chain segment can be treated as of Gaussian type. This assumption requires that the

[12] W. L. Holt and A. T. McPherson, Rubber Chem. Tech. **10**, 412 (1937).

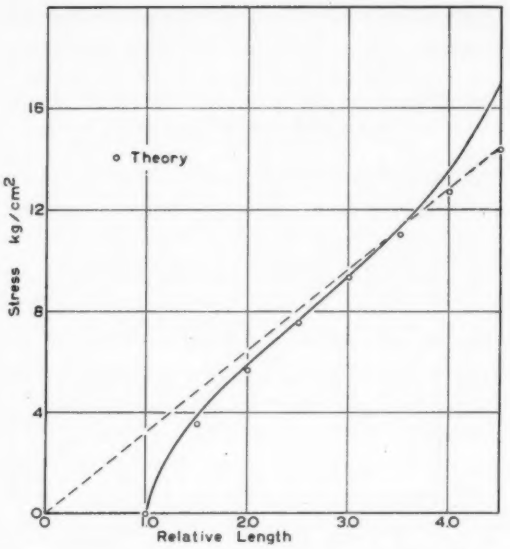

FIG. 2. Comparison of experiment with theory using Gaussian chains. Solid line, experiment. Circles, theoretical values. Dashed line, asymptote approached by theoretical values at large extensions.

segments of chains between junctions all contain very many links and (as will be apparent later) that these segments normally have extensions small compared with their maximum length. For the purposes of the present section it is sufficient for us to make use of results established in the Appendix: The forces exerted by a network of Gaussian segments, irregular in detail but homogenous and isotropic in the average, with fixed points constrained to lie on the six planes $x=0$, $x=L_x$, $y=0$, $y=L_y$, $z=0$, $z=L_z$, are the same as those exerted by a simplified network in which one set of Gaussian chains runs between the planes $x=0$, and $x=L_x$, a second completely independent set runs between the planes $y=0$ and $y=L_y$, and a third between the planes $z=0$, and $z=L_z$. Each set of chains can be taken to include M chains, each of N links, and each chain may be thought of as parallel to an edge of the parallelopiped, in the sense that its fixed ends lie on a straight line parallel to that edge.

The Appendix establishes this result by a treatment which gives a picture of the behavior of the network in both unstretched and distorted conditions and indicates a method of computing the forces from the detailed picture of the network. There is also possible a more direct proof, which consists essentially of the reduction of a Gaussian distribution in many dimensions to a Gaussian distribution in a smaller number of dimensions by integrating over certain of the variables.

Replacing the irregular network of our model by the equivalent system of three sets of M chains of N links acting independently in the three coordinate directions, we can determine the internal pressure in the material by a consideration of one of the free surfaces, for which the outward push of this pressure is balanced by the pull of M molecular chains, each extended to length L_x and thus exerting an average force of $[kT/\langle L^2\rangle_{Nv}]L_x$. That is,

$$PL_yL_z=M[kT/\langle L^2\rangle_{Nv}]L_x,$$

or

$$P=M\cdot[kT/\langle L^2\rangle_{Nv}]L_x^{-1}. \tag{3.2}$$

Thus the internal pressure in bulk rubber decreases when the material is subjected to stretch.

To obtain the stress-strain relation for the cube, one needs only to consider similarly the equilibrium of one of the end faces, equating the outward push of the pressure plus the external force to the pull of the molecular chains. One finds at once

$$Z=M[kT/\langle L^2\rangle_{Nv}][L_x-1/L_x^2]. \tag{3.3}$$

The first term on the right is the force given by the bundle model of rubber already mentioned, while the second term is the correction for the effect of the decreasing internal pressure as the material is stretched.

Figure 2 shows a curve of the form given in Eq. (3.3), in comparison with an experimental curve.[13] It will be seen that the nature of the characteristic knee in the experimental curve is well reproduced by this simple theory, in which the only adjustable parameter governs the vertical scale of the figure. The form of this knee is determined by the decreasing internal pressure in the material. Figure 2 thus indicates immediately the importance of the internal pressure in the understanding of the form of the stress-strain curve of rubber. We defer more detailed comparison between theory and experiment to Section 7, after the theory has been further developed.

This theory gives a relation of Z to L_x which approaches linearity as L_x becomes large and the

[13] R. L. Anthony, R. H. Caston, and E. Guth, J. Phys. Chem. **46**, 826 (1942).

internal pressure becomes negligible in effect. The asymptote for large L_z passes through the origin of the (Z, L_z) plane, a feature which is possessed by the tangents to many rubber stress-strain curves in the nearly linear portion for intermediate stresses.

The differential Young's modulus is, of course, not a constant, since Hooke's law does not hold. Referred to the original cross section, we have

$$E(L_z)=\frac{dZ}{dL}=M\frac{kT}{\langle L^2\rangle_{Av}}\left[1+\frac{2}{L_z^3}\right]. \tag{3.4}$$

For large values of L_z this approaches $\frac{1}{3}$ of its value for $L_z=1$—another feature for which one can easily check in experimental stress-strain curves. Referred to the actual cross section by use of (4.1), the stress is given by

$$\zeta=\frac{Z}{L_x^2}=M\frac{kT}{\langle L^2\rangle_{Av}}\left[L_z^2-\frac{1}{L_z}\right], \tag{3.5}$$

and the differential Young's modulus is

$$E_\zeta(L_z)=\frac{d\zeta}{dL_z}=M\frac{kT}{\langle L^2\rangle_{Av}}\left[2L_z+\frac{1}{L_z^2}\right]. \tag{3.6}$$

Unlike $E(L_z)$ this increases indefinitely with L_z.

Introducing the perhaps more customary strain variable, the extension $\epsilon=L_z-1$, one finds

$$Z=3M[kT/\langle L^2\rangle_{Av}]\epsilon[1-\epsilon+\tfrac{4}{3}\epsilon^2-\cdots]. \tag{3.7}$$

This form exhibits well the large deviations from Hooke's law shown by rubber.

The internal pressure in the unstressed rubber is simply related to the differential Young's modulus for zero stress:

$$P_0=MkT/\langle L^2\rangle_{Av}=\tfrac{1}{3}E(1). \tag{3.8}$$

For the rubber sample of Fig. 2, P_0 is thus about 5 kg/cm², a value which can be taken as representative for soft gum compounds. When this pressure is reduced by stretching one might expect an increase in the volume of the material. Since the compressibility of rubber is about 10^{-4} cm²/kg, the increase in volume due to complete removal of the internal pressure would be some 0.05 percent, an amount quite compatible with the observations of Holt and McPherson. Generalization of the theory to take account of the compressibility of the material, while simply accomplished, is, accordingly, of little interest.

4. FURTHER APPLICATIONS OF NEW MODEL WITH GAUSSIAN CHAINS

We now illustrate the application of our model to the treatment of a number of other properties of rubber.

The correction for the volume thermal expansion of the material is of considerable interest. If one deals with a cube of rubber having unit volume at temperature T_0 and a coefficient of thermal expansion α, the volume becomes at temperature T

$$V=1+\alpha(T-T_0). \tag{4.1}$$

Generalizing (3.3) to apply to temperatures other than the original one, one finds

$$Z=M\frac{kT}{\langle L^2\rangle_{Av}}\left[L_z-\frac{1+\alpha(T-T_0)}{L_z^2}\right], \tag{4.2}$$

the correction for the internal pressure being changed by a factor V. According to this, the stress at constant strain will not be exactly proportional to T, but will involve also a small negative term proportional to T^2. The tendency, described by this quadratic term, of thermal expansion to decrease the stress in material heated under constant strain is of course the dominant tendency in the case of a stretched wire. It should be noted, however, that in ordinary materials the temperature dependence of this term is different from that in rubber, the stress going down linearly with increasing temperature.

The effect of this correction term appears most clearly when one plots stress against temperature at various constant strains. Each stress-temperature curve will appear nearly straight if the range of temperature considered is not excessive; the most striking effect of the new terms in (4.2) is the change in slope of these curves with changing strain. If the strain is small $(\partial Z/\partial T)_L$ is negative, and the behavior is that of an ordinary body, while if the strain is large $(\partial Z/\partial T)_L$ has the large positive value usually considered characteristic of rubber. From (4.2) one finds

$$(\partial Z/\partial T)_{T=T_0}$$
$$=[Mk/\langle L^2\rangle_{Av}][L_z-(1+\alpha T_0)/L_z^2]. \tag{4.3}$$

Thus the critical extension L_{zc} at which the stress-temperature curve changes its slope is given by the isometric thermoelastic inversion point

$$L_{zc}^3 = 1 + aT_0. \tag{4.4}$$

For a soft unaccelerated gum compound with 8 percent sulphur content, $\alpha = 6.2 \times 10^{-4}$. For $T = 300°\text{K}$ one then obtains $L_{zc} = 1.065$—the inversion should take place for a strain of about 7 percent.

Since

$$(\partial L_z/\partial T)_Z = -(\partial L_z/\partial Z)_T(\partial Z/\partial T)_{L_z}, \tag{4.5}$$

$(\partial L_z/\partial T)_Z$ and $(\partial Z/\partial T)_{L_z}$ must change sign together. Thus the thermoelastic inversion point is the same for isotonic curves as for isometrics.

We now compute the linear thermal expansion coefficients of stretched rubber, both parallel and perpendicular to the direction of stress. The expansion coefficient parallel to the stress is

$$\alpha_{\parallel}(L_z) = (1/L_z)(\partial L_z/\partial T)_Z. \tag{4.6}$$

Using (4.5) together with (4.2) we obtain for $T = T_0$

$$\alpha_{\parallel}(L_z) = -\frac{1}{T}\frac{L_z^3 - 1}{L_z^3 + 2} + \frac{\alpha}{L_z^3 + 2}. \tag{4.7}$$

The expansion coefficient perpendicular to the stress is

$$\alpha_{\perp}(L_z) = (1/L_y)(\partial L_y/\partial T)_Z. \tag{4.8}$$

Since

$$V = L_y^2 L_z = 1 + \alpha(T - T_0), \tag{4.9}$$

one has at $T = T_0$,

$$\alpha_{\perp}(L_z) = \frac{1}{2T}\frac{L_z^3 - 1}{L_z^3 + 2} + \frac{\alpha}{2}\frac{L_z^3 + 1}{L_z^3 + 2}. \tag{4.10}$$

In the unstretched state, $L_z = 1$, we have

$$\alpha_{\parallel}(1) = \alpha_{\perp}(1) = \alpha/3, \tag{4.11}$$

as for any material. But as soon as the rubber is appreciably stretched the terms involving α become negligible:

$$\alpha_{\parallel}(L_z) \cong -(1/T)(L_z^3 - 1)/(L_z^3 + 2), \tag{4.12}$$

$$\alpha_{\perp}(L_z) \cong (1/2T)(L_z^3 - 1)/(L_z^3 + 2). \tag{4.13}$$

When these equations hold, the changes of dimensions of the material are quite unrelated to its volume expansion; they are shifts in relative dimensions needed to restore equilibrium as the effective stresses in the flexible chains vary with temperature. The coefficient of "expansion" parallel to the stress is negative, while the other is positive, a striking illustration of the anisotropy of stretched rubber. These linear expansion coefficients are large, of the order of magnitude $1/T$ of the volume expansion coefficients for gases. Equation (4.7) will make it clear why rubber stretched by a weight will contract visibly when it is warmed.

The change in temperature ΔT on adiabatic stretching is given according to thermodynamics by the following formula:

$$\Delta T = (T/C_L)\int_1^L (\partial Z/\partial T)_{L_z} dL_z, \tag{4.14}$$

where C_L designates the specific heat at constant length.

Inserting for $(\partial Z/\partial T)_{L_z}$ its value from (4.3) and integrating we obtain

$$\Delta T = (KT/2C_L)[L_z^2 + L_z - 2(1 + \alpha T_0)] \times [(L_z - 1)/L_z]. \tag{4.15}$$

According to this formula ΔT starts with the value zero at $L_z = 1$, reaches a minimum for $L_z = L_{zc}$ as given by (4.4), then becomes zero for the adiabatic thermoelastic inversion point, determined by

$$L_{z0}^2 + L_{z0} - 2(1 + \alpha T_0) = 0, \tag{4.16}$$

and takes on positive values for $L_z > L_{z0}$. For $T = 300°\text{K}$ and $\alpha = 6.2 \times 10^{-4}$ one obtains $L_{z0} = 1.13$—ΔT becomes zero for a strain of 13 percent, i.e., twice the strain at the isometric thermoelastic inversion point.

This model permits consideration of other distortions than simple stretch of rubber. We shall discuss briefly three of these: stretching in two directions, shear, and swelling followed by stretching.

Let a piece of rubber, a unit cube in the unstretched state, be stretched to length L_x in the x direction, and thereafter stretched to length L_z in the z direction. Neglecting compressibility effects, one has then

$$L_y = 1/L_x L_z. \tag{4.17}$$

The internal pressure is found, as before, by con-

sideration of the equilibrium of the free faces of the material, to be

$$P=[MkT/\langle L^2\rangle_{Av}](1/L_x^2L_z^2). \quad (4.18)$$

Thus by consideration of the faces perpendicular to the z axis,

$$Z=[MkT/\langle L^2\rangle_{Av}][L_z-1/L_x^2L_z^3]. \quad (4.19)$$

To make a proper check on this expression care must be taken that L_x and L_z are not made excessively large, for the deviations from Gaussian behavior of the molecular chains in real rubber, which will be discussed in later portions of this paper, will be particularly important in this case. It is a familiar fact that rubber stretched strongly in one direction is difficult to stretch in a perpendicular direction. As ordinarily observed this behavior is, however, probably largely conditioned by crystallization induced in the stretched rubber.

Examination of Section 3 and of the Appendix will show that the reduction from the irregular network to the model with parallel molecular chains will apply also for the discussion of shears. If a shear slides the xy planes of the model over each other in the x direction, both x chains and y chains will have their extensions unchanged and will exert no restoring forces. The internal pressure will also give no restoring forces. The z chains, however, will be stretched and will exert a component of force opposing the shear. Considering, as before, a unit cube, now sheared through an angle θ, the mean force exerted by a z chain, stretched in length by a factor $1/\cos\theta$, will be $[kT/\langle L^2\rangle_{Av}][1/\cos\theta]$, and the total component of force opposing the shear will be[14]

$$F_s=M[kT/\langle L^2\rangle_{Av}]\tan\theta. \quad (4.20)$$

The shear modulus is thus

$$G=dF_s/d\theta=M[kT/\langle L^2\rangle_{Av}]\sec^2\theta, \quad (4.21)$$

or, for infinitesimal deformations,

$$G=M[kT/\langle L^2\rangle_{Av}]. \quad (4.22)$$

[14] It will be noted that the shearing force is strictly proportional to the shear displacement, this being equal to the thickness of the sample times $\tan\theta$. M. Mooney, J. App. Phys. **11**, 582 (1940), has discussed from the point of view of phenomenologic elasticity theory the form which may be taken by stress-strain curves of elastic incompressible bodies having this property, and our relation is of course to be found as a special case of his general result, as pointed out by Dr. Mooney to us some time ago. The dependency upon temperature, however, cannot be obtained from elasticity theory.

This, of course, satisfies the relation with Young's modulus,

$$G=E/2(1+\mu), \quad (4.23)$$

as found in the theory of elasticity for infinitesimal deformations, when Poisson's modulus μ has the value 0.5 valid for incompressible materials.

Rubber has the remarkable property of being able to absorb large quantities of liquid hydrocarbons without loss of shape or elastic properties. The behavior of the resulting swollen rubber suggests that the hydrocarbon molecules do not greatly affect the structure of the material, but merely serve to increase its bulk and tend to prevent crystallization. If this assumption is correct our model should be able to explain the elastic properties of swollen rubber.

Suppose a unit cube of rubber to be swollen by the addition of an inert hydrocarbon until its linear dimensions are increased by the swelling factor σ. If it is then stretched or compressed until its z dimension is L_z, one has

$$L_zL_x^2=\sigma^3. \quad (4.24)$$

Proceeding as before, one finds

$$P=M[kT/\langle L^2\rangle_{Av}][1/L_z], \quad (4.25)$$

which is identical with (3.2). It is to be noted, however, that in the absence of external forces

$$P_0=M[kT/\langle L^2\rangle_{Av}](1/\sigma). \quad (4.26)$$

Comparing with (3.8), one sees that, as rubber is swelled by the introduction of inert liquid molecules, the internal pressure falls, varying inversely with the linear dimensions of the material. The stress-strain relation for the swollen cube is found to be

$$Z=M[kT/\langle L^2\rangle_{Av}][L_z-\sigma^3/L_z^2]. \quad (4.27)$$

This equation is not entirely comparable to (3.3), which relates to a portion of material which, in the unstretched state, is a unit cube. Modifying (4.27) to relate to a unit cube of the swollen material, rather than a swollen unit cube, we have

$$Z=M[kT/\langle L^2\rangle_{Av}](1/\sigma)[L_z-1/L_z^2]. \quad (4.28)$$

That is, swelling of rubber should reduce its rigidity by a factor of $1/\sigma$, but leave the form of the stress-strain curve unchanged.

Results (4.26) and (4.28) are simply understood as follows: Swelling of the material diminishes the number of chains crossing unit area by the factor $1/\sigma^2$, and also the number of links per unit stretched length of chain by the factor of $1/\sigma$. The latter change increases the force per chain by the factor σ. Thus, finally, the forces per unit area exerted by the chains, as well as the pressure forces which resist them, will be changed by $(1/\sigma^2)\sigma = 1/\sigma$.

The decrease in the rigidity of swollen rubber described by (4.28) is well known to occur. Unfortunately there does not seem to be available any experimental material permitting satisfactory quantitative comparison with this theory. Tiltman and Porritt[15] have measured the effect of benzene on the elastic properties of one particular vulcanizate, but the high percentage of zinc oxide in their material makes their data unsatisfactory for our purposes. It may be noted that, at very high strains, they observe decreases of stress on the addition of relatively small amounts of benzene which are quite out of proportion to those indicated by this theory. Here the effect is doubtless that of a reduction of the strain-induced crystallization.

Now it is obvious that the results of Sections 3 and 4 can be valid only when the extensions of the chains in the molecular network are not too large compared with their total lengths, since only in this case can the assumed Gaussian configuration distribution be an adequate approximation. The Gaussian distribution assigns a nonzero probability to any extension of the chain, however great, whereas the actual function for any finite chain must become zero as soon as L exceeds the total length of the chain. As L approaches this limit the true distribution function must fall toward zero faster than the Gaussian function. Then $-\log C(L)$ must increase more rapidly than quadratically, and $Z(L)$ for a single chain must increase more rapidly than linearly, becoming infinite as L approaches $L_{\max}$. This deviation from the linear stress-strain relation will make itself felt when bulk rubber is subjected to large strains; the effect will be the introduction of an upward curvature into the stress-strain curve, the stress increasing indefinitely as the stretched length approaches the finite maximum extension of the network. It is thus evident that with a more careful treatment of the stress-strain relation in molecular chains our model will show an upward curvature in the stress-strain curve similar to that shown in the experimental curve of Fig. 2, but lacking in the theoretical results of the present section. (The observed upward curvature is not to be explained entirely as due to crystallization effects, as it is evident even for strains insufficient to induce crystallization, or when this is suppressed by swelling.)

We turn, then, to a consideration of the stress-strain relation in a flexible thermally agitated chain when its extension is comparable to its total length.

5. STATISTICAL TREATMENT OF HIGHLY EXTENDED FLEXIBLE CHAINS: GENERAL METHODS

In applying the equation

$$Z = -kTd[\log C(L, N)]/dL \qquad (5.1)$$

to the computation of the stress-strain relation for a flexible chain under thermal agitation, one is, essentially, considering the chain to have a fixed extension and computing the average force exerted by it. That is, one determines

$$Z = \bar{Z}(L). \qquad (5.2)$$

An alternative approach which offers marked advantages for our problem is that of considering the chain with constant forces exerted on its ends and computing the average extension:

$$L = \bar{L}(Z). \qquad (5.3)$$

For chains of few links, the instantaneous value of L may differ markedly from $\bar{L}$, and the same is true for Z and $\bar{Z}$. Under these circumstances, Eqs. (5.2) and (5.3) are by no means converse relations; only in the limit of very long chains will the methods lead to essentially identical results. The advantage of the approach through (5.3) will be made evident by the example at the end of the present section.

We consider first a one-dimensional chain. If a constant force Z be applied to the ends of the chain there will be a potential energy $-ZL$ associated with the extension L. Let the number of

[15] A. H. Tiltman and B. D. Porritt, India-Rubber J. **78**, 345 (1929).

configurations available to the chain when its extension is L to within dL be

$$dC = C(L)dL. \tag{5.4}$$

The probability that the chain acted on by the force Z will have the extension L to within dL will then be proportional to

$$dP = e^{+ZL/kT}dC = C(L)e^{+ZL/kT}dL. \tag{5.5}$$

Let

$$f = Z/kT. \tag{5.6}$$

Then

$$\bar{L}(f) = \int LC(L)e^{fL}dL \Big/ \int C(L)e^{fL}dL, \tag{5.7}$$

or

$$\bar{L}(f) = d\left[\log \int C(L)e^{fL}dL\right] \Big/ df. \tag{5.8}$$

If L can take on only discrete values we have, instead,

$$\bar{L} = d(\log \textstyle\sum_L C(L)e^{fL})/df. \tag{5.8'}$$

Let $G(x)$ be the generating function for $C(L)$. That is, for the continuous case

$$G(x) = \int C(L)x^L dL, \tag{5.9}$$

and for the discrete case

$$G(x) = \textstyle\sum_L C(L)x^L. \tag{5.10}$$

Then in either case[16]

$$\bar{L} = d[\log G(e^f)]/df. \tag{5.11}$$

Often the most convenient method of determining $C(L)$ is by use of the generating function. Equation (5.11) offers a method of passing from $G(x)$ directly to a relation of the form (5.3), thus obviating the necessity of determining $C(L)$ and applying (5.1) to obtain a relation of the form (5.2).

Another point of view is often useful. We have

$$\langle e^{fL}\rangle_{Av} = \int e^{fL}C(L)dL \Big/ \int C(L)dL. \tag{5.12}$$

Thus

$$\bar{L} = d(\log \langle e^{fL}\rangle_{Av})/df. \tag{5.13}$$

As a third approach, we expand the exponential in the integrand, Eq. (5.12). Then

$$\langle e^{fL}\rangle_{Av} = \textstyle\sum_\tau f^\tau/\tau! \int L^\tau C(L)dL \Big/ \int C(L)dL. \tag{5.14}$$

Let

$$\langle L^\tau\rangle_{Av} = \int L^\tau C(L)dL \Big/ \int C(L)dL, \tag{5.15}$$

the average of L^τ in the force-free case. Using these relations, (5.13) becomes

$$L = d[\log \textstyle\sum_\tau \langle L^\tau\rangle_{Av} f^\tau/\tau!]/df. \tag{5.16}$$

It is instructive to relate the statistical treatments of flexible chains at constant extension, $Z = \bar{Z}(L, T)$, and at constant stress, $L = \bar{L}(Z, T)$, with the corresponding thermodynamic approaches to the problem.

When temperature and extension are chosen as independent variables in the treatment of a thermodynamic system it is natural to introduce the Helmholtz free energy function $F(L, T)$ and to determine stress from this:

$$Z = (\partial F/\partial L)_T. \tag{5.17}$$

As we have already noted, the free energy is related to the number of configurations accessible to the system, $C(L)$. ($C(L)$ is the partition function.)

$$F(L, T) = -kT \log C(L). \tag{5.18}$$

Thus Eq. (5.1) is simply the statistical form of (5.17).

Now if temperature and stress are chosen as independent variables in treating a thermodynamic system, one introduces the Gibbs function, which, for our system, becomes

$$\mathfrak{G}(Z, T) = U - ZL - TS. \tag{5.19}$$

From this one determines the extension of the system,

$$L = -(\partial \mathfrak{G}/\partial Z)_T. \tag{5.20}$$

Statistically the Gibbs function is related to the sum over all accessible states of the statistical assembly, weighted with the factor $e^{ZL/kT}$. In analogy to (5.18) we have

$$\mathfrak{G}(Z, T) = -kT \log D(Z), \tag{5.21}$$

[16] The discrete case can be formally unified with the continuous case by taking the integrals in the Stieltjes sense.

where $D(Z)$ is a generalized partition function

$$D(Z)=\int C(L)e^{ZL/kT}dL, \tag{5.22}$$

which is essentially the Laplace transform of the partition function $C(L)$. Since from (5.9) we have

$$D(Z)=G(e^{Z/kT})=G(e^f), \tag{5.23}$$

it is evident that (5.11) is the statistical version of the thermodynamic relation (5.20).

That $Z=\bar{Z}(L)$ and $L=\bar{L}(Z)$ are converse relations only in the limit of very long chains becomes, in thermodynamic terms, the statement that only in this limit does there exist an equation of state

$$Z=Z(L, T) \qquad \text{or} \qquad L=L(Z, T)$$

describing the system.

Depending on the circumstances, each of (5.11), (5.13), and (5.16) may serve as useful alternatives to (5.1).

The extension of these results to the case of a chain in three dimensions involves no difficulty. Let one end of the chain be fixed at the origin. Then the number of configurations of the chain for which its free end will lie in the infinitesimal volume dV will be

$$dC=C(x, y, z)dV. \tag{5.24}$$

If there is no preferred orientation of the system C will be a function of $x^2+y^2+z^2$ only.

Let a constant force of components Z_x, Z_y, Z_z be applied to the free end of the chain. Then the probability of finding the end of the chain in volume dV will be proportional to

$$dP=\exp\{(xZ_x+yZ_y+zZ_z)/kT\}C(x, y, z)dV. \tag{5.25}$$

As before, letting

$$\begin{aligned} f_x&=Z_x/kT, \\ f_y&=Z_y/kT, \quad \text{etc.}, \end{aligned} \tag{5.26}$$

one has

$$\bar{x}=\frac{\partial}{\partial f_x}\log\int e^{(xf_x+yf_y+zf_z)}C(x, y, z)dV, \tag{5.27}$$

$$\bar{y}=\frac{\partial}{\partial f_y}\log\int e^{(xf_x+yf_y+zf_z)}C(x, y, z)dV. \tag{5.28}$$

Ordinarily there will be no preferred orientation of the chain in space. Then, if a force is applied in the x direction, one will have $\bar{y}=\bar{z}=0$. Defining

$$C_x(x)=\int\int C(x, y, z)dydz, \tag{5.29}$$

one finds

$$\bar{x}=\frac{d}{df}\log\int e^{fx}C_x(x)dx. \tag{5.30}$$

Thus, in this case, one can reduce the three-dimensional problem to a one-dimensional problem by projecting the configuration function onto the direction of the applied force. In particular, if the chain consists of independent links, the problem can be reduced to a one-dimensional case at the very start, by projecting the probability distribution for the individual links onto this direction, and employing this projection in the treatment of the chain as a whole. If the links of the chain are not independent—i.e., the probability distribution for each link depends on the orientation of the adjacent links—the projection method can still be applied. One has then to deal with probability distributions for the projections of link extensions onto the force direction, these depending on the values of the projections for adjacent links. Examples of such reductions will be found in succeeding sections.

As a simple illustration of the application of these methods, we consider a one-dimensional chain of N links, each of which will, in the absence of external forces, contribute to the extension of the chain an amount $+1$ or -1, with equal probability. The relative number of ways in which an extension L of the chain can be obtained is clearly the coefficient of x^L in $(1/2^N)(x+1/x)^N$. We have, thus,

$$G(x)=(1/2^N)(x+1/x)^N, \tag{5.31}$$

and

$$C(L, N)=\frac{1}{2^N}\frac{N!}{[(N+L)/2]![(N-L)/2]!}. \tag{5.32}$$

To apply Eq. (5.1) one must first use Stirling's approximation, $N!\cong(2\pi N)^{\frac{1}{2}}N^Ne^{-N}$, for the factorials. In the case of the factorial $[(N-L)/2]!$

this will not be legitimate for L arbitrarily close to N, but, by increasing N, this approximation can be made good for values of the fractional extension

$$t=L/L_{\max}=L/N \tag{5.33}$$

arbitrarily close to 1. In terms of the fractional extension one has

$$C(L, N)=\frac{2}{(2\pi N)^{\frac{1}{2}}}(1+t)^{-(N/2)(1+t)} \times(1-t)^{-(N/2)(1-t)}(1-t^2)^{-\frac{1}{2}} \tag{5.34}$$

and

$$\bar{Z}=\frac{kT}{2}\log\frac{1+t}{1-t}-\frac{2}{N}\frac{t}{1-t^2}+0\left(\frac{1}{N^2}\right). \tag{5.35}$$

To apply (5.11) we have simply to note that according to (5.31)

$$G(e^f)=[\cosh f]^N. \tag{5.36}$$

Then

$$\bar{L}=N\frac{d}{df}\log\cosh f=N\tanh f, \tag{5.37}$$

or

$$t=\tanh f \tag{5.38}$$

exactly. Equation (5.38) is the inverse of (5.35) only in the limit of N large, in which all terms on the right, except the first, are to be neglected. Its derivation is almost trivial, there being no terms of order $1/N$ to be separated out and dropped in passing to the limit. This illustrates the essential advantage in computing $\bar{L}(Z)$ instead of $\bar{Z}(L)$: it is the former quantity which varies the more simply with the number of links in the chain. In less simple problems the importance of this advantage is greatly increased, as it becomes much more difficult to construct $C(L, N)$ explicitly. Usually it will be necessary to derive $C(L, N)$ by an inverse Laplace transformation from $G(e^f)$, whereas, by use of (5.11), the desired stress-strain relation can be derived directly from $G(e^f)$.

The next section, and especially a later paper, will provide more elaborate illustrations of these methods.

6. EXTENDED MODEL OF BULK RUBBER: CHAINS WITH INDEPENDENT LINKS

The simplest type of flexible chain which one may use to represent a rubber molecule consists of links of fixed length l, each of which will tend to take on all orientations in space with equal probability, whatever may be the orientations of the neighboring links. In this model a link will correspond, not to a single carbon-carbon bond, but to a section of the chain so long that constraints on the relative orientations of the ends are negligible. Just what this length should be is not well defined, and there will be a corresponding uncertainty in the magnitude of the forces computed using this model. In attributing a fixed length to each link we are also making a simplifying assumption which will somewhat affect the form of the stress-strain curve. Nevertheless, this model constitutes so marked an advance over that with Gaussian chains as to deserve consideration. In a later paper we shall compare this model with a more refined, but more intractable, model.

A three-dimensional vector of magnitude l which takes on all orientations with equal probability will have all x components between $-l$ and $+l$ with equal probability. Our three-dimensional chain is thus equivalent to a one-dimensional chain in which the ith link may make any contribution x between $+l$ and $-l$ to the extension, with equal probability when external forces are absent.

To treat this system one may use Eq. (5.13). Note that

$$\langle e^{fL}\rangle_{Av}=\langle\exp f(x_1+x_2+\cdots)\rangle_{Av} =\prod_i\langle\exp fx_i\rangle_{Av}, \tag{6.1}$$

since the x's vary independently. Now

$$\langle\exp fx_1\rangle_{Av}=\frac{1}{2l}\int_{-l}^{+l}\exp fx_1dx_1=\sinh lf/lf. \tag{6.2}$$

Thus for a chain of N links

$$\langle e^{fL}\rangle_{Av}=\{\sinh lf/lf\}^N. \tag{6.3}$$

Applying (5.13), we have at once

$$t=\coth lf-1/lf=\mathfrak{L}(lf), \tag{6.4}$$

where $\mathfrak{L}(x)$ is the Langevin function.

It is not possible to pass rigorously from the stress-strain relation thus derived for a single chain to that for an arbitrary three-dimensional network, since the reduction of the network to an equivalent set of independent chains as carried

out in Section 3 is not exact for these non-Gaussian chains. So long, however, as the conditions of stretch of the network are not too extreme we will expect that reduction to lead to a satisfactory approximation. Without further justification of the procedure we pass to the consideration of a model of rubber similar to that previously considered, except that in the unstretched state of the material each independent chain is taken to have an extension equal to κ times its maximum length. The maximum stretch for the model is thus given by a factor of $1/\kappa$, a quantity which will vary with the sample of rubber and will, accordingly, enter our treatment as a variable parameter.

As before, we consider a unit cube of the material, taken, in a first approximation, as incompressible. In the stretched condition $L_xL_yL_z=1$, as before. If a chain is given an extension L its fractional extension will be $t=L\kappa$. The stress-strain relation for the individual chain may then be expressed as

$$L\kappa=\mathfrak{L}(lZ/kT). \tag{6.5}$$

This defines a relation between the fractional extension of the model in a given direction and the tension of the chains extended in that direction which we express as

$$lZ/kT=\mathfrak{L}^{-1}(t). \tag{6.6}$$

One then finds, for the internal pressure in the model stretched only in the z direction, $(L_x=L_y=L_z^{-\frac{1}{2}})$,

$$P=(MkT/lL_yL_z)\mathfrak{L}^{-1}(t_y). \tag{6.7}$$

The stress-strain relation for the model as a whole becomes

$$Z=(MkT/l)[\mathfrak{L}^{-1}(t_z)-(L_y/L_z)\mathfrak{L}^{-1}(t_y)] \tag{6.8}$$

or

$$Z=(MkT/l)[\mathfrak{L}^{-1}(L_z\kappa)-L_z^{-\frac{1}{2}}\mathfrak{L}^{-1}(L_z^{-\frac{1}{2}}\kappa)]. \tag{6.9}$$

This relation involves essentially two parameters; Mk/l, which determines the scale of the forces just as in the Gaussian case, and the new maximum stretch parameter κ.

If the argument of the second term in the stress, that due to the internal pressure, is small,

$$\mathfrak{L}^{-1}(t)\cong 3t, \tag{6.10}$$

$$Z\cong(MkT/l)[\mathfrak{L}^{-1}(L_z\kappa)-3\kappa/L_z^2]. \tag{6.11}$$

When this approximation can be applied to both terms—all extensions small compared to the maximum—one has simply

$$Z\cong(3M\kappa kT/l)[L_z-1/L_z^2], \tag{6.12}$$

as for a Gaussian model. Putting $\kappa=1/Nl$ the relation (6.12) reduces exactly to (3.3), remembering that $\langle L^2\rangle_{Av}=\frac{1}{3}Nl^2$.

It should be noted that predictions of the theory for shear, stretch in two directions, swelling, and so on, as given in Section 4 for Gaussian chains will also be modified for higher extensions. Since these modifications are not formally interesting, and are quite insignificant so long as one does not deal with extreme distortions of the material, we shall not discuss them at this point.

Comparison of these results with experiment is deferred to Section 7.

The appearance of the Langevin function in these results is most easily understood by consideration of a method of treating stress-strain relations which is applicable only to chains of independent links. In cases in which the contribution of each link to the extension is independent of that of every other link, the reduction of the total problem to a one-dimensional equivalent may be accomplished by making a corresponding reduction for each individual link. We consider then a chain of N identical independent links, each of which will, in the force-free case, contribute to the x component of the extension of the chain according to the probability distribution $c(x)$. Then

$$\langle e^{fL_x}\rangle_{Av}=[\langle e^{fx}\rangle_{Av}]^N, \tag{6.13}$$

the average on the right being computed for an individual link. Consequently,

$$L_x=Nd(\log\langle e^{fx}\rangle_{Av})/df, \tag{6.14}$$

or

$$\bar{x}=\int x\exp(xZ_x/kT)c(x)dx \Big/ \int \exp(xZ_x/kT)c(x)dx. \tag{6.15}$$

Here we do not deal with t, as before, since the maximum extension might be infinite, but rather with $\bar{x}$, the average contribution of each link to the extension.

Equation (6.15) states that the contribution of each independent link in a flexible chain can be computed as if it were the only link present and the external forces were applied directly to its ends. This is true whether or not all links in the chain are described by the same distribution function $c(x)$.

The situation of an independent link in an extended flexible chain is thus completely analogous to that of a polar molecule in an electric or a magnetic field. The thermal agitation of the chain tends to disorient the links, to make the average contribution to the extension vanish, while the tension of the chain, in effect, is equivalent to a uniform field of force tending to align the links. The computations of the average contribution of a link to the extension and of the average contribution of a polar molecule to, say, the magnetic moment of a material are thus formally identical. If the link has a fixed length, the molecule a fixed moment, the computations are identical in detail; the Langevin function appears in each result.

In the same way the function $\tanh f$ which appears in Eq. (5.38) for the extension of a chain of links for which only two configurations are possible is the function which appears in Ehrenfest's classical theory of magnetism, which assumed the existence in crystals of polar atoms having two orientations of equal potential energy in the absence of a magnetic field. A chain model in which each link could take on a discrete set of orientations would similarly lead to the Brillouin function, of which Ehrenfest's $\tanh x$ is the simplest special case.[17]

We conclude this section with a more explicit statement of the role of the Gaussian distribution as an approximation in the case of chains of independent links. We assume that $c(x)$ is an even function of x, as it must be if there is no preferred direction in space. Then, expanding the exponentials of Eq. (6.15), one has

$$t=\int\left\{fx^2+\frac{1}{3!}f^3x^4+\frac{1}{5!}f^5x^6+\cdots\right\}c(x)dx \Big/ \int\left\{1+\frac{1}{2!}f^2x^2+\cdots\right\}c(x)dx, \quad (6.16)$$

or

$$t=f\langle x^2\rangle_{Av}+f^3\{\tfrac{1}{6}\langle x^4\rangle_{Av}-\tfrac{1}{2}(\langle x^2\rangle_{Av})^2\}+\cdots. \quad (6.17)$$

For very small f and t, the relation between these quantities is determined by the value of $\langle x^2\rangle_{Av}$, and is otherwise independent of the form of the distribution function. For larger extensions there will be deviations from the linear relation between t and f which will be determined by the relative values of $\langle x^2\rangle_{Av}$, $\langle x^4\rangle_{Av}$, $\cdots$, for a single link. If these are all in the same ratio as for a Gaussian chain, the higher terms in (6.17) all vanish, and $t=\langle x^2\rangle_{Av}f$ always. Otherwise, there is a deviation from the linear relation of f and t which is quite unaffected by any increase in the number of links in the chain. That is, as the number of links in the chain increases, the linear relation of Z and L holds to greater and greater values of L, but not of L/N; deviations from the linear relation of L and Z depend only on the fractional extension. Correspondingly, an increase in the number of links will make $C(L)$ approach the Gaussian form for any given range of L, but, in general, only for L small as compared with the maximum extension of the chain. Similarly, by making the chain long enough, one can make the $\langle L^r\rangle_{Av}$ of (5.15) approach the values for a Gaussian chain, for any given range of r. There will, however, always be deviations of these quantities from the Gaussian values at larger r, and these deviations will be important if the fractional extension of the chain becomes large. In short, the Gaussian approximation for the distribution function is dependable only if the fractional extension of the chain is sufficiently small —smaller, as our results show, than extensions actually encountered in bulk rubber.

The nature of the Gaussian form as an approximation to the more exact form of the configuration function may be illustrated more explicitly by reference to the one-dimensional problem treated in Section 5. Neglecting a slowly

[17] P. Ehrenfest, Proc. Amst. Akad. Sci., Dec. 18, 1920 or Leiden Communications, Suppl. 44b; cf. also P. Debye in Marx, *Handbuch der Radiologie*, Vol. VI, p. 712. For the Brillouin function, L. Brillouin, J. de phys. et rad. **8**, 74 (1927); also P. Debye, *loc. cit.*, p. 713. More recent accounts are given by J. H. van Vleck, *The Theory of Electric and Magnetic Susceptibilities* (Oxford, 1932), pp. 257, 289; and R. H. Fowler and E. A. Guggenheim, *Statistical Thermodynamics* (Cambridge, 1939), pp. 629–630.

varying factor $(1-t^2)^{-\frac{1}{2}}$ in (5.34), we have

$$C(L, N) \cong \frac{2}{(2\pi N)^{\frac{1}{2}}}(1+t)^{-(N/2)(1+t)}(1-t)^{-(N/2)(1-t)}. \tag{6.18}$$

This can be written without further approximation as

$$C(L, N) \cong \frac{2}{(2\pi N)^{\frac{1}{2}}} \exp\left\{-\frac{N}{2}\int \log\frac{1+t}{1-t}dt\right\}. \tag{6.19}$$

Since

$$\log[(1+t)/(1-t)] = 2(t+t^3/3+t^5/5+\cdots), \tag{6.20}$$

it is evident that, for small enough t, where all terms but the first are negligible, we have essentially the Gaussian distribution. Deviations from the Gaussian law set in when

$$(N/2)\int \tfrac{2}{3}t^3dt = Nt^4/4$$

becomes appreciably different from zero—for greater absolute extensions Nt and smaller relative extensions t as N is increased—and are very great when t is comparable to 1.

7. COMPARISON OF THEORY WITH EXPERIMENT

In explanation of the method to be used in comparing this theory with experiment we may survey briefly the approximations which have been made. A rather elaborate attempt has been made to treat the changes in entropy of the molecular network when the bulk material is deformed, as this accounts for much the greater part of the rigidity of the material. Here we were forced to neglect steric hindrances between chains —an approximation which we expect to be significant only for compact networks (highly vulcanized materials) or extreme deformations—and to carry out the reduction from an irregular to a regular one in an approximate way which will be increasingly in error as the deformation is increased. By including thermal expansion in our model phenomenologically we have introduced terms in the entropy which occur also in ordinary liquids, and also some terms in the internal energy. On the whole, however, the effects of changes in the internal energy have been ignored. We have neglected van der Waals forces between the atoms in a single molecule, which may affect the behavior of the material for small extensions by changing both the internal energy and the entropy, and also van der Waals forces between essentially independent chains of atoms. At the smaller extensions we may expect these latter forces to be largely taken into account by inclusion of the thermal expansion, but at large extensions they give rise to crystallization, a large effect which is entirely outside the domain of the present theory. On the whole it is apparent that the theory is essentially one of entropy forces, valid at most for extensions which do not induce crystallization. It will be reasonable and desirable to resolve both theoretical and experimental results so as to separate forces due to entropy changes from those due to changes in internal energy, and to deal with these separately, anticipating the better agreement for the entropy forces.

The division of the total force in unilaterally stretched materials into parts associated with the entropy and internal energy is expressed in Eq. (1.2). Since

$$Z_U = \left(\frac{\partial U}{\partial L}\right)_T = Z - T\left(\frac{\partial Z}{\partial T}\right)_L = Z - Z_S, \tag{7.1}$$

the two terms in Z can be determined separately as soon as $Z(L, T)$ is given, whether experimentally or theoretically. Proceeding from Eq. (4.2) and from the analogue of Eq. (6.11) which takes account of thermal expansion, for the cases of Gaussian and independent link chains, respectively, one finds for the entropy forces

$$Z_S = KT\{L_z - [1+\alpha(2T-T_0)]L_z^{-2}\}, \tag{7.2}$$

$$Z_S = K'T\{\mathfrak{L}^{-1}(L_z\kappa) - 3\kappa[1+\alpha(2T-T_0)]L_z^{-2}\}, \tag{7.3}$$

respectively. The forces associated with the internal energy are

$$Z_U = K\alpha T^2 L_z^{-2}, \tag{7.4}$$

$$Z_U = 3K'\kappa\alpha T^2 L_z^{-2}, \tag{7.5}$$

in the two approximations. In both cases the thermoelastic inversion point is given by

$$L_{zc}^3 = 1+\alpha T_0. \tag{7.6}$$

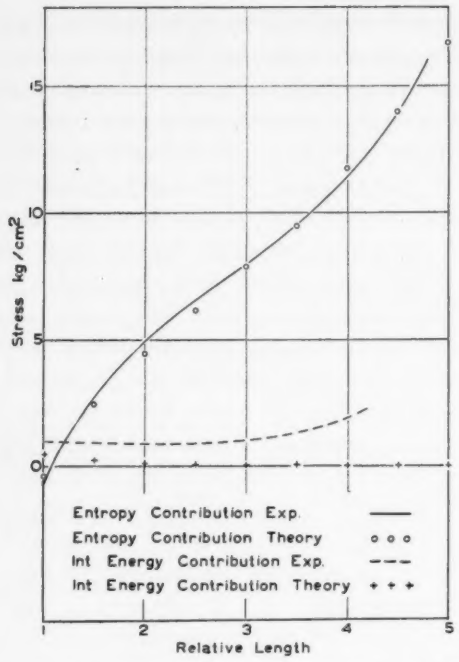

FIG. 3. Comparison of theory and experiment for natural rubber *A*.

Experimental stress-strain curves obtained under conditions carefully enough controlled to permit satisfactory comparison with our theoretical results are not abundant in the literature. In our preliminary report[4] comparisons were made between (7.2), with $\alpha=0$, and total stress-strain curves from the literature, with very encouraging results in the range of validity of that simplest theory. However, all the older experimental results are very incomplete, and, in particular, they do not permit a resolution of the observed stresses into parts Z_S and Z_U. To make possible a more satisfactory comparison with experiment some very careful and complete observations have been made and have been described elsewhere, by our experimental associates at Notre Dame, Dr. R. L. Anthony, Dr. R. H. Caston, Dr. L. E. Peterson, and Mr. S. L. Dart. We shall describe here the results with two types of vulcanized rubber and one synthetic rubberlike material of widely different composition.

A. Unaccelerated Natural Pure Gum[13]

This material was an unaccelerated pure gum stock containing 8 parts of sulfur and 100 parts of pale crepe rubber, cured for 3 hours at 147°C. It shows little permanent set and no crystallization for extensions up to 350 percent at room temperature. At higher temperatures greater extensions are possible without crystallization.

For this compound $\alpha=6.2\times10^{-4}$. The experimental value of L_{ze} is approximately 1.10, as compared with 1.065 as given by (7.6).

Z_S was found to be proportional to T, to within the experimental error.

Figure 3 shows the experimental values for both Z_S and Z_U in comparison with the values predicted by Eqs. (7.3), (7.5) for a model with chains of independent links, with $K'=24$, $\kappa=0.12$.

B. Accelerated Natural Pure Gum[18]

This stock was an accelerated pure gum compound containing 5 parts sulfur, 3 parts diphenylguanidine, 1 part zinc oxide, 100 parts pale crepe. It was cured for 30 minutes at 147°C. This compound showed little permanent set. Crystallization began at 250 percent extension at room tem-

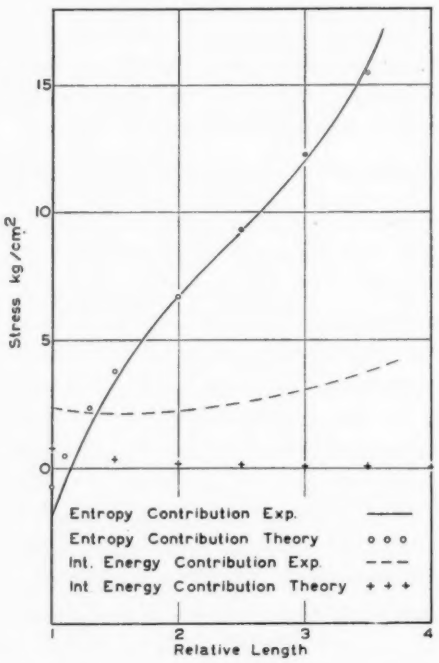

FIG. 4. Comparison of theory and experiment for natural rubber *B*.

[18] R. H. Caston, Notre Dame Thesis.
R. H. Caston, R. L. Anthony, and E. Guth, Detroit meeting of the American Physical Society, February, 1942; cf. Phys. Rev. **60**, 542 (1942).

perature, and at somewhat higher extensions when the temperature was raised.

For this compound, $\alpha = 7 \times 10^{-4}$. This leads to a calculated value $L_{xc} = 1.07$, against the value 1.14 given in reference 18. More recent work at Notre Dame, still unpublished, gives an improved experimental value $L_{xc} = 1.09$, in better agreement with the theory.

Z_S was found to be proportional to T, to within the experimental error.

Figure 4 shows experimental values for both Z_S and Z_U as functions of L, measured at 20°C. The indicated theoretical values were computed by Eq. (7.3), with $K' = 30$, $\kappa = 0.143$. In this case the fit was made in the middle of the range of L, since the discrepancy between the observed and computed thermoelastic inversion points indicated the presence of either errors or additional entropy terms in the forces measured at low extensions.

Figure 5 compares experimental[19] and theoretical values for the temperature rise in this material on stretching. These experiments give the isometric inversion point (ΔT a minimum) at $L = 1.07$ and the adiabatic inversion point ($\Delta T = 0$) at $L = 1.15$, in excellent agreement with the theoretical values of 1.065 and 1.13, respectively. Theoretical and experimental values of ΔT agree well over the whole range considered.

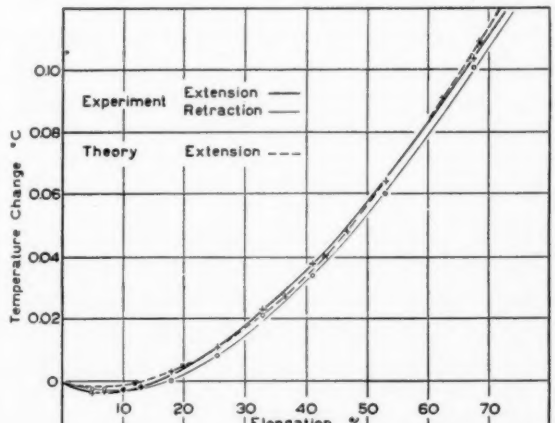

FIG. 5. Temperature changes of material *B* on stretching. +: Value measured after extension. ○: Value measured after retraction. ×: Theoretical value.

[19] Experimental work by S. L. Dart (unpublished).

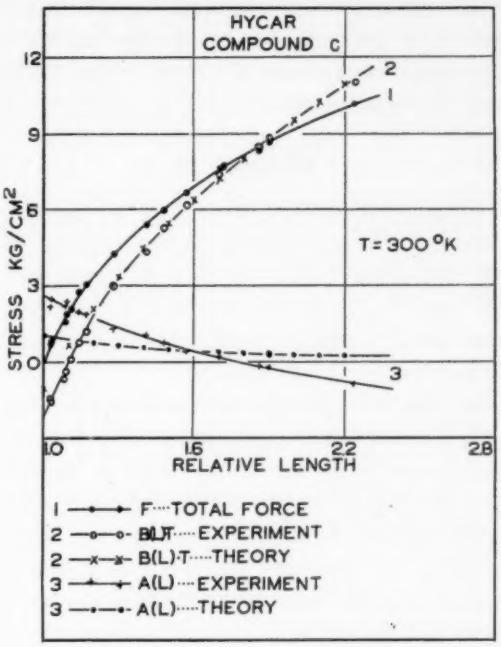

FIG. 6. Comparison of theory and experiment for Hycar compound *C*.

C. Accelerated Pure Gum Hycar[20]

The composition of this stock was as follows: 1 part sulfur, 1 part crude lauric acid, 5 parts zinc oxide, 100 parts Hycar *OR*. This compound, like all synthetics, exhibits considerable permanent set if stretched to higher extensions. Curing is not enough to restrict plasticity; it is necessary in addition to use reinforcing agents such as carbon black. We have wished to avoid consideration of compounds in which the reinforcing material adds a new element to the behavior of the material, and have accordingly been forced here to deal with extensions not exceeding 130 percent. Within this range the Gaussian approximation equations (7.2) and (7.4), are valid. No crystallization whatever was observed on stretching this material.

From the observed $\alpha = 5 \times 10^{-4}$ one computes $L_{xc} = 1.05$, as compared with the observed $L_{xc} = 1.10$.

Z_S was found to be proportional to T, to within the experimental error.

Figure 6 compares experimental and theo-

[20] L. E. Peterson, Thesis, Notre Dame, 1942; cf. L. E. Peterson, R. L. Anthony, and E. Guth, Ind. Eng. Chem. **34**, 1349 (1942).

retical results for this material. Again the fit was made with reference to moderate rather than very small extensions of the material. No estimate of κ is possible.

DISCUSSION

The proportionality of Z_S to T at constant L, shown by all these samples, is in complete accord with the theory. The terms in T^2 appearing in (7.3) are too small to produce an appreciable disturbance of this proportionality over the temperature range investigated.

The observed entropy stress-strain curves are in very satisfactory agreement with the theory in all cases, over the whole range of extensions here considered. At the very highest extensions of compounds A and B the observed stress is beginning to increase more rapidly than the theoretical. This may be considered as an effect of incipient crystallization, or it may be due to the approximate replacement of an irregular network by bundles of chains all with the same fractional extension in the unstretched state of the material. A more satisfactory approximation would certainly require the use of chains with a variety of initial fractional extensions. This would lead to just the behavior here observed—a more rapid increase in stress at large extensions than one would expect from the behavior at moderate extensions, due to the increasing relative importance of the shortest chains.

Compound B shows in addition an appreciable discrepancy in Z_S for L near 1, associated with a nearly equal and opposite discrepancy in Z_U. Compound C shows a similar discrepancy which vanishes for $L=1.2$—that is, rather more rapidly than in the case of compound B. The variability of this discrepancy and its rapid decrease with decreasing internal pressure in the material suggests that it is due to van der Waals forces neglected in the theory. The close agreement of the theoretical and experimental thermoelastic inversion points indicates that the actual discrepancy is even smaller than it appears to be in Figs. 3, 4, and 6.

Aside from the small effect just mentioned, synthetic rubber C gives excellent agreement with the theory. It is thus proved, apparently for the first time, that synthetics behave quantitatively in the same way as natural rubber under conditions for which thermoplasticity is negligible. It is to be emphasized that rubberlike elasticity requires the presence of a coherent network of flexible molecular chains, but does not depend on the special nature of the chains. The form of the stress-strain curves for small extensions (at least in the absence of excessive van der Waals forces) is then universal; variability in the behavior enters when plasticity is not completely suppressed, or the network approaches its maximum extension.

Experimentally, the entropy forces account for 80 percent or more of the total stress. As was to be expected, our theory gives a less satisfactory account of the smaller internal energy force. For very small extensions the predicted force is about half that observed. Whereas the theory predicts that this force will continually decrease as L increases, actually in the natural rubber compounds it passes through a minimum and then increases. In the case of the Hycar compound C this rise does not appear. The effect appears to be due to the increasing importance, as the chains are straightened and aligned, of those van der Waals forces which eventually lead to crystallization of the natural compounds.

The values of κ indicate immediately that in compounds of the type here considered the chains of the molecular network are, in the unstretched state of the bulk material, extended to some 10 percent of their maximum extension.

By combining this result with the observed Young's modulus of the material one can gain some idea as to the density of the active coherent network. At small extensions we have

$$E \cong 9MkT/Nl^2, \tag{7.7}$$

M being as before the effective number of chains in one coordinate direction and N the number of links per chain crossing a unit cube of unstretched material. Since each link contributes an amount l to the maximum extension of the chain we have

$$N=1/\kappa l. \tag{7.8}$$

Now as a measure of the fraction of the material actively involved in the network we may take the quantity

$$\Delta=3MNm/A\rho, \tag{7.9}$$

A being Avogadro's number, ρ the density of the material, and m the atomic weight per link in the chain. Combining these expressions, one obtains

$$\Delta = Em/3\kappa^2 A\rho kT. \tag{7.10}$$

Each link in our model chain will correspond, not to a carbon-carbon bond, as these are not independent of each other, but to a segment of chain just long enough for the orientations of neighboring sections to be nearly independent. If we suppose that each isoprene group should be represented by the links we have $m=35$. Introducing experimental values into Eq. (7.10) we then find $\Delta \sim \frac{1}{4}$. We thus estimate that some 25 percent of the molecular chains are active in the formation of the network, the remainder forming a relatively inert medium through which the network extends. This result, which appears to us to be physically reasonable, of course applies only to compounds similar to those here considered, for it may be much affected by the degree of vulcanization of the material. Increasing vulcanization, forming new links within the network and tending to link new material into it will tend to increase κ, E, M, and probably Δ. It would be very interesting to have more information on the way in which these quantities depend on the vulcanization of the material.

The idea of a molecular weight does not appear in the network theory of rubber, which considers essentially a single enormous molecule. There is, however, an interesting quantity, the mean weight of the chain segments between junctions in the network, which plays essentially the same role in this theory as mean molecular weight does in the theory of Kuhn. To determine this quantity one must go beyond the proper bounds of the present work, setting up a more detailed theory of the structure of the network in unstressed rubber, presumably on the basis of consideration of the processes by which it is formed.

Kuhn's theory leads to an estimated molecular weight because it does involve a definite picture of the conditions in unstressed rubber, the assumption that the distribution of extensions of the molecules is then essentially that which would obtain at any instant if the molecules were freely suspended in a fluid. On this basis the mean contribution of a molecule to the elastic constant becomes independent of its length, and one can determine from this constant the total number of molecules irrespective of length. With Kuhn's effective distribution of extensions one has

$$E(1) = 7G_0 kT, \tag{7.11a}$$

G_0 being the total number of molecules per unit volume. An at least equally reasonable theory which considers only the distribution of distances between the ends of the molecules would give

$$E(1) = 3G_0 kT. \tag{7.11}$$

(Note that under these assumptions the valence angle does not enter into the expression for the molecular weight.) From G_0 one can at once determine a mean molecular weight

$$\mu = \rho A/G_0. \tag{7.12}$$

Now we have shown in the Appendix that in the network theory of rubber (at least in the case of Gaussian chains) the mean positions of the junctions of the network move in just the way that Kuhn assumes the ends of the molecules to move when the material is distorted. Correspondingly the lengths of chain between these junctions will enter our theory in the same way that the molecular weight enters Kuhn's. If we were to assume that the mean extensions of the chain segments were related to their lengths by the same distribution function which would apply to thermal agitation of the free segments, we would obtain the same result as in the above modification of Kuhn's theory, with G_0 now the number of active chain segments between junctions. For the mean weight of chains between junctions we would then obtain

$$\mu = \rho A\Delta/G_0, \tag{7.13}$$

the presence of the factor Δ marking an essential change from the point of view of Kuhn. The mean weight of a chain between junctions thus comes out on our theory to be of the order of one-fourth of Kuhn's molecular weight. Combining this relation with (4.15) and (4.16), one has

$$\mu = m/\kappa^2, \tag{7.14}$$

while the number of links between junctions is simply

$$\mu/m = 1/\kappa^2. \tag{7.15}$$

On this basis we would estimate that the number of links between junctions is of the order of 100 in the materials considered. We do not wish to emphasize this result unduly, as it is not clear that it would arise from a more detailed theory of network structure, in which, we suspect, the relatively large extensions would appear more frequently than in the thermal distribution.

One of us (H. M. J.) wishes to express his appreciation of the grant of a Guggenheim Memorial Fellowship, during the tenure of which part of this work was done. We wish to acknowledge very helpful discussions with Professor R. H. Fowler during the early part of our work on this problem. We are also indebted to Professor G. E. Uhlenbeck for reading the manuscript of our paper and for constructive suggestions.

APPENDIX. FORCES EXERTED BY AN IRREGULAR NETWORK OF FLEXIBLE CHAINS: REDUCTION OF AN IRREGULAR NETWORK TO A REGULAR NETWORK

In this Appendix we shall discuss the average forces exerted by an irregular network of Gaussian flexible chains, by a method which involves rather detailed consideration of the statistical behavior of such a network. The method, as an approach to the final result, is not the most direct one possible, but it gives a particularly clear picture of the situation and provides useful intermediate results. It seems to offer a basis for further study of the behavior of these networks, and indeed of non-Gaussian networks, to which our basic theorem equally applies.

Consider a network of flexible chains of arbitrary type, certain junction points of which are subject to external constraints which may, for instance, force the network to extend through a given volume in space. The constrained junctions (on which alone the network can exert a non-zero average force) will be indicated by roman letter subscripts, their positions being indicated by $\mathbf{r}_a$ or x_a, y_a, z_a, while free junctions will be distinguished by numerical subscripts; greek letters may indicate either type.

As already noted, we can compute the average components of force exerted by the network on fixed junction a as

$$F_{xa}(x,y,z)=-kT\frac{\partial}{\partial x}\log \mathfrak{Z}(x,y,z), \tag{8.1}$$

$$F_{ya}(x,y,z)=-kT\frac{\partial}{\partial y}\log \mathfrak{Z}(x,y,z),$$

where $\mathfrak{Z}(x,y,z)$ is the number of configurations available to the network when the fixed junction a is at the point x,y,z, all other constraints on the network being taken into account.

One can also compute this average force as the sum of the average forces due to all chains reaching the ath junction. The average force due to the chain running from the ath junction to the τth junction (fixed or free) can be computed by treating the τth junction as fixed and averaging the results over all possible positions of the τth junction, with weights proportional to the probabilities with which these positions occur. We shall show that this procedure is valid, in the absence of steric hindrances, by proving that it gives the same result as the preceding method.

Let the number of links in the chain between the ath and τth junction be $N_{a\tau}$, the number of configurations available to this chain be $c(N_{a\tau}, \mathbf{r}_a-\mathbf{r}_\tau)$. Then, neglecting steric hindrances, the number of configurations available to the network as a whole, when the position of every junction is specified, is

$$C(\mathbf{r}_1, \mathbf{r}_2, \cdots, \mathbf{r}_a, \mathbf{r}_b\cdots) = c(N_{12}, \mathbf{r}_1-\mathbf{r}_2)c(N_{23}, \mathbf{r}_2-\mathbf{r}_3)\cdots, \tag{8.2}$$

with one factor on the right for every chain joining a pair of junctions. The number of configurations available to the network for specified positions of the fixed junctions only is

$$\mathfrak{Z}(\mathbf{r}_a, \mathbf{r}_b, \cdots)=\int dV\cdot C(\mathbf{r}_1, \mathbf{r}_2, \cdots \mathbf{r}_a, \mathbf{r}_b\cdots), \tag{8.3}$$

the indicated integration being over the positions of all free junctions. If we indicate by $\int dV_\tau$ integration over the coordinates of all free junctions *except* the τth, then the probability distribution for the τth free junction is

$$P_\tau(\mathbf{r}_\tau; \mathbf{r}_a, \mathbf{r}_b, \cdots) = \int dV_\tau C(\mathbf{r}_1, \mathbf{r}_2, \cdots) \Big/ \int dV C(\mathbf{r}_1\mathbf{r}_2, \cdots). \tag{8.4}$$

As indicated, this is a function of the position of all fixed junctions as well as of the τth free one.

In this notation the x component of force on the ath fixed junction is by the standard method,

$$F_{xa}(\mathbf{r}_a, \mathbf{r}_b, \cdots)=-kT\frac{\partial}{\partial x_a}\log \mathfrak{Z}(\mathbf{r}_a, \mathbf{r}_b, \cdots). \tag{8.5}$$

We now compute this force as given by the proposed method.

The x component of force exerted on the ath junction by the chain running to the τth junction, considered as fixed at $\mathbf{r}_\tau$, is

$$f_{xa\tau}=-kT\frac{\partial}{\partial x_a}\log c(N_{a\tau}, \mathbf{r}_a-\mathbf{r}_\tau). \tag{8.6}$$

By the proposed method the total x component of force is then

$$F_{xa}=\Sigma_\tau\int d\mathbf{r}_\tau P_\tau(\mathbf{r}_\tau; \mathbf{r}_a, \mathbf{r}_b, \cdots)f_{xa\tau}, \tag{8.7}$$

the sum being over all chains ending at the ath junction. Using (8.4) and (8.6) this becomes

$$F_{xa}=-kT\int dVC(\mathbf{r}_1, \mathbf{r}_2, \cdots)\frac{\partial}{\partial x_a}\Sigma_\tau \log c(N_{a\tau}, \mathbf{r}_a-\mathbf{r}_\tau) \Big/ \int dVC(\mathbf{r}_1, \mathbf{r}_2, \cdots). \tag{8.8}$$

Remembering the form of C as given in (8.2), we can

express this as

$$F_{xa}=-kT\frac{\partial}{\partial x_a}\int dVC(\mathfrak{r}_1, \mathfrak{r}_2, \cdots \mathfrak{r}_a \cdots)\Big/\int dVC(\mathfrak{r}_1, \mathfrak{r}_2, \cdots), \tag{8.9}$$

which is identical with (8.5) as required.

This method is particularly easy to apply when the chains are all of Gaussian type. It then becomes a trivial matter to average over the positions of the free junctions, all of which are subject to probability distributions of Gaussian form. For a Gaussian chain between the τth and νth junctions we have as the x component of force on the νth junction

$$f_{x\nu\tau}=\frac{2kT}{l^2N_{\tau\nu}}(x_\tau-x_\nu). \tag{8.10}$$

If $P_\tau(\mathfrak{r}_\tau)$ is of Gaussian form,

$$\int d\mathfrak{r}_\tau x_\tau P_\tau(\mathfrak{r}_\tau)=x_{o\tau}, \tag{8.11}$$

where $x_{o\tau}$ is the x coordinate of the center of the distribution. The average x component of force between the τth and νth junctions is then

$$\int\int d\mathfrak{r}_\tau d\mathfrak{r}_\nu P_\tau(\mathfrak{r}_\tau)P_\nu(\mathfrak{r}_\nu)f_{x\tau\nu}(\mathfrak{r}_\tau-\mathfrak{r}_\nu)$$

$$=\frac{2kT}{l^2N_{\tau\nu}}(x_{o\nu}-x_{o\tau})=f_{x\tau\nu}(\mathfrak{r}_{o\tau}-\mathfrak{r}_{o\nu}). \tag{8.12}$$

Thus the average force between the junctions is the same as if both were fixed at the centers of their respective Gaussian distributions, and is entirely independent of the extent of these distributions. Accordingly, for the special case of Gaussian chains we can get the mean force on any fixed point by determining (1) the elastic constants $(2kT/l^2N)$ of the chains attached to this point, and (2) the mean position of the other ends of these chains.

It remains to prove the above statement that all junctions of an irregular network of Gaussian chains have probability distributions of Gaussian form. We have, when all chains are Gaussian,

$$C(\mathfrak{r}_1, \mathfrak{r}_2, \cdots)=\exp\left\{-\frac{1}{l^2}\left[\frac{|\mathfrak{r}_1-\mathfrak{r}_2|^2}{N_{12}}+\frac{|\mathfrak{r}_2-\mathfrak{r}_3|^2}{N_{23}}+\cdots\right]\right\}, \tag{8.13}$$

or

$$C(\mathfrak{r}_1, \mathfrak{r}_2, \cdots)=\exp\left\{-\frac{1}{l^2}\sum_{\tau>\nu}\sum\frac{1}{N_{\tau\nu}}\times[(x_\tau-x_\nu)^2+(y_\tau-y_\nu)^2+(z_\tau-z_\nu)^2]\right\}, \tag{8.14}$$

in which expression we can sum over all pairs of junctions (τ, ν) if we take $N_{\tau\nu}=\infty$ whenever there is no chain connecting the τth and νth junctions.

Let us now consider the most probable configuration of the junctions in the network—the positions of the free junctions which make C a maximum. The coordinates of these points we shall denote by $x_{o\tau}$, $y_{o\tau}$, $z_{o\tau}$, and we shall let $x_{oa}=x_a$, etc., in the case of the fixed junctions. Then these quantities can be determined from the equations

$$\left.\begin{aligned}\sum_\tau\frac{1}{N_{\tau\nu}}(x_{o\tau}-x_{o\nu})=0\\ \sum_\tau\frac{1}{N_{\tau\nu}}(y_{o\tau}-y_{o\nu})=0\\ \sum_\tau\frac{1}{N_{\tau\nu}}(z_{o\tau}-z_{o\nu})=0\end{aligned}\right\}\nu=1, 2, 3, \cdots, \tag{8.15}$$

where the sum is over all junctions, free or fixed. These equations determine the coordinates $x_{o\tau}$, $y_{o\tau}$, $z_{o\tau}$ of the free junctions as linear expressions in the corresponding coordinates of the fixed junctions:

$$\begin{aligned}x_{o\tau}&=c_{\tau a}x_a+c_{\tau b}x_b+\cdots,\\ y_{o\tau}&=c_{\tau a}y_a+c_{\tau b}y_b+\cdots,\\ z_{o\tau}&=c_{\tau a}z_a+c_{\tau b}z_b+\cdots.\end{aligned} \tag{8.16}$$

The coefficients c which appear in these equations are functions of the N's only.

If we introduce as new variables

$$\begin{aligned}X_\tau&=x_\tau-x_{o\tau},\\ Y_\tau&=y_\tau-y_{o\tau},\\ Z_\tau&=z_\tau-z_{o\tau},\end{aligned} \tag{8.17}$$

specifying the position of each free junction with respect to its position in the most probable configuration, the expression for C becomes

$$C(\mathfrak{r}_1, \mathfrak{r}_2, \cdots)=\exp\left\{-\frac{1}{l^2}\sum_{\tau>\nu}\sum\frac{1}{N_{\tau\nu}}\times[(x_{o\tau}-x_{o\nu})^2+(y_{o\tau}-y_{o\nu})^2+(z_{o\tau}-z_{o\nu})^2]\right\}$$

$$\times\exp\left\{-\frac{1}{l^2}\sum_{\tau>\nu}\sum\frac{1}{N_{\tau\nu}}\times[(X_\tau-X_\nu)^2+(Y_\tau-Y_\nu)^2+(Z_\tau-Z_\nu)^2]\right\}. \tag{8.18}$$

In reducing (8.14) to this form we have used (8.15) and the fact that for fixed junctions $X=Y=Z=0$. The first factor on the right is, by (8.16), a quadratic form in the coordinates of the fixed junctions only, while the second factor involves coordinates of both free and fixed junctions.

If one integrates (8.18) over the coordinates of the free junctions only the second factor is affected. One obtains then

$$\mathfrak{P}(\mathfrak{r}_a, \mathfrak{r}_b, \cdots)=K\exp\left\{-\frac{1}{l^2}\sum_{\tau>\nu}\sum\frac{1}{N_{\tau\nu}}\times[(x_{o\tau}-x_{o\nu})^2+(y_{o\tau}-y_{o\nu})^2+(z_{o\tau}-z_{o\nu})^2]\right\}, \tag{8.19}$$

with K a function of the N's only. Using this expression together with (8.1), one can proceed to a discussion of the forces exerted by the network. Instead, we pass on to the evaluation of $P_\mu(\mathfrak{r}_\mu)$. This we can write as

$$P_\mu(\mathfrak{r}_\mu)=\frac{1}{K}\mathfrak{P}(\mathfrak{r}_a, \mathfrak{r}_b, \cdots)\int dV_\mu\exp\left\{-\frac{1}{l^2}\sum_{\tau>\nu}\sum\frac{1}{N_{\tau\nu}}\times[(X_\tau-X_\nu)^2+(Y_\tau-Y_\nu)^2+(Z_\tau-Z_\nu)^2]\right\}, \tag{8.20}$$

or as

$$P_\mu(\mathfrak{r}_\mu)=\frac{1}{K}\mathfrak{P}(\mathfrak{r}_a, \mathfrak{r}_b\cdots)I(X_\mu)I(Y_\mu)I(Z_\mu), \tag{8.21}$$

with

$$I(X_\mu)=\int dX_1\cdots dX_{\mu-1}dX_{\mu+1}\cdots \times\exp\left\{-\frac{1}{l^2}\sum_\tau\sum_{\nu>\tau}\frac{1}{N_{\tau\nu}}(X_\tau-X_\nu)^2\right\}. \quad (8.22)$$

Now one can write the sum in the exponent as

$$\left(\sum_\tau\frac{1}{N_{1\tau}}\right)\{X_1-L(X_2, X_3\cdots)\}^2+Q(X_2, X_3, \cdots),$$

where X_1 is singled out for special treatment, and L is a linear form, Q a quadratic form in the other variables. Integrating over X_1, one gets

$$I(X_\mu)=k\int dX_2\cdots dX_{\mu-1}dX_{\mu+1}\cdots \times\exp\left\{-\frac{1}{l^2}Q(X_2, X_3, \cdots)\right\}, \quad (8.23)$$

where k depends only on the N's. Proceeding similarly to carry out the other integrations, one finally obtains

$$I(X_\mu)=[K']^{\frac{1}{2}}\exp\left\{-\frac{1}{l^2}\frac{1}{N_\mu}X_\mu^2\right\}, \quad (8.24)$$

where N_μ is the number of links in a chain which would give a similar distribution; it depends on the number of links in all the various chains in the network. We have then, from (8.21) and (8.24),

$$P_\mu(\mathbf{r}_\mu)=\frac{K'}{K}\mathfrak{L}(\mathbf{r}_a, \mathbf{r}_b, \cdots)\exp\left\{-\frac{1}{l^2}\frac{1}{N_\mu}|\mathbf{r}_\mu-\mathbf{r}_{o\mu}|^2\right\}, \quad (8.25)$$

a Gaussian distribution, as was to be proved. It will be noted that the extent of the distribution is independent of the positions of the fixed junctions, i.e., the way in which the network is stretched. The position of its center turns out to be the point $\mathbf{r}_{o\mu}$ and is related to the position of the fixed junctions by

$$\mathbf{r}_{o\mu}=c_{\mu a}\mathbf{r}_a+c_{\mu b}\mathbf{r}_b+\cdots. \quad (8.16')$$

We now note a useful and suggestive classical analogue to the network of Gaussian flexible chains. In this model each molecular chain, e.g., that of $N_{\tau\nu}$ links connecting the τth and νth junctions, is to be replaced by a classical elastic thread with the same elastic constant,

$$Z/L=2kT/l^2N_{\tau\nu}. \quad (8.26)$$

The equilibrium positions of the junctions of this classical network are just the mean positions of the corresponding junctions of the molecular network. This becomes evident at once when we write (8.14) as

$$C(\mathbf{r}_1, \mathbf{r}_2, \cdots)=\exp\{-V(\mathbf{r}_1, \mathbf{r}_2, \cdots)/kT\}, \quad (8.27)$$

where

$$V(\mathbf{r}_1, \mathbf{r}_2, \cdots\mathbf{r}_a, \cdots)=\frac{kT}{l^2}\sum_\tau\sum_{\nu>\tau}\frac{1}{N_{\tau\nu}} \times[(x_\tau-x_\nu)^2+(y_\tau-y_\nu)^2+(z_\tau-z_\nu)^2] \quad (8.28)$$

is the potential energy of the classical thread model. The condition that C shall be a maximum is also the condition that V shall be a minimum; (8.15) determines not only the mean positions of the free junctions of the molecular chains, but also the equilibrium positions of the junctions in its classical analogue.

It follows at once that the classical analogue and the molecular network, being similar in all relevant respects, will exert exactly the same mean forces on their corresponding fixed junctions. Thus if one wishes to treat the elastic properties of massive rubber using a model involving a network of Gaussian chains, one can go a step farther in the discussion of forces and mean positions of junctions, completing a cycle, by returning to a classical model in which each molecular chain is replaced by a corresponding elastic thread.

Now it is evident from (8.16), or on examination of the classical analogue, that if the x coordinates of all fixed junctions are increased by a constant factor the same will be true of the mean x coordinates of all free junctions, while the mean y and z coordinates will be unchanged. Generalizing this, it follows easily that if the fixed junctions of a network are given the motion of points in a classical uniform elastic continuum under uniform stretch in one or more directions, with or without superimposed shears, then the mean positions of the free junctions will also move like points in that elastic continuum. For example, if the fixed junctions of the network are constrained to lie on the surface of a parallelepiped, which is then distorted by stretches and shears, the interior free junctions will undergo, as concerns their mean positions, displacements corresponding to those same stretches and shears. It should be noted, however, that there is no corresponding effect on the form or extent of the probability distributions for the positions of the free junctions.

Another observation of importance is that the forces exerted by a network are the same whether any given junction is treated as free, or as fixed at what would be its most probable position if it were free. This is evident from (8.12), or from the fact that the classical analogue to the chain network is the same in either case. This observation, together with the preceding one, forms the basis of our discussion in Section 7 of the relation of our model to that of Kuhn. If the network is regarded as imbedded in and exerting its forces, at the fixed junctions, on a continuum which is subject only to uniform distortions, one obtains a model which corresponds to that of Kuhn. Since we can consider *all* junctions as fixed, as above, and acting on the continuum, it is evident that the connectivity of the network is not of importance; we can introduce a parallel displacement of the fixed ends of any chains we may select without changing the net force on the continuum, and in this way we could break up or modify the connectivity of the network to any desired degree, arriving in the limit at a model which is essentially that of Kuhn. What are of prime importance in determining the magnitude of the forces exerted by a network are the mean separation and relative orientation of the ends of each chain; the connectivities enter only through their influence on these quantities. Indeed, to determine the effective elastic constants of a Gaussian network one need only specify the number of chain segments and the distribution of their mean fractional extensions (since these determine the mean forces); in the isotropic material all orientations of the segments would of course be equally probable.

Now, as in our model for bulk rubber, let us consider a network of Gaussian chains stretched through a unit cube by having certain junctions constrained to lie on each of the six cube faces, $x=0$, $x=1$, $y=0$, $y=1$, $z=0$, $z=1$. The free junctions will then all have mean positions within or on the surface of the cube. If the separation between the x faces is changed from 1 to L_x there will be a corresponding change in the difference in the x coordinates of any pair of junctions, the force between those junctions [cf. (8.10)], and the total normal force on the x faces. The y and z coordinates of all junctions will, however, be unchanged, as will the total forces between the y planes and the z planes. In short, the normal force between opposing forces of the model will be proportional to the separation of those faces, and independent of all other dimensions. This is exactly the behavior of a model in which sets of independent chains run between opposite faces of the cube without interfering with or affecting each other in the least. If the network is isotropic in the mean then this equivalent but simplified network can be chosen as having equal numbers M, of chains, with equal numbers of links, N, stretching between opposite faces of the cube. This is the model with which, for ease of visualization, we have made our calculations. It should be noted that the forces between opposite faces depend only on M/N so long as we deal with Gaussian networks. Thus it is not possible to determine either M or N separately from any observation on rubber under conditions in which this model is adequate.

It is easily shown that this simplified model will give results equivalent to those with the original irregular network when shears are present.

It can be shown by simple examples that reduction of an arbitrary irregular network to an equivalent set of three independent bundles of chains of equal length, acting in the three coordinate directions, is not always possible. So long as the departure from Gaussian behavior is not extreme it should, however, provide a serviceable approximation.

THE JOURNAL OF CHEMICAL PHYSICS VOLUME 11, NUMBER 10 OCTOBER, 1943

Frequency Spectrum of Crystalline Solids. II. General Theory and Applications to Simple Cubic Lattices

ELLIOTT W. MONTROLL
Palmer Physical Laboratory, Princeton University, Princeton, New Jersey

(Received July 23, 1943)

At temperatures not too close to its melting point, the molecules in a crystalline solid vibrate with simple harmonic motion about fixed equilibrium positions in a space lattice. In order to calculate the thermodynamic properties of the solid, one must know the distribution of frequencies of the normal modes of vibration of the component oscillators. On the basis of the Born-Kármán model, the frequencies of the normal modes are the characteristic roots of a matrix. The moments of the frequency distribution can be found from the traces of powers of the matrix. Methods are developed for calculating the frequency spectrum and thermodynamic functions from these moments. The frequency spectrum of a simple cubic lattice is studied by deriving its polynomial approximation from its moments. The spectrum has two maxima, one near the middle of its frequency range and the other at the high frequency end. As the ratio of the interactions between next nearest neighbors to those of nearest neighbors increases, the height of the low frequency maximum increases and that of the high frequency maximum decreases. Specific heats are calculated from the moments of the frequency distribution.

INTRODUCTION

A CRYSTALLINE solid, to a first approximation, can be pictured as a set of atoms or molecules whose equilibrium positions form a periodic lattice in space and which at a given time, due to thermal motion or interactions with neighbors, may be displaced slightly from their equilibrium positions. Neglecting non-harmonic displacements (which tend to become increasingly important at higher temperatures) every possible state of motion of the crystal is a linear combination of its so-called normal modes of vibration.

According to classical mechanics and classical statistics, to find the thermodynamic properties of such a system one needs only to know its number of normal modes or degrees of freedom.[1] For example, the specific heat C_v, at constant

[1] J. Mayer and M. Mayer, *Statistical Mechanics* (J. Wiley and Sons, New York, 1940), Chapter 11.

volume is the product of the number of normal modes and Boltzmann's constant k. Such a theory leads to the old Dulong-Petit result of a constant C_v independent of temperature. To eliminate the contradiction between this classical result and the experimentally observed decrease in C_v with temperature, Einstein[2] suggested that the contribution of a normal mode with a frequency ν_i is that of a quantized oscillator in the Planck sense, so

$$C_v = k \sum_i (h\nu_i/2kT)^2/\sinh^2 (h\nu_i/2kT), \quad (1)$$

where h is Planck's constant and T is the absolute temperature. By assuming independence of molecules or atoms at individual lattice points and equality of frequencies of normal modes Einstein obtained his well-known results which agree qualitatively with experiments but quantitatively deviate somewhat at low temperatures. Debye[3-5] improved the situation at low temperatures by treating a solid as a continuous elastic medium in which the fraction of normal modes with frequencies in a small interval $d\nu$ at ν are proportional to $\nu^2 d\nu$. Now the Debye theory involves a parameter Θ_D (related to the largest frequency), the Debye temperature of the solid, which theoretically should be a constant independent of the temperature. Actually if one plots as a function of the temperature the values of Θ_D necessary to make the Debye C_v agree exactly with the experimental ones at the same temperatures, the resulting curve is far from a constant in the low temperature region.[6] Born and Kármán[7] have proposed a molecular approach to the frequency spectrum problem that seems to explain the variation of Θ_D at low temperatures and which, at the same time, is sounder than the Debye model in that it provides a molecular picture of a molecular situation.

Born and Kármán in a straightforward manner deduce the equations of motion for the set of atoms in the crystal and by substituting periodic solutions into these equations they find that the squares of the frequencies of the normal modes of vibration are characteristic values of a matrix which we shall leave undefined at the present and merely signify by M^2. That is, to find the frequencies of the normal modes one must find the characteristic values of

$$M^2\psi = \lambda\psi = \nu^2\psi. \quad (2)$$

(ψ is an unknown vector which satisfies (2) and which shall not interest us here.) For every $\lambda_i = \nu_i^2$ which is a characteristic value of M^2, there are two frequencies $+\nu_i$ and $-\nu_i$, the positive one of which is to be used for finding thermodynamic properties (i.e., to be substituted into equations like (1)). The frequencies $\{\nu_i\}$ turn out to be so densely distributed between $-\nu_L$ and ν_L ($\lambda_L = \nu_L^2$ is the largest characteristic value of (2)) that one can define a continuous function $g(\nu)$ such that $g(\nu)d\nu/3N$ is the fraction of frequencies in the interval $d\nu$ at ν. From (2) it is apparent that

$$g(\nu) = g(-\nu)$$

causing the odd moments of the distribution function $g(\nu)$ to vanish:

$$\int_{-\nu_L}^{\nu_L} \nu^{2n+1} g(\nu) d\nu = 0 \quad (3a)$$

and

$$\int_{-\nu_L}^{\nu_L} \nu^{2n} g(\nu) d\nu = 2\int_0^{\nu_L} g(\nu)\nu^{2n} d\nu. \quad (3b)$$

Now it is well known that if $\{\lambda_i\}$ is the set of characteristic values of the matrix M^2

$$\text{Trace } M^2 = \sum_i \lambda_i = \sum_i \nu_i^2$$

and

$$\text{Trace } M^{2k} = \sum_i \lambda_i^k = \sum_i \nu_i^{2k}.$$

If the order of M^2 is $3N$, the average value of the $2k$th powers of the frequencies are

$$(1/3N)\ \text{Trace } M^{2k} = (1/3N) \sum_i \nu_i^{2k}$$

and since this by definition is the $2k$th moment of $g(\nu)$

$$(1/6N)\int_{-\nu_L}^{\nu_L} g(\nu)\nu^{2k} d\nu = (1/3N)\ \text{Trace } M^{2k} = \mu_{2k}. \quad (4)$$

---

[2] A. Einstein, Ann. d. Physik **22**, 180 (1906); **34**, 170 (1911).
[3] P. Debye, Ann. d. Physik **39**, 789 (1912).
[4] E. Schroedinger, *Handbuch der Physik*, X (1926).
[5] R. Fowler, *Statistical Mechanics* (University Press, Cambridge, and Macmillan Company, New York, 1936), Chapter IV.
[6] M. Blackman, Proc. Roy. Soc. **148**, 365, 384 (1935); **159**, 416 (1937).
[7] M. Born and T. von Kármán, Physik. Zeits. **13**, 297 (1912); **14**, 15 (1913).

With a knowledge of M^2 for a given crystal one can (at least with an infinite amount of patience) calculate all the moments of the function $g(\nu)$ and the problem of determining $g(\nu)$ is reduced to the moment problem of statistics—given a set of moments $\{\mu_{2k}\}$, to find the distribution function which has these moments.[8]

The first part of this paper will be devoted to outlining some applications of the moments of $g(\nu)$ to the direct calculation of thermodynamic quantities and to a discussion of methods of solution of the moment problem. In the second part a detailed study of the Born-Kármán model of a monatomic crystal with a simple cubic lattice will be made.

I. USES OF THE MOMENTS OF THE FREQUENCY SPECTRUM

A. Calculation of Thermodynamic Quantities

1. General Considerations

In order to calculate the average value of a thermodynamic quantity f (as a function of the temperature) of a crystalline solid one must evaluate integrals of the form

$$f(T)=\int_0^\infty f(\nu, T)g(\nu)d\nu. \tag{5}$$

For certain models of crystals (with $3N$ degrees of freedom) it is not difficult to evaluate the moments[8]

$$\mu_{2k}=\int_0^\infty \nu^{2k}g(\nu)d\nu/3N \tag{6}$$

of $g(\nu)$. With this in mind, we shall derive an expression for $f(T)$ involving the moments of $g(\nu)$ instead of $g(\nu)$ itself. Let us define

$$F(x, T)=(2/\pi)^{\frac{1}{2}}\int_0^\infty f(\nu, T)\cos \nu x d\nu, \tag{7a}$$

$$G(x)=(2/\pi)^{\frac{1}{2}}\int_0^\infty g(\nu)\cos \nu x d\nu. \tag{7b}$$

Then by the well-known Parseval formula[9]

$$f(T)=\int_0^\infty F(x, T)G(x)dx. \tag{8}$$

[8] E. Montroll, J. Chem. Phys. **10**, 218 (1942).

[9] E. Titchmarsh, *Introduction to the Theory of Fourier Integrals* (Oxford University Press, Oxford, 1937), p. 50.

The quantity $F(x, T)$ can usually be expressed in closed form—for example, consider the temperature-dependent component of the average internal energy:

$$E(T)=\int_0^\infty h\nu g(\nu)d\nu/(e^{h\nu/kT}-1). \tag{9}$$

The cosine transform of

$$\epsilon(\nu, T)=h\nu/(-1+\exp(h\nu/kT))$$

is the integral

$$E(x, T)=\left(\frac{2}{\pi}\right)^{\frac{1}{2}}kT\int_0^\infty \frac{\theta\nu\cos \nu x d\nu}{e^{\theta\nu}-1}, \tag{10}$$

when $\theta=h/kT$. It is not difficult to show that[10]

$$\int_0^\infty \frac{\sin \alpha z dz}{e^{2\pi z}-1}=\frac{e^\alpha+1}{4(e^\alpha-1)}-\frac{1}{2\alpha}. \tag{11a}$$

Therefore, differentiation with respect to α yields

$$2\int_0^\infty \frac{z\cos \alpha z dz}{e^{2\pi z}-1}=\frac{1}{\alpha^2}-\frac{e^\alpha}{(e^\alpha-1)^2} \tag{11b}$$

and

$$E(x, T)=\frac{2\pi^2h}{\theta^2}\left(\frac{2}{\pi}\right)^{\frac{1}{2}}\left\{\frac{\theta^2}{4\pi^2x^2}-\frac{e^{2\pi x/\theta}}{(e^{2\pi x/\theta}-1)^2}\right\}. \tag{12}$$

The cosine transformation of the distribution function $g(\nu)$ is

$$\begin{aligned}G(x)&=\left(\frac{2}{\pi}\right)^{\frac{1}{2}}\int_0^\infty g(\nu)\cos \nu x d\nu\\&=\left(\frac{2}{\pi}\right)^{\frac{1}{2}}\int_0^\infty \sum_{n=0}^\infty \frac{(-1)^n(\nu x)^{2n}}{(2n)!}g(\nu)d\nu\\&=\left(\frac{2}{\pi}\right)^{\frac{1}{2}}\sum_{n=0}^\infty \frac{(-1)^n x^{2n}}{(2n)!}\int_0^\infty \nu^{2n}g(\nu)d\nu\\&=3N\left(\frac{2}{\pi}\right)^{\frac{1}{2}}\sum_{n=0}^\infty \frac{(-1)^n x^{2n}\mu_{2n}}{(2n)!}.\end{aligned} \tag{13}$$

Therefore, from (8),

$$E(T)=E_0+(12\pi hN/\theta^2)\int_0^\infty \left\{\frac{\theta^2}{4\pi^2x^2}-\frac{e^{2\pi x/\theta}}{(e^{2\pi x/\theta}-1)^2}\right\}\sum_{n=0}^\infty \frac{(-1)^n x^{2n}\mu_{2n}dx}{(2n)!} \tag{14}$$

[10] E. Whittaker and G. Watson, *Modern Analysis* (Cambridge University Press, Cambridge, 1935), p. 122.

and

$$C_v/3Nk=\frac{2\pi}{\theta}\int_0^\infty \operatorname{csch}^2\frac{\pi x}{\theta}\times\left\{\frac{\pi x}{\theta}\coth\frac{\pi x}{\theta}-1\right\}\sum_{n=0}^{\infty}\frac{(-1)^n x^{2n}\mu_{2n}dx}{(2n)!}. \quad (15)$$

E_0 is proportional to the sum $\sum\nu_i$ which in a Born-Kármán model is the trace of the positive square root of the matrix M^2.

2. *High Temperature Series*

Of course at high temperatures a useful formula results immediately from the expansion of $f(\nu, T)$ as a power series in $1/T$. Again, consider the internal energy

$$E(T)=\sum_{i=1}^{3N}\{h\nu_i/2+h\nu_i/(e^{h\nu_i/kT}-1)\}. \quad (16)$$

Since

$$x/(e^x-1)=1-x/2-\sum_{n=1}^{\infty}(-1)^n B_n x^{2n}/(2n)!,$$

where the B_n's are Bernoulli numbers and $|x|<2\pi$,

$$E(T)=kT\sum_{i=1}^{3N}\left[\frac{h\nu_i}{2kT}+1-\frac{h\nu_i}{2kT}-\sum_n\frac{(-1)^n(h\nu_i/kT)^{2n}}{(2n)!}B_n\right],$$

when $|h\nu_{\max}/kT|<2\pi$. Now the moments of the frequency distribution are

$$(1/3N)\int_0^\infty \nu^n g(\nu)d\nu=\sum\nu_i{}^n/3N=\mu_n,$$

therefore[11]

$$E(T)=3NkT-3NkT\sum_{n=1}^{\infty}\frac{(-1)^n B_n}{(2n)!}\times\left(\frac{h}{kT}\right)^{2n}\mu_{2n} \quad (17)$$

and

$$C_v=3Nk-3Nk\sum_{n=1}^{\infty}\frac{(-1)^n B_n(1-2n)}{(2n)!}\times\left(\frac{h}{kT}\right)^{2n}\mu_{2n}, \quad (18a)$$

when

$$T>h\nu_{\max}/2\pi k.$$

Remembering that $B_1=1/6; B_2=1/30; B_3=1/42;$ $\cdots$ we have (if $\theta=h/kT$)

$$C_v/3Nk\sim 1-\frac{\theta^2\mu_2}{12}+\frac{\theta^4\mu}{240}-\frac{\theta^6\mu_6}{6048}+\cdots. \quad (18b)$$

B. Solution of the Moment Problem

This section will be devoted to introducing several methods of finding the distribution function $g(\nu)$ from its moments. The first procedure will be based on the Fourier integral theorem and the others will be applications of the method of least squares.

If the Fourier integral of $g(\nu)$ is $G(x)$ (Eq. (13)),

$$G(x)=(2/\pi)^{\frac{1}{2}}\int_0^\infty g(\nu)\cos\nu x d\nu=3N(2/\pi)^{\frac{1}{2}}\sum_{n=0}^{\infty}(-1)^n x^{2n}\mu_{2n}/(2n)!, \quad (13)$$

the inversion of (13) by the Fourier integral theorem yields

$$g(\nu)=\left(\frac{2}{\pi}\right)^{\frac{1}{2}}\int_0^\infty G(x)\cos x\nu dx=\frac{6N}{\pi}\int_0^\infty\sum_{n=0}^{\infty}\frac{(-1)^n x^{2n}\mu_{2n}\cos\nu x dx}{(2n)!}. \quad (14)$$

In general, the power series representation of $G(x)$ cannot be expressed in closed form in terms of well-known functions, so one must resort to numerical integration actually to obtain $g(\nu)$ from (14). This is unfortunate, for in order to obtain a complete $g(\nu)$ curve one would have to make a numerical integration for every value of ν; and, furthermore, the resulting $g(\nu)$ would not be in an analytic form, as one might like to have it. However, as will be shown later in a discussion

[11] This type of development was first made by H. Thirring, Physik. Zeits. **14**, 867 (1913); **15**, 127, 180 (1914).

of the method of least squares, some results derivable from (13) and (14) are useful in the determination of errors involved in the application of the method of least squares.

Although the properties of Fourier integrals do not seem to be suited to our problem, those of Fourier series are. Since we are interested only in $g(\nu)$ when $|\nu| \leq \nu_L$ (ν_L is the largest frequency of a normal mode) and

$$g(\nu)=0 \qquad \text{if} \qquad |\nu|>\nu_L, \tag{15}$$

we can express $g(\nu)$ in the interval $<-\nu_L, \nu_L>$ by the cosine series:

$$g(\nu)=a_0/2+\sum_{n=1}^{\infty} a_n \cos(n\pi\nu/\nu_L), \tag{16}$$

where the coefficients $\{a_n\}$ are computed by the well-known scheme of multiplying (16) by $\cos(n\pi\nu/\nu_L)d\nu$ and observing the orthogonality of the elements of the set $\{\cos(n\pi\nu/\nu_L)\}$:

$$a_0=\mu_0/\nu_L \tag{17a}$$

and

$$\begin{aligned} a_n &= (1/\nu_L)\int_{-\nu_L}^{\nu_L} g(\nu)\cos(\pi n\nu/\nu_L)d\nu \\ &= (1/\nu_L)\int_{-\nu_L}^{\nu_L} g(\nu) \\ &\qquad \times\sum_{m=0}^{\infty}(-1)^m(n\pi\nu/\nu_L)^{2m}d\nu/(2m)! \\ &= (6N/\nu_L)\sum_{m=0}^{\infty}(-1)^m(n\pi/\nu_L)^{2m}\mu_{2m}/(2m)!. \end{aligned} \tag{17b}$$

Thus the coefficients of the $(\cos n\pi\nu/\nu_L)$'s are linear combinations of the moments of $g(\nu)$.

This Fourier development of $g(\nu)$ is really a special example of the method of least squares. Suppose we try to approximate $g(\nu)$ by a function $G(a_0, a_1, \cdots, a_k; \nu)\equiv G(a;\nu)$ of a set of parameters $\{a_n\}$ chosen in such a manner that

$$\begin{aligned} I(a_0, a_1, \cdots, a_k) &= I(a) \\ &= \int_{-\nu_L}^{\nu_L}[g(\nu)-G(a;\nu)]^2 d\nu \end{aligned} \tag{18}$$

(where $a=(a_1, \cdots, a_k)$) is a minimum. According to the calculus of variations, the necessary condition for $I(a)$ to be a minimum is

$$\partial I(a)/\partial a_n=0; \quad n=0, 1, \cdots, k \tag{19a}$$

or

$$\int_{-\nu_L}^{\nu_L} g(\nu)(\partial G/\partial a_n)d\nu - \int_{-\nu_L}^{\nu_L} G(a;\nu)(\partial G/\partial a_n)d\nu=0. \tag{19b}$$

The simplest way of finding a set of a's to satisfy (18) is to choose $G(a, \nu)$ as a linear combination of a set of functions

$$\varphi_0(x), \varphi_1(x), \cdots, \varphi_n(x) \qquad (x=\nu/\nu_L)$$

orthonormal in the interval $<-1, 1>$, i.e.,

$$\int_{-1}^{1}\varphi_i(x)\varphi_j(x)dx=\delta_{ij}. \tag{20}$$

For, in that case,

$$G(a;\nu)=\sum_{n=0}^{k} a_n\varphi_n(\nu/\nu_L) \tag{21}$$

and Eq. (19) becomes

$$\int_{\nu_L}^{\nu_L} g(\nu)\varphi_n(\nu/\nu_L)d\nu - \int_{-\nu_L}^{\nu_L}\sum_m \varphi_m(\nu/\nu_L)\varphi_n(\nu/\nu_L)a_m d\nu=0$$

or by (20)

$$a_n=\int_{-1}^{1} g(x\nu_L)\varphi_n(x)dx. \tag{22}$$

In the special case

$$\varphi_n(x)=\cos xn\pi,$$

the coefficients are the linear combinations of the moments of $\{\mu_{2n}\}$ that were given in (17). And for any finite number k, the coefficients determined in (17) are just those which give the best k-term Fourier approximation in the least square sense. This development has the disadvantage that each coefficient depends on all the moments of $g(\nu)$. Actually it is possible to find other approximations to $g(\nu)$ such that a_k depends only on the first k μ_{2n}'s.[8] For example, if

$$\varphi_n(x)=[(2n+1)/2]^{\frac{1}{2}}P_n(x),$$

where $P_n(x)$ is the nth Legendre polynomial,

$$a_n=[(2n+1)/2]^{\frac{1}{2}}\int_{-1}^{1}g(x\nu_L)P_n(x)dx. \quad (23)$$

When n is odd, $a_n=0$, for $g(x\nu_L)P_n(x)$ is an even function and when n is even (say $2n$)

$$P_{2n}(x)=\sum_{r=0}^{n}\frac{(-1)^r(4n-2r)!x^{2n-2r}}{2^{2n}r!(2n-r)!(2n-2r)!}.$$

Therefore

$$a_{2n}=[(4n+1)/2]^{\frac{1}{2}}\int_{-1}^{1}g(x\nu_L)\times\sum_{r=0}^{n}\frac{(-1)^r(4n-2r)!x^{2n-2r}dx}{2^{2n}r!(2n-r)!(2n-2r)!}$$

$$=3N[(4n+1)/2]^{\frac{1}{2}}\times\sum_{r=0}^{n}\frac{(-1)^r(4n-2r)!\mu_{2n-2r}}{r!(2n-r)!(2n-2r)!\nu_L{}^{2n-2r+1}2^{2n}} \quad (24)$$

and a_{2n} depends only on the moments μ_{2k} with $k\leq n$. Finally

$$g(\nu)=\sum_{n=0}^{\infty}[(4n+1)/2]^{\frac{1}{2}}a_{2n}P_{2n}(\nu/\nu_L). \quad (25)$$

Another type of approximating function whose k parameters depend only on the first k even moments of $g(\nu)$ is (assuming that $x=\nu/\nu_L$)

$$G(a_0, a_1, \cdots, a_{2k}; x)=\sum_{n=0}^{2k}a_nx^n.$$

Since $g(\nu)=g(-\nu)$ and we would also want $G(a:x)$ to be an even function, all the odd coefficients a_{2n+1} vanish and

$$G(a_0, a_2, a_4, \cdots, a_{2k}; x)=\sum_{n=0}^{k}a_{2n}x^{2n}. \quad (26)$$

From (19b)

$$\int_{-\nu_L}^{\nu_L}g(\nu)(\nu/\nu_L)^{2n}d\nu-\sum_{m=0}^{k}a_{2m}\int_{-\nu_L}^{\nu_L}(\nu/\nu_L)^{2(m+n)}d\nu=0 \quad (27)$$

$$n=0, 1, 2, \cdots, k.$$

But

$$\int_{-\nu_L}^{\nu_L}g(\nu)\nu^{2n}d\nu=6N/\mu_{2n} \quad (28a)$$

and

$$\int_{-\nu_L}^{\nu_L}\nu^{2(m+n)}d\nu=2\nu_L/[2(m+n)+1]. \quad (28b)$$

Therefore the set of $k+1$ equations (27) become

$$\begin{aligned}
a_0/1+a_2/3+a_4/5+\cdots+a_{2k}/(2k+1)&=3N\mu_0/\nu_L,\\
a_0/3+a_2/5+a_4/7+\cdots+a_{2k}/(2k+3)&=3N\mu_2/\nu_L{}^3,\\
a_0/5+a_2/7+a_4/9+\cdots+a_{2k}/(2k+5)&=3N\mu_4/\nu_L{}^5,\\
&\cdots\cdots\cdots\cdots\cdots\cdots\cdots\cdots\\
a_0/(2k+1)+a_2/(2k+3)+\cdots+a_{2k}/(4k+1)&=3N\mu_{2k}/\nu_L{}^{2k+1}.
\end{aligned}$$

Or, if we write the matrix of this set of linear equations as

$$A(k)=\begin{pmatrix}1 & 1/3 & 1/5 & \cdots & 1/(2k+1)\\ \cdots & \cdots & \cdots & \cdots & \cdots\\ 1/(2k+1) & 1/(2k+3) & \cdots & \cdots & 1/(4k+1)\end{pmatrix} \quad (29)$$

and define

$$a(k)=(a_0, a_2, a_4, \cdots, a_{2k}), \quad (30)$$

$$\mu(k)=(3N/\nu_L)(\mu_0, \mu_2/\nu_L{}^2, \mu_4/\nu_L{}^4, \cdots, \mu_{2k}/\nu_L{}^{2k}), \quad (31)$$

our set of linear equations becomes the matrix equation

$$a(k)\cdot A(k)=\mu(k). \quad (32)$$

Now suppose $A^{-1}(k)$ is the inverse of $A(k)$. Then

$$a(k)=\mu(k)\cdot A^{-1}(k) \quad (33)$$

and each component of $a(k)$ can be found from $\mu(k)$ and $A^{-1}(k)$. By direct multiplication it is possible to verify that

$$A^{-1}(1)=1,$$

$$A^{-1}(2)=\frac{1}{(1!)^2 2^2}\begin{pmatrix}(1\cdot3)(1\cdot3)/1 & -(1\cdot3)(3\cdot5)/3\\ -(3\cdot5)(1\cdot3)/3 & (3\cdot5)(3\cdot5)/5\end{pmatrix}$$

$$=\frac{1}{4}\begin{pmatrix}9 & -15\\ -15 & 45\end{pmatrix},$$

$$A^{-1}(3)=\frac{1}{(2!)^2 2^4}\begin{pmatrix}(1\cdot3\cdot5)(1\cdot3\cdot5)/1 & -2(1\cdot3\cdot5)(3\cdot5\cdot7)/3 & 1(1\cdot3\cdot5)(5\cdot7\cdot9)/5\\ -2(3\cdot5\cdot7)(1\cdot3\cdot5)/3 & 4(3\cdot5\cdot7)(3\cdot5\cdot7)/5 & -2(3\cdot5\cdot7)(5\cdot7\cdot9)/7\\ (1\cdot3\cdot5)(5\cdot7\cdot9)/5 & -2(5\cdot7\cdot9)(3\cdot5\cdot7)/7 & (5\cdot7\cdot9)(5\cdot7\cdot9)/9\end{pmatrix}$$

and, in general, the element in the ith row and jth column of $A^{-1}(k)$, $a^*_{ij}(k)$, is*

$$a^*_{ij}(k)=\frac{(-1)^{i+j}(2i-1)(2i+1)(2i+3)\cdots(2i+2k-3)(2j-1)(2j+1)\cdots(2j+2k-3)\binom{k-1}{j-1}\binom{k-1}{i-1}}{(k-1)!2^{2k-2}[2(i+j)-3]}$$

$$=\frac{(-1)^{i+j}(2i+2k-3)!(2j+2k-3)!(k-1)!}{2^{4k-4}(2i-2)!(2j-2)!(i+k-2)!(j+k-2)!(k-j-2)!(k-i-2)![2(i+j)-3]}. \tag{34}$$

Therefore

$$a_i=\sum_{j=0}^{k}\mu_{2j}a^*_{ji}(k)$$

$$=\frac{(2i+2k-1)!(k-1)!}{2^{4k-4}(2i-2)!(i+k-2)!(k-i-2)!}\sum_{j=0}^{k}\frac{(-1)^{i+j}(2i+2k-3)!\mu_{2j}}{(2j-2)!(j+k-2)!(k-j-2)![2(i+j)-3]}. \tag{35}$$

Anyone using the method of least squares soon realizes that the accuracy with which an approximating function represents an initial function after a best set of constants have been chosen depends significantly on the form of the approximating function. With a given set of moments one can determine the best (in the least square sense) approximating function to $g(\nu)$ of all those discussed above by seeing which minimizes the integral

$$I(a)=\int_{-\nu_L}^{\nu_L}g^2(\nu)d\nu-2\int_{-\nu_L}^{\nu_L}g(\nu)G(a;\nu)d\nu+\int_{-\nu_L}^{\nu_L}G^2(a;\nu)d\nu\geqslant 0.$$

The component of $I(a)$: $\int G^2(a;\nu)d\nu$ depends only on the approximating function under investigation, so its calculation causes no trouble. And when $G(a;\nu)$ is taken to be a Fourier series, a sum of Legendre functions, or a polynomial, it is clear that

$$\int_{-\nu_L}^{\nu_L}g(\nu)G(a;\nu)d\nu$$

can be evaluated in terms of the set of constants a and the moments of $g(\nu)$. Inasmuch as we do not know $g(\nu)$ itself, there is no direct way of finding $\int g^2(\nu)d\nu$. However, if $G(x)$ is the Fourier integral of $g(\nu)$, Parseval's theorem yields

$$\int_{-\nu_L}^{\nu_L}g^2(\nu)d\nu=\int_{-\infty}^{\infty}g^2(\nu)d\nu=\int_{-\infty}^{\infty}G^2(x)dx.$$

Now from direct calculation in special cases it

* The author is indebted to Mr. W. Bower of Cornell University for calculating the inverse matrices $A^{-1}(k)$ for several small values of k. His calculations indicated how the general inverse could be obtained.

seems that $G(x)$ has a strong greatest maximum at the origin. This indicates that $G^2(x)$ would have an even stronger greatest maximum there and that the integral of $G^2(x)$ could be calculated numerically. With a knowledge of the three components of $I(a)$ one could find the mean square deviation of an approximating function $G(a, \nu)$ from $g(\nu)$.

It is also possible to find the maximum error in thermodynamic quantities calculated on the basis of a frequency spectrum $G(a; \nu)$ instead of the exact one $g(\nu)$. Suppose we wish to find the thermodynamic function

$$f(T)=\int_0^\infty f(\nu, T)g(\nu)d\nu.$$

Writing

$$g(\nu)=G(a; \nu)+\epsilon(\nu),$$

where $\epsilon(\nu)$ is the error in approximating $g(\nu)$ by $G(a; \nu)$ at ν,

$$f(T)=\int_0^\infty f(\nu, T)G(a; \nu)d\nu+\int_0^\infty f(\nu, T)\epsilon(\nu)d\nu.$$

Our problem now is to find an upper bound in the error resulting from writing

$$f(T)=\int_0^\infty f(\nu, T)G(a; \nu)d\nu.$$

Since

$$\int_0^\infty f(\nu, T)\epsilon(\nu)d\nu=\int_0^{\nu_L} f(\nu, T)[g(\nu)-G(a; \nu)]d\nu,$$

the Schwartz inequality[12] indicates that

$$\int_0^{\nu_L} f(\nu, T)[g(\nu)-G(a; \nu)]d\nu$$

$$\leq\left\{\left[\int_0^{\nu_L} f^2(\nu, T)d\nu\right]\left[\int_0^{\nu_L}[g(\nu)-G(x, \nu)]^2d\nu\right]\right\}^{\frac{1}{2}}$$

$$=\left[\left[\int_0^{\nu_L} f^2(\nu, T)d\nu\right]I(a)/2\right]^{\frac{1}{2}}$$

and

$$f(T)=\int_0^\infty f(\nu, T)G(a; \nu)d\nu$$

$$+\phi\left[(I(a)/2)\int_0^{\nu_L} f^2(\nu, T)d\nu\right]^{\frac{1}{2}}, \quad (36)$$

where ϕ is some number such that $|\phi|\leq 1$.

II. BORN-KÁRMÁN MODEL WITH CENTRAL FORCES

This section will be devoted to developing a method of calculating the moments of the frequency distribution of a Born-Kármán crystal in which only central forces exist and in which only nearest and next nearest neighbors of a given atom directly influence its motion. From the moments corresponding to a three-dimensional simple cubic lattice, its frequency spectrum will be obtained.

In following the Born-Kármán approach one first writes the equations of motion for a system of N atoms. Assuming central forces, the total potential energy is

$$V(\mathbf{r}_1, \cdots, \mathbf{r}_N)=\sum_{i<j=1}^{N} V_{ij}(\mathbf{r}_i-\mathbf{r}_j). \quad (37)$$

Expanding this function in a Taylor series about the coordinates of the molecules at equilibrium at absolute zero, choosing the zero point of energy as the constant term obtained from such a development, remembering that, at equilibrium, no forces act on any atom, and assuming that displacements from equilibrium are sufficiently small so that their powers higher than the second may be neglected,

$$V(\mathbf{r}_1\cdots\mathbf{r}_N)=\sum_{i<j=1}^{N}(\xi_i-\xi_j)^2V_{ij}''(a_{ij})/2, \quad (38)$$

where ξ_i is the displacement vector of the ith atom from its absolute zero equilibrium position and $V_{ij}''(a_{ij})$ is the second derivative of the potential energy function due to interactions between the ith and jth atoms evaluated at their equilibrium positions. Now if the interatomic forces are sufficiently short ranged so that only

[12] R. Courant and D. Hilbert, *Methoden der Mathematischen Physik* (J. Springer, Berlin, 1931), Vol. 1, p. 40.

nearest and next nearest neighbor interactions are important, $V(\mathbf{r}_1, \cdots, \mathbf{r}_N)$ becomes a function of two parameters, $\alpha = V''(a_{ij})/2$ with i and j a pair of nearest neighbors and $\gamma = V''(a_{kl})/2$ with k and l a pair of next nearest neighbors. In this case

$$V(\mathbf{r}_1, \cdots, \mathbf{r}_N) = \alpha \sum_{\text{(nearest)}} (\xi_i - \xi_j)^2 + \gamma \sum_{\text{(next nearest)}} (\xi_k - \xi_l)^2. \quad (39)$$

Of course $\alpha \gg \gamma$.

Saving details until special cases are introduced in the next section, let us merely recall[6] that the matrix of the secular equation from which one obtains the characteristic frequencies of a Born-Kármán crystal is of the form

$$M = 2\alpha A + 4\gamma B, \quad (40)$$

where A is a diagonal matrix and B a symmetrical one.

$$\begin{aligned} M^n &= (2\alpha A + 4\gamma B)^n \\ &= (2\alpha)^n \{A^n + (2\gamma/\alpha) \sum_{n_1=1}^{n} A^{n-n_1} B A^{n_1-1} \\ &\quad + (2\gamma/\alpha)^2 \sum_{n_1=2}^{n} \sum_{n_2=2}^{n_1} A^{n-n_1} B A^{n_1-n_2} B A^{n_2-2} \\ &\quad + (2\gamma/\alpha)^3 \sum_{n_1=3}^{n} \sum_{n_2=3}^{n_1} \sum_{n_3=3}^{n_2} \\ &\quad \times A^{n-n_1} B A^{n_1-n_2} B A^{n_2-n_3} B A^{n_3-3} + \cdots \} \\ &= (2\alpha)^n \sum_{s=1}^{n} (2\gamma/\alpha)^{s-1} q_{s,n}. \end{aligned} \quad (41)$$

If the order of M is m, the $2n$th moment of the distribution of its characteristic values is

$$\mu_{2n} = \text{Trace } M^n/m. \quad (42)$$

Since $2\gamma/\alpha$ is small (of order 0.1), we have, in (41) and (42), an expression for μ_{2n} as a polynomial in $2\gamma/\alpha$, whose first terms are the most important.

A. Moment Calculations for a Simple Cubic Lattice

The frequencies of normal modes of vibration of a Born-Kármán model of a simple cubic lattice of $2N \times 2N \times 2N$ identical atoms are solutions of the secular determinant[6]

$$\begin{vmatrix} a_{11}(\varphi_1, \varphi_2, \varphi_3) - 4\pi^2 M\nu^2 & a_{12}(\varphi_1, \varphi_2) & a_{13}(\varphi_1, \varphi_3) \\ a_{21}(\varphi_2, \varphi_1) & a_{22}(\varphi_1, \varphi_2, \varphi_3) - 4\pi^2 M\nu^2 & a_{23}(\varphi_2, \varphi_3) \\ a_{31}(\varphi_3, \varphi_1) & a_{32}(\varphi_3, \varphi_2) & a_{33}(\varphi_1, \varphi_2, \varphi_3) - 4\pi^2 M\nu^2 \end{vmatrix} = 0 \quad (43)$$

with $\varphi_i = \pi a_i/N$ where the a_i's are integers satisfying

$$-N \leq a_1, a_2, a_3 \leq N$$

and

$$\begin{aligned} a_{11} &= 2\alpha(1 - \cos\varphi_1) + 4\gamma(2 - \cos\varphi_1 \cos\varphi_2 - \cos\varphi_1 \cos\varphi_3), \\ a_{22} &= 2\alpha(1 - \cos\varphi_2) + 4\gamma(2 - \cos\varphi_2 \cos\varphi_1 - \cos\varphi_2 \cos\varphi_3), \\ a_{33} &= 2\alpha(1 - \cos\varphi_3) + 4\gamma(2 - \cos\varphi_3 \cos\varphi_1 - \cos\varphi_3 \cos\varphi_2), \\ a_{ij}(\varphi_i, \varphi_j) &= 4\gamma \sin\varphi_i \sin\varphi_j \quad i \neq j. \end{aligned} \quad (44)$$

Incorporating the $4\pi^2 M$ into ν^2, the kth power of the entire Born-Kármán matrix is

$$M^{2k} = \begin{pmatrix} M^{2k}(-N, -N, -N) & 0 & 0 \cdots 0 & 0 \\ 0 & M^{2k}(-N, -N, -N+1) & 0 \cdots 0 & 0 \\ \cdots & \cdots & \cdots & \cdots \\ 0 & 0 & 0 \cdots 0 & M^{2k}(N, N, N) \end{pmatrix}$$

$(2N+1)^3$ rows and columns

TABLE I. Coefficients c_{nm} of the $2n$th moments $\mu_{2n}/(2\alpha)^n = \sum_{m=0}^{n} c_{nm}(2\gamma/\alpha)^m$.

n \ m	0	1	2	3	4	5	6	7
0	1	*	*	*	*	*	*	*
1	1	2	*	*	*	*	*	*
2	3/2	4	5	*	*	*	*	*
3	5/2	9	15	57/4	*	*	*	*
4	35/8	20	179/4	57	703/16	*	*	*
5	63/8	175/4	990/8	210	3515/16	4549/32	*	*
6	231/16	189/2	10,365/32	690	15,321/16	13,467/16	30,353/64	*
7	429/16	1617/8	26,075/32	133,959/64	58,037/16	272,167/64	212,471/64	827,031/512

Since all of the small $M^2(a_1, a_2, a_3)$ matrices are of the same form

$$M^2(a_1, a_2, a_3) = \begin{pmatrix} a_{11} & a_{12} & a_{13} \\ a_{21} & a_{22} & a_{23} \\ a_{31} & a_{32} & a_{33} \end{pmatrix} \tag{45}$$

and

$$\text{Trace } M^{2k} = \sum_{a_1=-N}^{N} \sum_{a_2=-N}^{N} \sum_{a_3=-N}^{N} \text{Trace } M^{2k}(a_1, a_2, a_3).$$

So, we need only find the traces of one general triple (a_1, a_2, a_3), and sum over all a_i's. Now

$$\text{Trace } M^2(a_1a_2a_3) = \sum_{i=1}^{3} a_{ii}(a_1a_2a_3)$$

and

$$\text{Trace } M^2 = 3 \sum_{a_1a_2a_3} a_{11}(a_1a_2a_3) = 3 \sum_{a_1a_2a_3} a_{11}.$$

By using the fact that the trace of the nth power of the matrix (43) is

$$\sum_{\alpha_1=1}^{3} \sum_{\alpha_2=1}^{3} \cdots \sum_{\alpha_n=1}^{3} a_{\alpha_1\alpha_2} a_{\alpha_2\alpha_3} \cdots a_{\alpha_n\alpha_1},$$

it is not difficult to show (taking into account all symmetries of matrix elements and summation operations) that if we let

$$\Sigma = \sum_{a_1} \sum_{a_2} \sum_{a_3},$$

$$\text{Trace } M^0 = 3\,\Sigma\, 1,$$

$$\text{Trace } M^2 = 3\,\Sigma\, a_{11},$$

$$\text{Trace } M^4 = 3\,\Sigma\, (a_{11}^2 + 2a_{12}^2),$$

$$\text{Trace } M^6 = 3\,\Sigma\, (a_{11}^3 + 6a_{11}a_{12}^2 + 2a_{12}a_{13}a_{23}),$$

$$\text{Trace } M^8 = 3\,\Sigma\, (a_{11}^4 + 8a_{11}^2a_{12}^2 + 4a_{12}^2a_{23}^2 + 4a_{11}a_{22}a_{12}^2 + 8a_{11}a_{12}a_{23}a_{31} + 2a_{12}^4),$$

$$\begin{aligned}\text{Trace } M^{10} = 3\,\Sigma\, (&a_{11}^5 + 10a_{11}^3a_{12}^2 + 10a_{11}a_{23}^2a_{12}^2 + 10a_{11}^2a_{12}a_{13}a_{32} + 10a_{11}^2a_{12}^2a_{22} \\ &+ 10a_{11}a_{12}a_{23}a_{33}a_{31} + 10a_{11}a_{12}^4 + 10a_{12}^3a_{13}a_{32} + 10a_{11}a_{12}^2a_{13}^2),\end{aligned} \tag{46}$$

$$\begin{aligned}\text{Trace } M^{12} = 3\,\Sigma\, (&a_{11}^6 + 12a_{11}^4a_{12}^2 + 2a_{12}^6 + 6a_{11}^2a_{22}^2a_{12}^2 + 12a_{11}a_{22}a_{12}^4 + 18a_{11}^2a_{12}^4 \\ &+ 12a_{11}^3a_{22}a_{21}^2 + 24a_{11}^2a_{12}a_{13}a_{33}a_{23} + 18a_{11}^2a_{12}^2a_{31}^2 + 12a_{11}^3a_{12}a_{23}a_{31} \\ &+ 4a_{11}a_{13}a_{33}a_{32}a_{22}a_{21} + 48a_{11}a_{12}^3a_{23}a_{31} + 24a_{11}a_{12}^2a_{13}^2a_{33} + 12a_{11}a_{12}a_{23}^3a_{31} \\ &+ 12a_{21}^4a_{13}^2 + 8a_{12}^2a_{13}^2a_{32}^2 + 6a_{11}a_{12}^2a_{23}^2a_{33} + 12a_{11}^2a_{12}^2a_{23}^2).\end{aligned}$$

Traces of higher powers of M become longer and more tedious to calculate by this method, so it is desirable to attempt to develop power series expressions in $(2\gamma/\alpha)$ as was suggested in the last section. Actually to calculate the moments of our distribution function we proceed as follows:

$$\mu_0 = \text{Trace } M^0/3(2N+1)^3 = 1,$$

$$\mu_2 = \text{Trace } M^2/3(2N+1)^3 = (2N+1)^{-3} \sum a_{11}$$

$$= (2N+1)^{-3} \sum [2\alpha(1-\cos\varphi_1)+4\gamma(2-\cos\varphi_1\cos\varphi_2-\cos\varphi_1\cos\varphi_3)].$$

However, from the expressions[8]

$$\sum_{a=-N}^{N} \cos^k \pi a/N = \begin{cases} 0 \text{ if } k \text{ is odd} \\ 1+2^{1-k}N(k!)/(k/2)!(k/2)! \text{ if } k \text{ is even.} \end{cases}$$

$$\sum_{a=-N}^{N} \sin^k \pi a/N = \begin{cases} 0 \text{ if } k \text{ is odd} \\ N(k)!/2^{k-1}(k/2)!(k/2)! \text{ if } k \text{ is even.} \end{cases}$$

It is clear that

$$\textstyle\sum_a 1 = (2N+1) \quad \text{and} \quad \sum_{a_1} \cos\varphi_1 = 1$$

and

$$\mu_2 = 2(\alpha+4\gamma)(2N+1)^{-3}[(2N+1)^3+0(N^2)]$$

$$= 2\alpha[1+2(2\gamma/\alpha)]+O(1/N).$$

Likewise, if $c_i = \cos(\pi a_i/N)$ and $s_i = \sin(\pi a_i/N)$, we have

$$\mu_4 = (2N+1)^{-3} \sum [(2\alpha)^2(1-c_1)^2+2(2\alpha)(4\gamma)(1-c_1)(2-c_1c_2-c_1c_3)$$

$$+(4\gamma)^2(2-c_1c_2-c_1c_3)^2+2(4\gamma)^2s_1^2s_2^2]$$

$$= (2\alpha)^2[3/2+4(2\gamma/\alpha)+5(2\gamma/\alpha)^2]+O(1/N).$$

In a similar manner we have derived expressions for $\mu_6, \mu_8, \cdots, \mu_{14}$ which are correct to within terms of order $(1/N)$. These results are collected in Table I where the coefficients c_{nm} of

$$\mu_{2n}/(2\alpha)^n = \sum_{m=0}^{n} c_{nm}(2\gamma/\alpha)^m \tag{47}$$

are tabulated.

From Eq. (42),

$$\mu_{2n} = (1/24N^3) \text{ Trace } M^n + O(1/N)$$

and in the Born-Kármán model of a simple cubic lattice, the trace of the first coefficient in (41) becomes

$$\text{Trace } q_{1,n} = \text{Trace } A^n$$

$$= 3 \sum (1-c_1)^n = 12N^2 \sum_{a_1=-N}^{N} (1-c_1)^n,$$

where $c_1=\cos(a_1\pi/N)$. But, as can be verified for $n\geq 0$,[13]

$$\sum_{a_1}(1-c_1)^n=N[(2n-1)!/n!(n-1)!2^{n-2}+0(1/N)] \tag{48}$$

or

$$(1/24N^3)\ \text{Trace}\ q_{1,n}=(2n-1)!/n!(n-1)!2^{n-1}$$

and, to a first approximation,

$$\mu_{2n}\sim(2\alpha)^n[(2n-1)!/n!(n-1)!2^{n-1}+O(2\gamma/\alpha)]. \tag{49}$$

To obtain the next approximation to μ_{2n} we must find

$$\text{Trace}\ q_{2,n}=\text{Trace}\sum_{n_1=1}^{n}A^{n-n_1}BA^{n_1-1}.$$

If the A matrix is represented by

$$A=\begin{pmatrix}A_{11}&0&0\\0&A_{22}&0\\0&0&A_{33}\end{pmatrix}$$

and the B matrix by $B=(B_{ij})$, it is a simple matter to obtain

$$A^{n-n_1}BA^{n_1-1}=\begin{pmatrix}A_{11}^{n-1}B_{11}&A_{11}^{n-n_1}A_{22}^{n_1-1}B_{12}&A_{11}^{n-n_1}B_{13}A_{33}^{n_1-1}\\A_{22}^{n-n_1}B_{21}A_{11}^{n_1-1}&A_{22}^{n-1}B_{22}&A_{22}^{n-n_1}B_{23}A_{33}^{n_1-1}\\A_{33}^{n-n_1}B_{31}A_{11}^{n_1-1}&A_{33}^{n-n_1}B_{32}A_{22}^{n_1-1}&A_{33}^{n-1}B_{33}\end{pmatrix}$$

and

$$\text{Trace}\ A^{n-n_1}BA^{n_1-1}=A_{11}^{n-1}B_{11}+A_{22}^{n-1}B_{22}+A_{33}^{n-1}B_{33}$$

is independent of n_1. Therefore:

$$\begin{aligned}\text{Trace}\ q_{2,n}&=3n\sum A_{11}{}^{n-1}B_{11}\\&=3n\sum(1-c_1)^{n-1}(2-c_1c_2-c_1c_3)\\&=(6n)(4N^2)\textstyle\sum_{a_1}(1-c_1)^{n-1}\end{aligned}$$

or, for $n>1$,

$$[1/3(2N)^2]\ \text{Trace}\ q_{2,n}=n(2n-3)!/(n-1)!(n-2)!2^{n-3}.$$

So

$$\mu_{2n}\sim(2\alpha)^n\left[\frac{(2n-1)!}{n!(n-1)!2^{n-1}}+(2\gamma/\alpha)\frac{n(2n-3)!}{(n-1)!(n-2)!2^{n-3}}+O\left(\left(\frac{2\gamma}{\alpha}\right)^2\right)\right]. \tag{50}$$

The calculation of Trace $q_{3,n}$ and higher coefficients is more complicated, but can be accomplished in essentially the same manner. The results of these calculations are not as simple as those for Trace $q_{1,n}$ and Trace $q_{2,n}$ so they are not recorded in their most general form here, but are incorporated into Table I.

---

[13] Note that when $n=0$, we must write $(2n-1)!/(n-1)!=(2n)!n/(n!)2n=0!/2(0!)=\frac{1}{2}$.

B. Frequency Spectrum for Born-Kármán Model

1. Frequency Spectrum at Low Frequencies

If one expands all the trigonometric functions in the Born-Kármán matrix into power series and neglects terms of order $(a_i/N)^4$ and of order $(2\gamma/\alpha)^2$, it is clear that when $|a_i| \ll N$, the normal modes ν are obtainable from the three equations

$$4\pi^2\nu_1^2M=\alpha[\varphi_1^2+(2\gamma/\alpha)(2\varphi_1^2+\varphi_2^2+\varphi_3^2)] +O[(2\gamma/\alpha)^2;\varphi_i^4],$$

$$4\pi^2\nu_2^2M=\alpha[\varphi_2^2+(2\gamma/\alpha)(2\varphi_2^2+\varphi_1^2+\varphi_3^2)] +O[(2\gamma/\alpha)^2;\varphi_i^4],$$

$$4\pi^2\nu_3^2M=\alpha[\varphi_3^2+(2\gamma/\alpha)(2\varphi_3^2+\varphi_1^2+\varphi_2^2)] +O[(2\gamma/\alpha)^2;\varphi_i^4],$$

$$\varphi_i=a_i\pi/N.$$

Therefore the number of frequencies less than ν (if ν is very small) is the total number of lattice points of (a_1, a_2, a_3) space which are included in the ellipsoid

$$\nu^2=a_1^2(\alpha+4\gamma)/MN^2 +a_2^2(2\gamma)/MN^2+a_3^2(2\gamma)/MN^2,$$

and the corresponding ellipsoids obtained by permuting a_1 with a_2 and a_1 with a_3. This number is approximately the sum of the volumes of the three ellipsoids, and since, upon rotation of coordinate axes, all three ellipsoids can be shown to be identical, the number of frequencies less than ν is

$$n(\nu)=(3)(4\pi/3)(N^3M^{\frac{3}{2}}\nu^3)/2\gamma(\alpha+4\gamma)^{\frac{1}{2}}.$$

Now $g(\nu)d\nu$ was defined to be the number of frequencies in the frequency interval $d\nu$ at ν; therefore

$$g(\nu)=\partial n/\partial\nu=12\pi N^3M^{\frac{3}{2}}\nu^2/2\gamma(\alpha+4\gamma)^{\frac{1}{2}}.$$

They obtain the same $g(\nu)$ that we have used in the last section (that is, the distribution function whose moments are given by Eq. (47)), and that we shall use in the next section. We incorporate $4\pi^2M$ into ν^2, so

$$g(\nu)=3N^3M^{\frac{3}{2}}\nu^2/2\pi\gamma(\alpha+4\gamma)^{\frac{1}{2}}.$$

However, as has been shown by Blackman, the square of the largest frequency ν_L, is given by

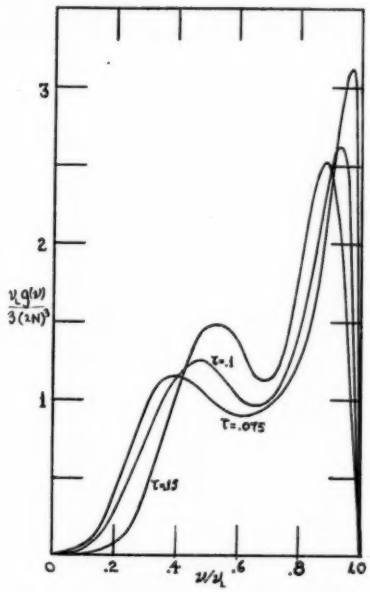

FIG. 1. Frequency spectrum of simple cubic lattice. $\nu_L g(\nu)/3(2N)^3$ plotted as a function of (ν/ν_L) for $\tau=0.075$, 0.1, 0.15.

$4\pi^2M\nu_L^2=4(\alpha+4\gamma)$. Using this fact, incorporating the $4\pi^2M$ into ν^2, and defining a new parameter

$$\tau=8\gamma/\nu_L^2, \tag{51}$$

we finally obtain

$$\nu_L g(\nu)/3(2N)^3=(\nu/\nu_L)^2/2\pi^2\tau, \tag{52}$$

when ν is very small.

2. Polynomial Approximation of Frequency Spectrum

Using Eq. (35) and Table I one can calculate the coefficients a_n of the polynomial approximation

$$G(\nu/\nu_L)=\sum_{n=0}^{7} a_{2n}(\nu/\nu_L)^{2n}$$

of $g(\nu)$. In order to find the a_n's it is necessary to know μ_{2n}/ν_L^{2n} for various n's. Table I gives this ratio as a function of two parameters, but by making the substitution (51), $\tau=8\gamma/\nu_L^2$, it is possible to express μ_{2n}/ν_L^{2n} as a one-parameter function. With this transformation the coefficients b_{nm} of

$$\mu_{2n}/\nu_L^{2n}=\sum_{m=0}^{n} b_{nm}\tau^m$$

TABLE II. Coefficients b_{nm} of the $2n$th moments $\mu_{2n}/\nu_L^{2n}=\sum_{m=0}^{n} b_{nm}\tau^m$.

n \ m	0	1	2	3	4	5	6	7
0	1	*	*	*	*	*	*	*
1	1/2	0	*	*	*	*	*	*
2	3/8	−1/2	3/4	*	*	*	*	*
3	5/16	−3/4	9/8	1/32	*	*	*	*
4	35/128	−15/16	119/64	−11/8	303/256	*	*	*
5	63/256	−35/32	355/128	−225/64	1515/512	25/1024	*	*
6	231/1024	−315/256	7845/2048	−1725/256	7941/1024	−4389/1024	10,313/4096	*
7	429/2048	−693/512	20,531/4098	−91,861/8192	34,419/2048	−126,217/8192	79,947/8192	−58,233/65,536

TABLE III. Coefficients c_{ms} of (53). The large number of significant figures is necessary because of the alternate nature of the signs. When sums are calculated in (53) the first four or five significant figures usually cancel out.

Coefficient of x^{2s} \ Coefficients of τ^m	0	1	2	3	4	5	6	7
0	.5079	−22.337	297.733	−1,751.79	4,999.17	3,556.2	−9,563	−13,216
1	15.7644	458.440	−11,104.119	76,955.12	−221,267.41	65,651.5	1,257,181	1,387,740
2	−295.8016	5,394.480	−15,777.088	−45,293.70	−80,087.89	−6,819,465.1	−26,662.539	−23,591,576
3	2091.4481	−85,986.577	1,017,799.282	−5,767,333.61	19,496,814.16	71,690,894.7	172,648,360	149,413,313
4	−6937.2931	374,647.254	−5,196,670.653	31,787,179.83	−104,419,659.56	−284,259,563.8	−557,900,611	−448,239,940
5	11,680.7148	−722,493.189	10,672,356.522	−67,064,585.68	218,258,344.87	523,471,667.7	906,057,942	687,301,241
6	−9661.1765	645,337.459	−9,829,994.779	62,531,485.03	−202,398,644.57	−452,304,050.3	−718,614,110	−520,682,759
7	3115.7088	−217,697.878	3,367,593.382	−21,542,684.29	69,437,373.44	148,283,675.4	221,355,300	154,488,291

TABLE IV. Coefficients p_n of $\nu_L g(\nu/\nu_L)/3(2N)^3=\Sigma p_n\tau^n$.

ν/ν_L	p_1	$p_2\times10^{-1}$	$p_3\times10^{-2}$	$p_4\times10^{-3}$	$p_5\times10^{-4}$	$p_6\times10^{-5}$	$p_7\times10^{-6}$	$p_8\times10^{-7}$
0.10	0.6379	−1.7296	1.8608	−0.9922	0.2797	−0.0360	0.0007	−0.0001
.20	.7901	.0016	−1.1879	.9594	−.2978	.0082	.0110	.0012
.30	.6639	2.0580	−3.7038	−2.3246	−.7017	.0930	−.0020	.0004
.35	.5734	2.3233	−3.3595	1.9042	−.5616	.0999	−.0113	−.0006
.40	.5483	1.6921	−1.5638	.5696	−.1351	.0546	−.0147	−.0013
.45	.6269	.3110	1.1881	−1.2908	.4554	−.0365	−.0094	−.0012
.50	.7799	−1.1941	3.6712	−2.8309	.9392	−.1336	.0045	−.0004
.55	.9190	−1.9153	4.3579	−3.0462	.9924	−.1736	.0171	.0008
.60	.9469	−1.1807	2.3076	−1.3744	.4319	−.1060	.0190	.0015
.65	.8367	.7892	−1.7894	1.6279	−.5651	.0595	.0054	.0010
.70	.7059	2.6126	−5.1835	4.0281	−1.3715	.2225	−.0163	−.0004
.75	.7689	2.2524	−4.2461	3.3304	−1.1671	.2255	−.0268	−.0016
.80	1.1393	−.9159	2.1389	−1.2523	.3315	−.0165	−.0084	−.0011
.85	1.5409	−3.6352	8.2282	−5.8836	1.9172	−.3187	.0277	.0010
.90	1.3918	.7153	1.9310	−2.3062	.9061	−.1935	.0262	.0017
.95	1.4819	9.1287	−14.8749	9.1985	−2.8059	.4689	−.0435	−.0019

are tabulated in Table II. Introduction of these moments into (33) permit one to calculate a seven-term polynomial approximation to $g(\nu)$ $(x=\nu/\nu_L)$:

$$\nu_L g(\nu)/3(2N)^3=\sum_{m=0}^{7}\Big(\sum_s c_{ms}x^{2s}\Big)\tau^m. \qquad (53)$$

The c_{ms}'s are tabulated in Table III. To facilitate numerical calculations, $\sum_s c_{ms}x^{2s}$ has been calculated for various x's in the interval $<0, 1>$ and tabulated in Table IV. This table is sufficient to give $\nu_L g(\nu)/3(2N)^3$ for all expected values of τ. The largest relative error probably occurs with very small x's, so in this range one should use the asymptotic expression (52). In Fig. 1 we have plotted $\nu_L g(\nu)/3(2N)^3$ for $\tau=0.075$, 0.1, and 0.15, on the basis of Table IV and (52). It is to be noted that there are two maxima in each curve, with the height of the low frequency maximum increasing with increasing τ and the height of the high frequency maximum decreasing with increasing τ. If one interpolates between the $\tau=0.075$ and $\tau=0.10$ excellent agreement is obtained with Blackman's[6] calculations for $\tau=0.085$.

C. Specific Heats

For a simple cubic lattice it is possible to calculate the specific heat at high temperatures

from Eq. (18). This series converges when $kT/h\nu_L > 0.159$; the first fourteen moments tabulated in Table II being sufficient to determine C_v to within one percent when $kT/h\nu_L > 0.2$. At higher temperatures

$$C_v/3(2N)^3k \simeq 1-(kT/h\nu_L)^2/24 + (kT/h\nu_L)^4(3-4\tau+6\tau^2)/1920-. \quad (54)$$

At very low temperatures we can derive an asymptotic T^3 law by introducing (52) into

$$C_v = k\int_0^{\nu_L} g(\nu)(h\nu/2kT)^2 d\nu/\sinh^2(h\nu/2kT).$$

Thus, at low temperatures

$$C_v/3k(2N)^3 \simeq (kT/h\nu_L)^3/2\pi^2 \times \int_0^{h\nu_L/kT} x^4 e^x dx/(1-e^x)^2,$$

and at very low temperatures the upper limit can be made infinite. Since

$$\int_0^{\infty} x^4 e^x dx/(1-e^x)^2 = 4\pi^2/15,$$

we have

$$C_v/3k(2N)^3 \simeq (2\pi^2/15\tau)(kT/h\nu_L)^3. \quad (55)$$

Letters to the Editor

PROMPT publication of brief reports of important discoveries in physics may be secured by addressing them to this department. The closing date for this department is the third of the month. Because of the late closing date for the section no proof can be shown to authors. The Board of Editors does not hold itself responsible for the opinions expressed by the correspondents. Communications should not in general exceed 600 words in length.

Statistical Mechanics of Binary Mixtures

T. ALFREY AND H. MARK
Polytechnic Institute of Brooklyn, Brooklyn, New York
August 11, 1943

IN a previous brief note[1] on the statistical mechanics of binary mixtures, we started with the usual assumptions —that the free energy of mixing is determined by a purely configurational partition function, that a given configuration can be described by specifying the occupants of a set of lattice points, and that the energy of interaction is predominantly that of nearest neighbors. We then introduced a method of describing a configuration in terms of the occupants of a reference set of non-overlapping lattice point pairs, rather than of the lattice points themselves. This was done in order to avoid the usual complexity of the relation between the variables used in determining the distinctness of a configuration and those used in calculating the energy of a configuration.

In the process of counting configurations, each lattice point is ordinarily considered separately; i.e., the lattice specifications are the elements of the statistical analysis. However, since the configurational energy depends upon *interaction*, it cannot be expressed as a simple function of the separate lattice point specifications. This energy is a sum of terms, each of which depends upon the simultaneous specification of two *different* lattice points.

By the use of the above lattice point pair method of specification, and the further *assumption* that the probable *total* number of molecular pairs of a given type was directly proportional to the number of such pairs in the reference set of lattice point pairs, it was possible to derive directly and simply the equilibrium configurational relationships for a binary mixture.

In a recent paper[2] Dr. Kottler has presented objections to our treatment. Dr. Kottler states that we did not present a sufficient justification for replacing the configurational partition function by its maximum term. As Dr. Kottler himself points out, this is a step "which is usually taken for granted." We felt this mathematical step to be a well-known and standard procedure in the evaluation of this type of sum, and to require no elaborate justification in a communication as brief as ours.

Dr. Kottler further objects to the assumption that the probable total number of pairs of a given type is proportional to the number of such pairs in the reference set. This objection is based upon the argument that "the pairs overlap and therefore are interdependent." We specifically stated as a restriction on the reference set of lattice point pairs that they were to be chosen in such a fashion that each lattice point was the member of one and only one reference pair and in this way precluded overlapping in the reference set of pairs. It is true that M_{AB}, the total number of AB pairs among the total pairs of all kinds, is not *geometrically identical* with $z \cdot X$, where X is the number of AB pairs among the reference pairs. We reaffirm, however, that the *probable value* of M_{AB} is given by $z \cdot X$ and that in the absence of any long range order the distribution function for a given value of X is very sharp about $z \cdot X$.

[1] T. Alfrey and H. Mark, J. Chem. Phys. 10, 303 (1942).
[2] F. Kottler, J. Chem. Phys. 11, 153 (1943).

Specific Heat Ratios in CO_2

LEON KATZ
Electronic Department, Westinghouse Research Laboratories, East Pittsburgh, Pennsylvania
August 9, 1943

TABLE I showing experimentally measured values of the ratio of specific heats for a number of gases (γ^0 exp.) was recently published by Clark and Katz.[1]

TABLE I.

Gas	Temp. Deg. Cent.	γ^0 exp.	γ^0 spec.	% Diff.
Argon	24.2	1.666_7	1.6667	0.00
Helium	23.0	1.666_9	1.6667	−0.01
Nitrogen	23.0	1.400_6	1.3999	+0.05
Hydrogen	24.4	1.404_5	1.4050	−0.04
Sulphur dioxide	25.1	1.264_2	1.2642	0.00
Nitrous oxide	25.1	1.278_2	1.2735	+0.38
Carbon dioxide	23.8	1.294_8	1.2886	+0.49

We measured gamma as a function of pressure at constant temperature in the range of 1 to 20 atmos. and then extrapolated by the method of least squares to zero pressure. These experimentally determined zero pressure values (γ^0 exp.) were then compared to γ^0 spec., calculated from the spectroscopically determined vibrational energy levels. It will be seen that excellent agreement was obtained for monatomic and diatomic gases, but rather large discrepancies were found for the triatomic gases N_2O and CO_2 but not SO_2. These discrepancies are in the opinion of the authors outside the limits of the accuracy of their measurements.

It is the purpose of this letter to point out that similar discrepancies exist between all reliable experimentally determined values of γ for CO_2 found in the literature and those calculated by the spectroscopic method.

Since most published values are given at one atmosphere, it is necessary first to reduce these to zero pressure. This was done with the aid of Berthelot's equation of state, which gives

$$(\gamma^1-1)=(\gamma^0-1)\frac{(1+\theta)^2}{1+(\gamma^0-1)\theta(1-\theta)},$$

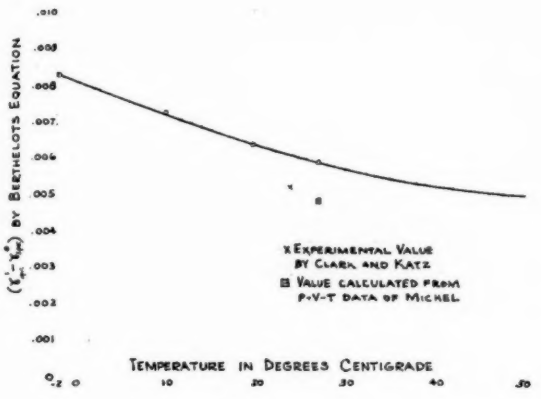
BY BERTHELOTS EQUATION
x EXPERIMENTAL VALUE BY CLARK AND KATZ
⊟ VALUE CALCULATED FROM P-V-T DATA OF MICHEL
TEMPERATURE IN DEGREES CENTIGRADE

FIG. 1.

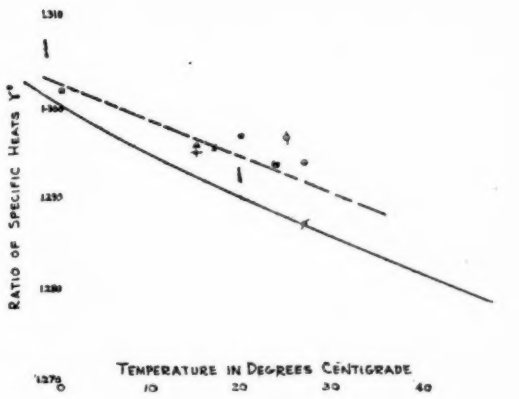

FIG. 2. x Partington; ⊙ Partington and Cant; —⊙— Shilling; Eucken and Lude; △ King and Partington; ⊕ Hubbard and Hodge; ⊡ Sherret and Griffiths; ⊙ Jatkar; ⊡ Kistiakowski and Rice; ⊗ Clark and Katz; ------ Straight line through experimental values by method of least squares; —— Spectroscopic values.

where γ^1 = ratio of specific heats at 1 atmosphere,
γ^0 = ratio of specific heats at zero pressure,

$$\theta = \frac{27}{32}\frac{1}{P_c}\left(\frac{T_c}{T}\right)^3,$$

with P_c = critical pressure = 72.85 atmos. for CO_2,
T_c = critical temperature = 304.19°C for CO_2.

Using this equation and γ^0 spec., the values of γ^1 spec. are calculated, giving (γ^1 spec. $-\gamma^0$ spec.) Berth.

This difference, for CO_2, is shown in Fig. 1 as a function of temperature. A value experimentally determined by Clark and Katz and one calculated from $P-V-T$ data of Michel[2] are also shown. The difference between these two points and the above "Berthelot" values corresponds to a difference of about 0.07 percent in γ.

TABLE II.

Source	Temperature	γ^1 exp.	γ^0 exp.
Partington[1]	17°C	1.3022	1.2956
Partington and Cant[2]	20	1.303	1.297
Shilling[3]	15	1.3020	1.2952
Euchen and Lude[4]	−1.7		1.3046
Euchen and Lude[4]	19.7		1.2928
King and Partington[5]	15		1.2960
Hubbard and Hodge[6]	27	1.300	1.294
Sherret and Griffiths[7]	0	1.310	1.302
Jatkar[8]	25	1.3028	1.2968
Kistiakowski and Rice[9]	27		1.2873
Clark and Katz[10]	23.8	1.3000	1.2938

[1] J. R. Partington, Proc. Roy. Soc. London **A100**, 27–49 (1921).
[2] J. R. Partington and H. J. Cant, Proc. Roy. Soc. London 369–80 (1922).
[3] W. G. Shilling, Phil. Mag. **3**, 273–301 (1927).
[4] A. Eucken and Lude, Zeits. f. physik. Chemie **5B**, 413 (1929).
[5] J. R. Partington and F. E. King, Phil. Mag. **9**, 1020–26 (1930).
[6] J. C. Hubbard and A. W. Hodge, J. Chem. Phys. **5**, 978–79 (1937).
[7] Sherret and Griffiths, Proc. Roy. Soc. London **A156**, 504–17 (1936).
[8] S. K. K. Jatkar, Ind. Inst. Sci. **2**, 1–11 (1937).
[9] G. B. Kistiakowski and W. W. Rice, J. Chem. Phys. **7**, 281 (1939).
[10] See reference 1, in text.

Table II summarizes the most reliable values of gamma at one atmosphere (γ^1 exp.) for CO_2 as found in the literature and their corresponding values at zero pressure (γ^0 exp.) obtained from the one atmosphere values with the aid of Fig. 1. Where we have assumed that

$$(\gamma^1 \text{ exp.} - \gamma^0 \text{ exp.}) = (\gamma^1 \text{ spec.} - \gamma^0 \text{ spec.})$$

and that this difference can be calculated with sufficient accuracy from Berthelot's equation of state.

These values of γ^0 exp. are compared with the spectroscopic values in Fig. 2. It will be seen that all the experimental values, except the one by Kistiakowski and Rice are higher in value than the corresponding calculated ones.

It would be difficult to see why the values of Kistiakowski and Rice should be considered more accurate than those of the other workers. In their paper Kistiakowski and Rice point out in a footnote, that some of their earlier measurements of C_p gave values 0.4 percent lower than those published. This difference is in the proper direction to throw γ^0 exp. among the other experimental values.

The straight line shown dotted was fitted to the experimental values by the method of least squares.

[1] A. L. Clark and L. Katz, Can. J. Research **A21**, 1–7.
[2] A. Michels and C. Michels, Proc. Roy. Soc. London **A153**, 201–14 (1935); **A160**, 348–57 (1937).

THE AMERICAN INSTITUTE OF PHYSICS

INCORPORATED

ADMINISTRATIVE STAFF

HERBERT A. BARTON, *Director*

MADELINE M. MITCHELL, *Publications Manager*

JOHN T. TATE, *Adviser on Publications*

Office: 175 Fifth Avenue, New York 10, New York

JOURNALS

THE PHYSICAL REVIEW

REVIEWS OF MODERN PHYSICS
JOHN T. TATE, *Editor (on leave)*;
J. W. BUCHTA, *Acting Editor*

JOURNAL OF THE OPTICAL SOCIETY OF AMERICA
GEORGE R. HARRISON, *Editor*

THE JOURNAL OF THE ACOUSTICAL SOCIETY OF AMERICA
FLOYD A. FIRESTONE, *Editor*

AMERICAN JOURNAL OF PHYSICS
DUANE ROLLER, *Editor*

THE REVIEW OF SCIENTIFIC INSTRUMENTS
GAYLORD P. HARNWELL, *Editor*

THE JOURNAL OF CHEMICAL PHYSICS
JOSEPH E. MAYER, *Editor*

JOURNAL OF APPLIED PHYSICS
ELMER HUTCHISSON, *Editor*

GOVERNING BOARD

PAUL E. KLOPSTEG, *Chairman*
Central Scientific Company

GEORGE B. PEGRAM, *Secretary*
Columbia University

For the American Physical Society:

JOHN T. TATE
University of Minnesota

L. A. DUBRIDGE
University of Rochester

GEORGE B. PEGRAM
Columbia University

For the Optical Society:

A. C. HARDY
Massachusetts Institute of Technology

K. S. GIBSON
National Bureau of Standards

R. C. GIBBS
Cornell University

For the Acoustical Society of America:

HARVEY FLETCHER
Bell Telephone Laboratories

FLOYD A. FIRESTONE
University of Michigan

WALLACE WATERFALL
The Celotex Corporation

For the Society of Rheology:

R. B. DOW
Aberdeen Proving Ground

HERMANN MARK
Brooklyn Polytechnic Institute

N. W. TAYLOR
The Pennsylvania State College

For the American Association of Physics Teachers:

A. G. WORTHING
University of Pittsburgh

PAUL E. KLOPSTEG
Central Scientific Company

T. D. COPE
University of Pennsylvania

The American Institute of Physics is [illegible]. The broad purpose of the Institute is to represent, in cooperation of which five societies are the [illegible] all matters of wide or common interest, the five thousand bers. The five societies are the principal [illegible] more members and subscribers associated with the devoted to pure and applied physics in [illegible] founder Societies and the journals. It aims to advance science, and places of their representatives [illegible] the science and profession of physics, and to promote Governing Board of the Institute, are given [illegible] cooperation between pure research, the applied sciences principal work of the Institute is the [illegible] and the industries. To achieve these aims, it is greatly journals sponsored by the societies or by [illegible] in need of an endowment and is empowered by law to manag[illegible] and the editors of the journals are also [illegible] administer grants and funds of any kind.

CONTENTS

THE JOURNAL OF CHEMICAL PHYSICS, VOL. 11, NO. 10 OCTOBER, 1943

Atomic and Electronic Distributions in Liquid Nitrogen, Nitric Oxide, and Nitrous Oxide . . . . . PAUL C. SCHERRER 435

Magnetic Susceptibility of Oxygen and Nitric Oxide at Low Field Strengths . . . . . A. BURRIS AND C. J. HAUBE 442

Depolarization Studies of Raman Lines. A Simplified Method . . . . . GEORGE GLOCKLER AND HAROLD T. BARNES 448

Raman Spectra of Acetylenes. VII. Symmetrical-Top Acetylenes . . . . . FORREST F. CLEVELAND AND M. J. MURRAY 450

Theory of the Kinetic Properties of Binary . . . . . HUBERT M. JAMES AND EUGENE GUTH 455

Frequency Spectrum of Crystalline Solids. I. General Theory and Applications to Simple Cubic . . . . . ELLIOTT W. MONTROLL 481

Letters to the Editor

. . . . . T. ASHLEY AND H. HUSE AND 496

LANCASTER PRESS, INC., LANCASTER, PA.